

Volumetric Calculations
 North King Camp (Devonian)
 Chaves County, New Mexico

(Based On Conditions Existing As Of October 1, 1989)

Classification	Santa Fe	Stevens	NE/4	Total
	Holmstrom #1	Deemar Fed #1	Section 9 29E-14S	
Productive Acreage (acres)	80.9	38.8	87.8	207.5
Gross Reservoir Volume (ac-ft)	5,270	4,524	6,088	15,882
Current Producing Reservoir Volume (ac-ft)	3,974	4,431	0	8,405
Producing Reservoir Volume Behind-Pipe (ac-ft)	864	29	0	893
Undeveloped Reservoir Volume-Regular Location (ac-ft)	0	0	5,706	5,706
Total Producing Reservoir Volume (ac-ft)	4,838	4,460	5,706	15,004
Non-Producing Reservoir Volume (ac-ft)	432	64	382	878
Original Oil-In-Place (MBBL)	2,278	1,955	2,631	6,857
Ultimate Proved Developed Producing Reserves (MBBL)	601	670	0	1,271
Ultimate Proved Developed Behind-Pipe Reserves (MBBL)	131	4	0	135
Ultimate Proved Undeveloped Reserves (MBBL)	0	0	863	863
Ultimate Total Proved Reserves (MBBL)	732	674	863	2,268
Recoverable Oil In Non-Producing Zones (MBBL)	65	10	58	133
Estimated Cumulative Production As Of October 1, 1989 (MBBL)	93.1	3.6	0	96.7
<i>Average Net Pay Thickness</i>	<i>65.1</i>	<i>116.1</i>	<i>69.3</i>	<i>76.5</i>

Parameters Used:

- BHT = 145° F
- API Gravity = 46°
- GOR = 40 CF/BBL
- FVF = 1.05
- Average Porosity = 7.8%
- Average Water Saturation = 25%
- Recovery Factor = 35%
- Bottom-Hole Flowing Pressure @ 536 BPD = 3704 psia
- Static Bottom-Hole Pressure @ August 25, 1989 = 3936 psia
- COIP = [7758(0.078)(1-0.25)] ÷ 1.05 = 432.2 STB/cu-ft
- ROIP = 432.2 x 0.35 = 151.3 STB/ac-ft

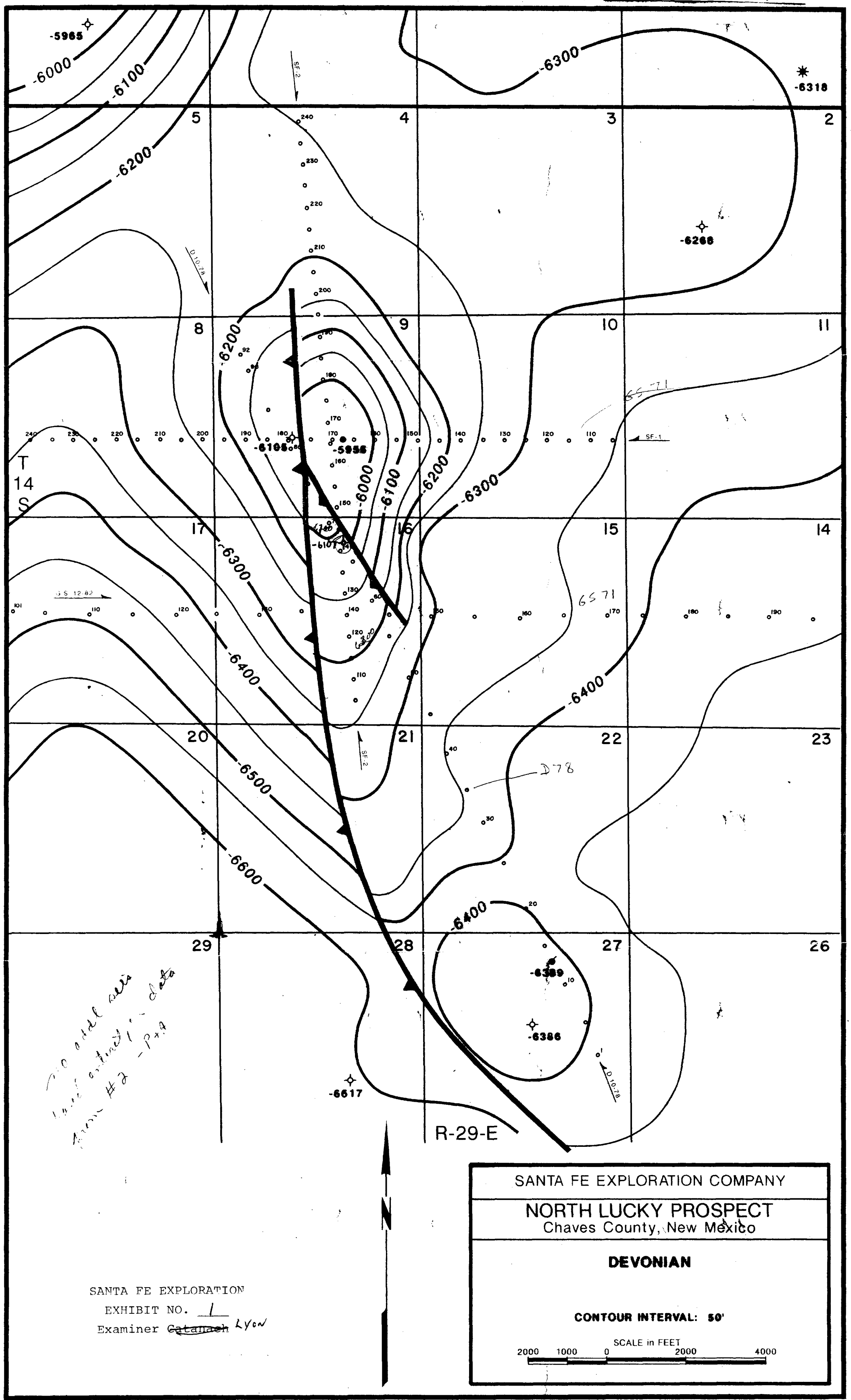
BEFORE THE
 OIL CONSERVATION COMMISSION
 Santa Fe, New Mexico

Case No. 9611-4005 Exhibit No. 2

Submitted by WILLIAM

Hearing Date 10/11/89

Santa Fe
Exhibits 1 through 3



200 odd wells
have activity - data
from #2 - P+4

SANTA FE EXPLORATION
EXHIBIT NO. 1
Examiner ~~Catanaeh~~ Lyon

SANTA FE EXPLORATION COMPANY
NORTH LUCKY PROSPECT Chaves County, New Mexico
DEVONIAN
CONTOUR INTERVAL: 50'
SCALE in FEET 2000 1000 0 2000 4000

Case No. 9617
S.F. Exh 1-3

HOLMSTROM FEDERAL #1
Sec. 9, T-14-S, R-29-E
1980' FSL & 1980' FEL
Chaves County, New Mexico
Proposed TD 10,000'
Wildcat Devonian

SANTA FE EXPLORATION
EXHIBIT NO. 52
Examiner Gatanaeh Lyon

DAILY DRILLING REPORT

1-21-89 TP 285#, 10/64" ck, made 259 B0 & 6 MCF in 23½ hrs.
1-22-89 TP 285#, 10/64" ck, made 257 B0 & 6 MCF in 23 hrs.
1-23-89 TP 285#, 10/64" ck, made 269 B0 & 6 MCF in 24 hrs.
1-24-89 TP 282#, 10/64" ck, made 251 B0 & 6 MCF in 24 hrs.
1-25-89 TP 300#, 10/64" ck, made 259 B0 & 6 MCF in 24½ hrs.
1-26-89 TP 290#, 10/64" ck, made 269 B0 & 6 MCF in 24 hrs.
1-27-89 TP 290#, 10/64" ck, made 269 B0 & 6 MCF in 24 hrs.
1-28-89 TP 285#, 10/64" ck, made 297 B0 & 6 MCF in 27 hrs.
1-29-89 TP 285#, 10/64" ck, made 198 B0 & 6 MCF in 23 hrs.
1-30-89 TP 285#, 10/64" ck, made 269 B0 & 6 MCF in 25 hrs.
1-31-89 TP 285#, 10/64" ck, made 264 B0 & 6 MCF in 23½ hrs.
2-01-89 TP 285#, 10/64" ck, made 241 B0, 6 MCF & 8 BW in 23 hrs.
2-02-89 TP 285#, 10/64" ck, made 270 B0, 6 MCF & 10 BW in 24½ hrs.
2-03-89 TP 264#, 10/64" ck, made 256 B0, 6 MCF & 10 BW in 23½ hrs.
2-04-89 TP 290#, 10/64" ck, made 264 B0, 6 MCF & 10 BW in 25 hrs.
2-05-89 TP 285#, 10/64" ck, made 231 B0, 6 MCF & 5 BW in 26-3/4 hrs.
2-06-89 TP 285#, 10/64" ck, made 259 B0, 6 MCF & 0 BW in 21½ hrs.
2-07-89 TP 285#, 10/64" ck, made 262 B0, 6 MCF & 10 BW in 23 hrs.
2-08-89 TP 285#, 10/64" ck, made 237 B0, 6 MCF & 20 BW in 23-3/4 hrs.
2-09-89 TP 285#, 10/64" ck, made 261 B0, 6 MCF & 8 BW in 24½ hrs.
2-10-89 TP 285#, 10/64" ck, made 264 B0, 6 MCF & 10 BW in 23½ hrs.
2-11-89 TP 285#, 10/64" ck, made 291 B0, 6 MCF & 8 BW in 28 hrs.
2-12-89 TP 285#, 10/64" ck, made 214 B0, 6 MCF & 10 BW in 20½ hrs.
2-13-89 TP 285#, 10/64" ck, made 259 B0, 6 MCF & 12 BW in 23-3/4 hrs.
2-14-89 TP 285#, 10/64" ck, made 225 B0, 6 MCF & 8 BW in 24 hrs.
2-15-89 TP 280#, 10/64" ck, made 253 B0, 6 MCF & 12 BW in 23½ hrs.
2-16-89 TP 280#, 10/64" ck, made 235 B0, 6 MCF & 8 BW in 25 hrs.
2-17-89 TP 280#, 10/64" ck, made 248 B0, 6 MCF & 10 BW in 23-3/4 hrs.
2-18-89 TP 280#, 10/64" ck, made 286 B0, 6 MCF & 10 BW in 27 hrs.
2-19-89 TP 280#, 10/64" ck, made 205 B0, 6 MCF & 11 BW in 20-3/4 hrs.
2-20-89 TP 280#, 10/64" ck, made 269 B0, 6 MCF & 8 BW in 24-3/4 hrs.
2-21-89 TP 280#, 10/64" ck, made 269 B0, 6 MCF & 12 BW in 24 hrs.
2-22-89 TP 280#, 10/64" ck, made 264 B0, 6 MCF & 10 BW in 24½ hrs.

HOLMSTROM FEDERAL #1
Sec. 9, T-14-S, R-29-E
1980' FSL & 1980' FEL
Chaves County, New Mexico
Proposed TD 10,000'
Wildcat Devonian

DAILY DRILLING REPORT

12-20-88 TP 320#, 10/64" ck, made 291 B0 & 6 MCF in 24 hrs.
12-21-88 TP 320#, 10/64" ck, made 280 B0 & 6 MCF in 24 hrs.
12-22-88 TP 320#, 10/64" ck, made 283 B0 & 6 MCF in 24 hrs.
12-23-88 TP 315#, 10/64" ck, made 264 B0 & 6 MCF in 24 hrs.
12-24-88 TP 310#, 10/64" ck, made 286 B0 & 6 MCF in 24½ hrs.
12-25-88 TP 310#, 10/64" ck, made 204 B0 & 6 MCF in 23½ hrs.
12-26-88 TP 310#, 10/64" ck, made 264 B0 & 6 MCF in 23 hrs.
12-27-88 TP 305#, 10/64" ck, made 281 B0 & 6 MCF in 24 hrs.
12-28-88 TP 305#, 10/64" ck, made 264 B0 & 6 MCF in 23½ hrs.
12-29-88 TP 300#, 10/64" ck, made 300 B0 & 6 MCF in 24½ hrs.
12-30-88 TP 300#, 10/64" ck, made 297 B0 & 6 MCF in 26½ hrs.
12-31-88 TP 300#, 10/64" ck, made 198 B0 & 6 MCF in 21 hrs.
1-01-89 TP 300#, 10/64" ck, made 308 B0 & 6 MCF in 26½ hrs.
1-02-89 TP 300#, 10/64" ck, made 275 B0 & 6 MCF in 25 hrs.
1-03-89 TP 300#, 10/64" ck, made 275 B0 & 6 MCF in 24-3/4 hrs.
1-04-89 TP 300#, 10/64" ck, made 264 B0 & 6 MCF in 23 hrs.
1-05-89 TP 300#, 10/64" ck, made 264 B0 & 6 MCF in 24½ hrs.
1-06-89 TP 300#, 10/64" ck, made 267 B0 & 6 MCF in 24 hrs.
1-07-89 TP 290#, 10/64" ck, made 286 B0 & 6 MCF in 26 hrs.
1-08-88 TP 290#, 10/64" ck, made 227 B0 & 6 MCF in 21 hrs.
1-09-88 TP 290#, 10/64" ck, made 264 B0 & 6 MCF in 25 hrs. (SI 1 hr to chg over to heater treater. Did a 1 hr pressure build-up test).
1-10-89 TP 287#, 10/64" ck, made 248 B0 & 6 MCF in 24½ hrs. Balanced out heater treater.
1-11-89 TP 290#, 10/64" ck, made 259 B0 & 6 MCF in 23½ hrs.
1-12-89 TP 285#, 10/64" ck, made 285 B0 & 6 MCF in 24½ hrs.
1-13-89 TP 285#, 10/64" ck, made 241 B0 & 6 MCF in 23½ hrs.
1-14-89 TP 285#, 10/64" ck, made 286 B0 & 6 MCF in 26 hrs.
1-15-89 TP 285#, 10/64" ck, made 219 B0 & 6 MCF in 20½ hrs.
1-16-89 TP 285#, 10/64" ck, made 301 B0 & 6 MCF in 26 hrs.
1-17-89 TP 282#, 10/64" ck, made 275 B0 & 6 MCF in 24 hrs.
1-18-89 TP 280#, 10/64" ck, made 249 B0 & 6 MCF in 24 hrs.
1-19-89 TP 280#, 10/64" ck, made 283 B0 & 6 MCF in 25 hrs.
1-20-89 TP 285#, 10/64" ck, made 285 B0 & 6 MCF in 24 hrs.

HOLMSTROM FEDERAL #1
Sec. 9, T-14-S, R-29-E
1980' FSL & 1980' FEL
Chaves County, New Mexico
Proposed TD 10,000'
Wildcat Devonian

DAILY DRILLING REPORT

11-17-88 TP 325#, 10/64" ck, made 330 BO & 6 MCF in 24 hrs. Sm amt of emulsion.
11-18-88 TP 320#, 10/64" ck, made 276 BO & 6 MCF in 22½ hrs. Sm amt of emulsion.
11-19-88 TP 320#, 10/64" ck, made 309 BO & 6 MCF in 25½ hrs. Sm amt of emulsion.
11-20-88 TP 315#, 10/64" ck, made 253 BO & 6 MCF in 21 hrs. Sm amt of emulsion.
11-21-88 TP 315#, 10/64" ck, made 330 BO & 6 MCF in 28 hrs. Sm amt of emulsion.
11-22-88 TP 310#, 10/64" ck, made 275 BO & 6 MCF in 21½ hrs. Sm amt of emulsion.
11-23-88 TP 310#, 10/64" ck, made 275 BO & 6 MCF in 24 hrs. Sm amt of emulsion.
11-24-88 TP 310#, 10/64" ck, made 281 BO & 6 MCF in 23½ hrs. Sm amt of emulsion.
11-25-88 TP 310#, 10/64" ck, made 243 BO & 6 MCF in 26½ hrs. "
11-26-88 TP 310#, 10/64" ck, made 226 BO & 6 MCF in 21 hrs.
11-27-88 TP 310#, 10/64" ck, made 292 BO & 6 MCF in 27 hrs.
11-28-88 TP 310#, 10/64" ck, made 299 BO & 6 MCF in 23 hrs.
11-29-88 TP 310#, 10/64" ck, made 275 BO & 6 MCF in 24 hrs.
11-30-88 TP 310#, 10/64" ck, made 265 BO & 6 MCF in 23½ hrs.
12-01-88 TP 310#, 10/64" ck, made 264 BO & 6 MCF in 24 hrs.
12-02-88 TP 310#, 10/64" ck, made 259 BO & 6 MCF in 23½ hrs.
12-03-88 TP 310#, 10/64" ck, made 314 BO & 6 MCF in 24½ hrs.
12-04-88 TP 310#, 10/64" ck, made 270 BO & 6 MCF in 23½ hrs.
12-05-88 TP 310#, 10/64" ck, made 264 BO & 6 MCF in 21-3/4 hrs.
12-06-88 TP 310#, 10/64" ck, made 252 BO & 6 MCF in 21½ hrs.
12-07-88 TP 310#, 10/64" ck, made 283 BO & 6 MCF in 26 hrs.
12-08-88 TP 310#, 10/64" ck, made 312 BO & 6 MCF in 26 hrs.
12-09-88 TP 310#, 10/64" ck, made 231 BO & 6 MCF in 22½ hrs.
12-10-88 SI due to weather (trucks unable to get to location - oil tanks full).
12-11-88 SI due to weather. When opened well TP 340#.
12-12-88 TP 315#, 10/64" ck, made 231 BO & 6 MCF in 21 hrs.
~~12-13-88 TP 330#, 10/64" ck, made 336 BO & 6 MCF in 27 hrs.~~
12-14-88 TP 330#, 10/64" ck, made 252 BO & 6 MCF in 21½ hrs.
12-15-88 TP 330#, 10/64" ck, made 318 BO & 6 MCF in 26 hrs.
12-16-88 TP 320#, 10/64" ck, made 308 BO & 6 MCF in 25½ hrs.
12-17-88 TP 320#, 10/64" ck, made 241 BO & 6 MCF in 20½ hrs.
12-18-88 TP 320#, 10/64" ck, made 253 BO & 6 MCF in 22 hrs.
12-19-88 TP 320#, 10/64" ck, made 323 BO & 6 MCF in 27 hrs.

HULMSTROM FEDERAL #1
Sec. 9, T-14-S, R-29-E
1980' FSL & 1980' FEL
Chaves County, New Mexico
Proposed TD 10,000'
Wildcat Devonian

DAILY DRILLING REPORT

10-19-88 TP 340#, 10/64" ck, made 286 BO & 6 MCF in 24½ hrs. Sm amt of emulsion.
10-20-88 TP 335#, 10/64" ck, made 286 BO & 6 MCF in 24 hrs. Sm amt of emulsion.
10-21-88 TP 335#, 10/64" ck, made 275 BO & 6 MCF in 23½ hrs. Sm amt of emulsion.
10-22-88 TP 335#, 10/64" ck, made 369 BO & 6 MCF in 28 hrs. Sm amt of emulsion.
10-23-88 TP 335#, 10/64" ck, made 220 BO & 6 MCF in 21 hrs. Sm amt of emulsion.
10-24-88 TP 335#, 10/64" ck, made 314 BO & 6 MCF in 26 hrs. Sm amt of emulsion.
10-25-88 TP 330#, 10/64" ck, made 290 BO & 6 MCF in 22½ hrs. Sm amt of emulsion.
10-26-88 TP 330#, 10/64" ck, made 275 BO & 6 MCF in 24 hrs. Sm amt of emulsion.
10-27-88 TP 330#, 10/64" ck, made 299 BO & 6 MCF in 24 hrs. Sm amt of emulsion.
10-28-88 TP 330#, 10/64" ck, made 299 BO & 6 MCF in 24 hrs. Sm amt of emulsion.
10-29-88 TP 330#, 10/64" ck, made 308 BO & 6 MCF in 25 hrs. Sm amt of emulsion.
10-30-88 TP 330#, 10/64" ck, made 286 BO & 6 MCF in 26 hrs. Sm amt of emulsion.
10-31-88 TP 330#, 10/64" ck, made 286 BO & 6 MCF in 23 hrs. Sm amt of emulsion.
11-01-88 TP 330#, 10/64" ck, made 275 BO & 6 MCF in 22½ hrs. Sm amt of emulsion.
11-02-88 TP 330#, 10/64" ck, made 236 BO & 6 MCF in 25½ hrs. Sm amt of emulsion.
11-03-88 TP 330#, 10/64" ck, made 269 BO & 6 MCF in 24 hrs. Sm amt of emulsion.
11-04-88 TP 330#, 10/64" ck, made 292 BO & 6 MCF in 24 hrs. Sm amt of emulsion.
11-05-88 TP 330#, 10/64" ck, made 275 BO & 6 MCF in 24 hrs. Sm amt of emulsion.
11-06-88 TP 330#, 10/64" ck, made 309 BO & 6 MCF in 24-3/4 hrs. Sm amt of emulsion.
11-07-88 TP 330#, 10/64" ck, made 325 BO & 6 MCF in 26½ hrs. Sm amt of emulsion.
11-08-88 TP 330#, 10/64" ck, made 303 BO & 6 MCF in 24½ hrs. Sm amt of emulsion.
11-09-88 TP 325#, 10/64" ck, made 254 BO & 6 MCF in 20½ hrs. Sm amt of emulsion.
11-10-88 TP 325#, 10/64" ck, made 275 BO & 6 MCF in 24 hrs. Sm amt of emulsion.
11-11-88 TP 325#, 10/64" ck, made 293 BO & 6 MCF in 24 hrs. Sm amt of emulsion.
11-12-88 TP 325#, 10/64" ck, made 299 BO & 6 MCF in 26½ hrs. Sm amt of emulsion.
11-13-88 TP 325#, 10/64" ck, made 292 BO & 6 MCF in 24 hrs. Sm amt of emulsion.
11-14-88 TP 325#, 10/64" ck, made 264 BO & 6 MCF in 22 hrs. Sm amt of emulsion.
11-15-88 TP 325#, 10/64" ck, made 309 BO & 6 MCF in 24½ hrs. Sm amt of emulsion.
11-16-88 TP 325#, 10/64" ck, made 267 BO & 6 MCF in 25 hrs. Sm amt of emulsion.

(FINAL DAILY REPORT - WELL TRANSFERRED TO PRODUCTION DEPT.
TO THE MONTHLY C-115 REPORT)

HOLMSTROM FEDERAL #1
Sec. 9, T-14-S, R-29-E
1980' FSL & 1980' FEL
Chaves County, New Mexico
Proposed TD 10,000'
Wildcat Devonian

DAILY DRILLING REPORT

9-24-88 TP 500#, 8/64" ck, made 242 BO, 4.5 MCF & no wtr in 22½ hrs.

9-25-88 TP 500#, 8/64" ck, made 266 BO, 4 MCF & no wtr in 24½ hrs.

9-26-88 TP 500#, 8/64" ck, made 253 BO, 4 MCF & no wtr in 24 hrs.

9-27-88 TP 500#, 8/64" ck, made 254 BO, 4 MCF & no wtr in 23½ hrs.

9-28-88 TP 500#, 8/64" ck, made 253 BO, 4 MCF & no wtr in 22 hrs (8AM on 9-27-88). Tefteller, Inc. collected fl samples for resevoir fluid analysis. Ran BHP. Flowed well 2 hrs on 10/64" ck, FTP 400 psi, made 27.3 BO, no wtr in 2 hrs. Flowing well 4 hrs on 12/64" ck, FTP 290 psi, 67.1 BO, no wtr in 4 hrs. Calculated 24 hrs: 403 BOPD, 13.8 MCFPD, GOR 34-1. Return to 10/64" ck @ 5:45 PM for extended flow test.

9-29-88 TP 400#, 10/64" ck, made 320 BO, 5.8 MCF & no wtr in 23½ hrs.

9-30-88 TP 375-380#, 10/64" ck, made 322 BO, 5 MCF & no wtr in 24 hrs.

10-01-88 TP 360-380#, 10/64" ck, made 313 BO, 5 MCF & no wtr in 24 hrs.

10-02-88 TP 360#, 10/64" ck, made 323 BO, 4.6 MCF & no wtr in 24½ hrs.

10-03-88 TP 360#, 10/64" ck, made 53 BO in tanks (unknown amount in pit because of malfunction in valve on seperator), 4 MCF & no wtr in 24 hrs.

10-04-88 TP 360#, 10/64" ck, made 248 BO, 4 MCF & no wtr in 23 hrs.

10-05-88 TP 360-375#, 10/64" ck, made 300 BO, 4.5 MCF & no wtr in 23 hrs.

10-06-88 TP 360#, 10/64" ck, made 280 BO, 4.5 MCF & no wtr in 22 hrs.

10-07-88 TP 350-360#, 10/64" ck, made 260 BO, 6 MCF & no wtr in 20½ hrs.

10-08-88 TP 355#, 10/64" ck, made 294 BO, 6 MCF & no wtr in 22-3/4 hrs.

10-09-88 TP 345#, 10/64" ck, made 294 BO, 6 MCF & no wtr in 24½ hrs.

10-10-88 TP 345#, 10/64" ck, made 308 BO, 6 MCF & no wtr in 24½ hrs.

10-11-88 TP 345#, 10/64" ck, made 350 BO, 6 MCF & no wtr in 25½ hrs.

10-12-88 Emulsion contained approximately 2% wtr. SI @ 11 AM on 10-10-88 for chemical & water analysis.

10-13-88 SI

10-14-88 TP 370#, 10/64" ck, made 279 BO & 6 MCF in 21 hrs. Well is still producing an emulsion (since Sunday, Oct 9th) that contains 2-5% water.

10-15-88 TP 360#, 10/64" ck, made 275 BO & 6 MCF in 24 hrs. Small amount of emulsion continues with approximately 1½% water.

10-16-88 TP 345#, 10/64" ck, made 302 BO & 6 MCF in 23 hrs. Sm amt of emulsion.

10-17-88 TP 340#, 10/64" ck, made 346 BO & 6 MCF in 27 hrs. Sm amt of emulsion.

10-18-88 TP 340#, 10/64" ck, made 297 BO & 6 MCF in 23½ hrs. Sm amt of emulsion.

HOLMSTROM FEDERAL #1
Sec. 9, T-14-S, R-29-E
1980' FSL & 1980' FEL
Chaves County, New Mexico
Proposed TD 10,000'
Wildcat Devonian

"CONFIDENTIAL"

DAILY DRILLING REPORT

9-12-88 SITP 700 psi. Open to tks @ 9 AM on 6/64" positive ck. At 11 AM flowing 6 BOPH w/no wtr. TP 610 psi. Testing to tks.

9-13-88 9:30 AM (9-12-88) ck 6/64", TP 610 psi, made 154.6 B0 in 24½ hrs, no wtr, 5 MCFPD. SI & change bonnett on tree & open on 8/64" ck @ 10:15 AM (9-12-88). Making 11 BOPH, TP 500#.

9-14-88 TP 500#, 8/64" ck, made 259 B0 & 4 MCF in 24 hrs (from 10:15 AM on 9-12-88 to 10:15 AM on 9-13-88)

9-15-88 TP 500#, 8/64" ck, made 257 B0, 4 MCF & no wtr in 24 hrs. (9/13-9/14 @ 10:15 AM).

9-16-88 TP 500#, 8/64" ck, made 257 B0, 4 MCF & no wtr in 24 hrs. (9/14-9/15 @ 10:15 AM).

9-17-88 TP 500#, 8/64" ck, made 260 B0, 4 MCF & no wtr in 24 hrs.

9-18-88 TP 500#, 8/64" ck, made 261 B0, 4 MCF & no wtr in 24 hrs.

9-19-88 TP 500#, 8/64" ck, made 258 B0, 4 MCF & no wtr in 24 hrs.

9-20-88 TP 500#, 8/64" ck, made 259 B0, 4 MCF & no wtr in 24 hrs.

9-21-88 TP 500#, 8/64" ck, made 251 B0, 4 MCF & no wtr in 23½ hrs.

9-22-88 TP 500#, 8/64" ck, made 265 B0, 4 MCF & no wtr in 24½ hrs.

9-23-88 TP 500#, 8/64" ck, made 271 B0, 4 MCF & no wtr in 25 hrs.

RESERVOIR SIMULATION RESULTS

North King Camp (Devonian) Field Chaves Co., New Mexico

Time (days)	Layer	Thickness (ft)	Cumulative Oil (MBBL)	Cumulative Water (MBBL)	Average BHP (psi)	Average Water Sat. (%)	Producing Well
0 (9-1-88)	1	11	0	0	3941	20.0	Deemar
	2	41	0	0	3949	20.1	
	3	30	0	0	3961	20.4	Holmstrom
	4	30	0	0	3971	25.5	
	5	39	0	0	3982	28.2	
				0	0		
420 (11-1-89)	1	11	7	0	3940	20.0	Deemar
	2	41	0	0	3948	20.1	
	3	30	0	0	3960	20.2	Holmstrom
	4	30	102	1	3920	24.5	
	5	39	0	0	3981	29.4	
				109	1		
570	1	11	84	0	3935	20.0	Deemar
	2	41	0	0	3944	20.0	
	3	30	74	1	3957	20.5	Holmstrom
	4	30	102	1	3966	24.0	
	5	39	0	0	3978	32.1	
				260	2		
750	1	11	177	0	3932	20.0	Deemar
	2	41	0	0	3942	20.0	
	3	30	124	14	3954	20.0	Holmstrom
	4	30	102	1	3964	23.5	
	5	39	0	0	3977	34.2	
				403	15		

BEFORE THE
OIL CONSERVATION COMMISSION
Santa Fe, New Mexico

Case No. 4617 4617 4617 4617 Exhibit No. 19

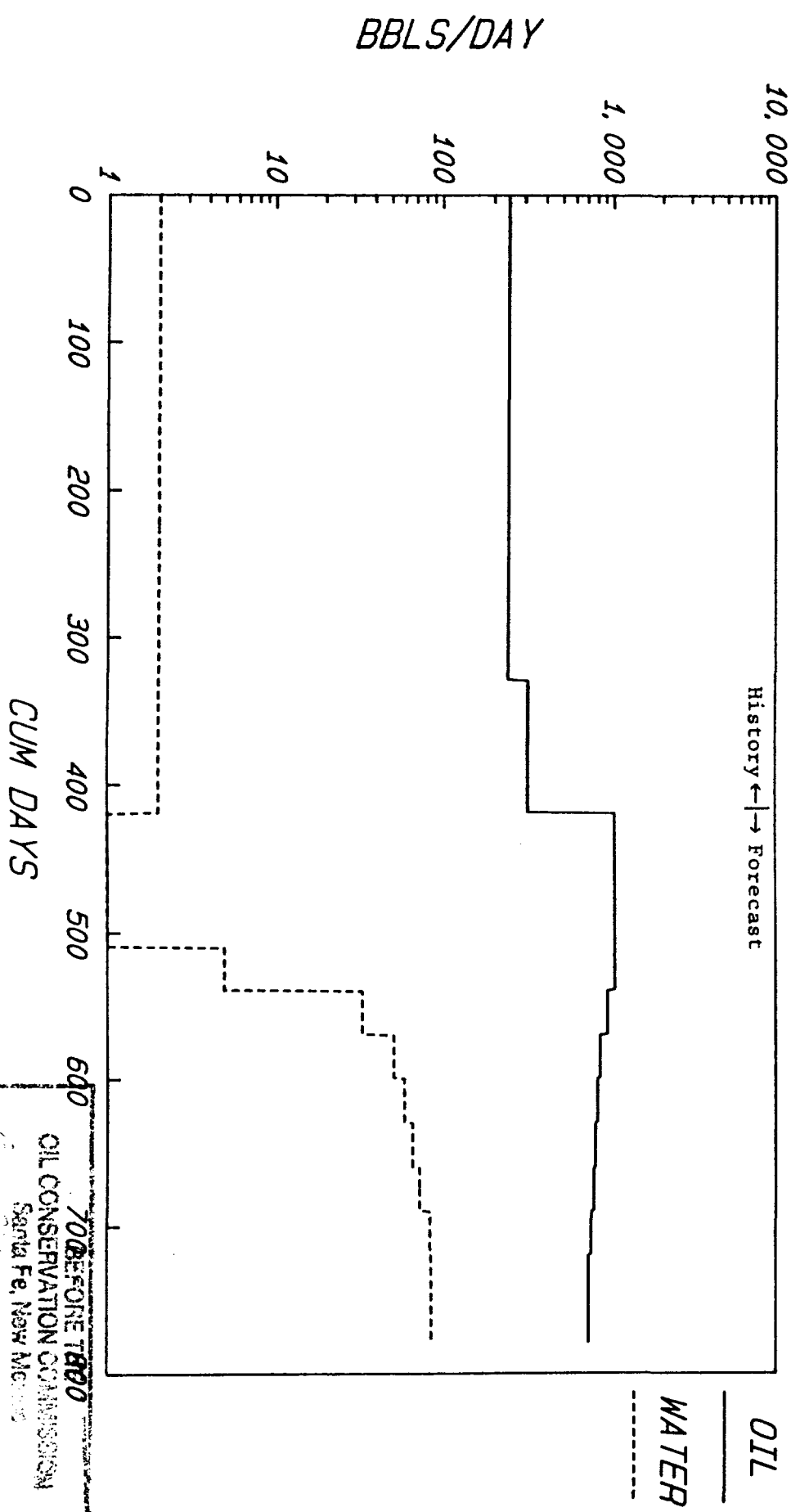
Submitted by 1/17/1989

Hearing Date 10/19/89

RESERVOIR SIMULATION PROJECTION

KING CAMP, N (DEVONIAN)

CHAVES COUNTY, NM

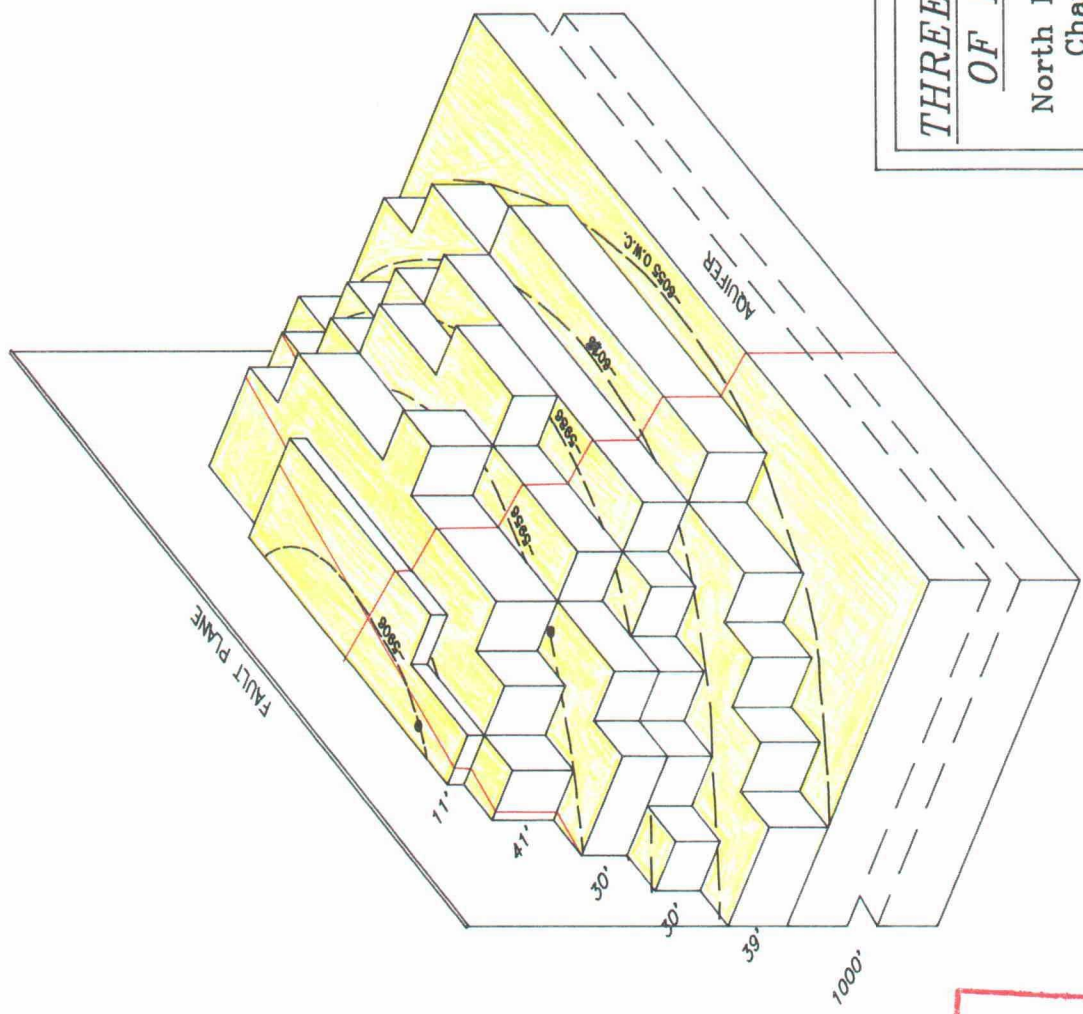


OIL CONSERVATION COMMISSION
 SANTA FE, NEW MEXICO

Case No. 2007-0011 EXHIBIT 1A

Submitted by Mason A.

Hearing Date 12/11/07



**THREE DIMENSIONAL VIEW
OF RESERVOIR MODEL**

North King Camp (Devonian) Field
Chaves County, New Mexico

Horizontal Scale is 1/10 of Vertical Scale

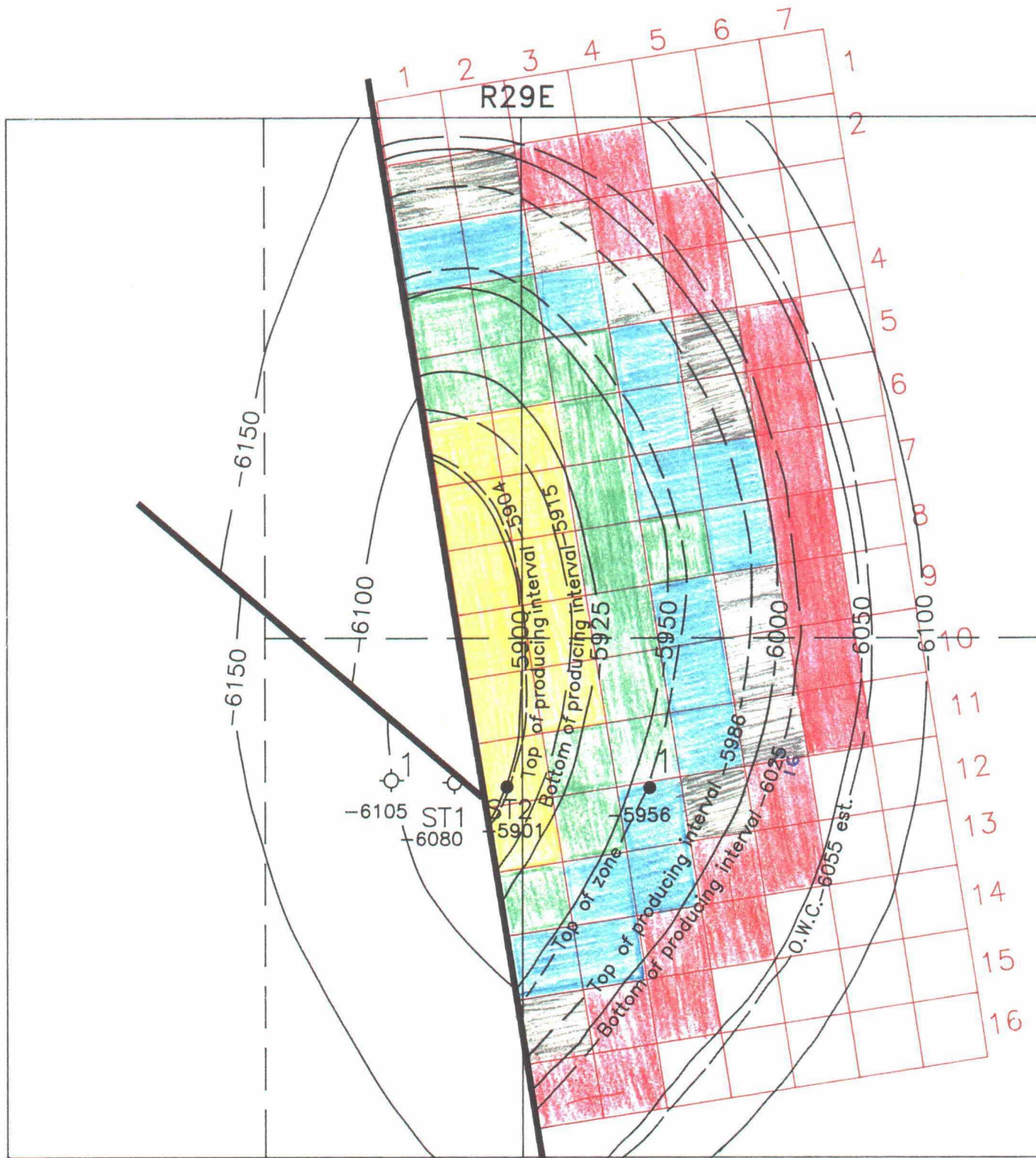
T. SCOTT HICKMAN & ASSOCIATES, INC.
PETROLEUM ENGINEERS

**BEFORE THE
OIL CONSERVATION COMMISSION**
Santa Fe, New Mexico

Case No. 9619, 9670 Exhibit No. 17

Submitted by HICKMAN

Hearing Date 10/19/89



North King Camp
 Chaves Co., New Mexico
DEVONIAN
STRUCTURE MAP
 Map Scale
 Date: 10-16-89
 0 1000'
T. SCOTT HICKMAN & ASSOCIATES, INC.
 PETROLEUM CONSULTANTS

BEFORE THE
OIL CONSERVATION COMMISSION
 Santa Fe, New Mexico
 Case No. 9617, 9670, 9697 Exhibit No. 16
 Submitted by HICKMAN
 Hearing Date 10/19/89

T14S

R29E

ST1
-6105
-6080

ST2
-5901
-5956

2
-6113

NORTH KING CAMP (DEVONIAN)

	<u>Total Recoverable Reserve BBLs</u>	<u>Per Cent</u>	<u>Total Standard Allowable</u>	<u>% Times Total Allowable</u>
Holmstrom SE/4	732,000	32.3	515	499
NE/4 Section 9	863,000	38.0	515	587
Deemar E/2W/2	674,000	29.7	515	459
TOTALS:	2,269,000	100.0%	1545 BO	1545 BO

BEFORE THE OIL CONSERVATION COMMISSION Santa Fe, New Mexico	
Case No. <u>9670</u>	Exhibit No. <u>15</u>
Submitted by <u>H. H. H. H. H.</u>	
Hearing Date <u>10/10/89</u>	

Comparison Of Cumulative Production
As Function Of Allowable
North King Camp (Devonian) Field
Chaves County, New Mexico

Time (Year)	Penalized Allowable		Top Allowable	
	Rate (BOPD)	Cumulative Production (MBBL)	Rate (BOPD)	Cumulative Production (MBBL)
1	34	12	515	188
2	34	25	515	376
3	34	37	515	564
4	34	50	515	752
5	34	62	515	940
6	34	74	515	1128
7	34	87	515	1316
8	34	99	515	1504
9	34	112	515	1692
10	34	124	515	1880

1128

1,670

BEFORE THE OIL CONSERVATION COMMISSION Santa Fe, New Mexico	
Case No. <u>9099</u>	Exhibit No. <u>14</u>
Submitted by <u>WILLIAM</u>	
Hearing Date <u>10/1/89</u>	

Description Of Numeric Simulator Used To Model Reservoir
North King Camp (Devonian) Field
Chaves County, New Mexico

Trade Name: PC - BOAST

Hardware: Sun 386i Engineering Workstation

Type of Simulator: Black Oil
3 - Dimensional
3 - Phase
Finite - Difference
Implicit Pressure-Explicit Saturation (IMPES)

Capability: Simulate oil and/or gas recovery by fluid expansion displacement, gravity drainage and capillary imbibition mechanism.

Dimensions: Individual Grid - 330' x 330' (2.5 ac)
Layer 1 - 12 Cells - 11' thick
Layer 2 - 27 Cells - 41' thick
Layer 3 - 43 Cells - 30' thick
Layer 4 - 54 Cells - 30' thick
Layer 5 - 75 Cells - 39' thick
Layer 6 - 112 Cells - 1000' thick (aquifer)

Reservoir Properties: Porosity = 7.0%
Water Saturation = 25.0% average (varies by height above OWC)
Permeability = 1000 md (vertically and horizontally)
Relative Permeability = Empirical correlation
PVT Data = Empirical correlation
Original Solution GOR = 40 SCF/BBL
Gas Gravity = 0.8
Oil Gravity = 46^o API
BHT = 145^o F

Volumetrics: OOIP = 6741 MBBL
Aquifer Volume = 1,940,323 MBBL

BEFORE THE OIL CONSERVATION COMMISSION Santa Fe, New Mexico	
Case No. <u>9617, 9618</u>	Exhibit No. <u>15</u>
Submitted by <u>Prokarian</u>	
Hearing Date <u>10/11/89</u>	

Bottom Hole Pressure Data
 North King Camp (Devonian) Field
 Chaves County, New Mexico

Well	Date	Type	Pressure @ -6000' (Psig)	Total Cumulative Production (MBBL)
Santa Fe-Holmstrom No. 1	8/88	DST	4012	0
	9/27/88	Build Up	3963	4
Stevens-Deemar-Fed No. 1	8/24/89	Build Up	3955	+88

Handwritten notes:
 10 July
 10/1/88
 10/1/88

Well Test Information
 North King Camp (Devonian) Field
 Chaves County, New Mexico

Well	Interval (TVD)	Date	Rate (BOPD)	Rate (BOPD)	GOR (SCF/BBL)	Choke (Inches)	FTP (Psi)
Santa Fe-Holmstrom No. 1	9728.0-58	9/28/88	403	0	35	NA	290
		11/24/88	287	10	21	NA	310
Stevens-Deemar-Fed No. 1		8/07/89	955	0	NA	12/64	320
			(4.5 Hrs)				
	9632.5-43	8/25/89	536	0	NA	12/64	320

PI = $\frac{536 \text{ BPD}}{3935.6 - 3704.0} = 2.31 \text{ BPD/Psi}$

BEFORE THE
 OIL CONSERVATION COMMISSION
 Santa Fe, New Mexico

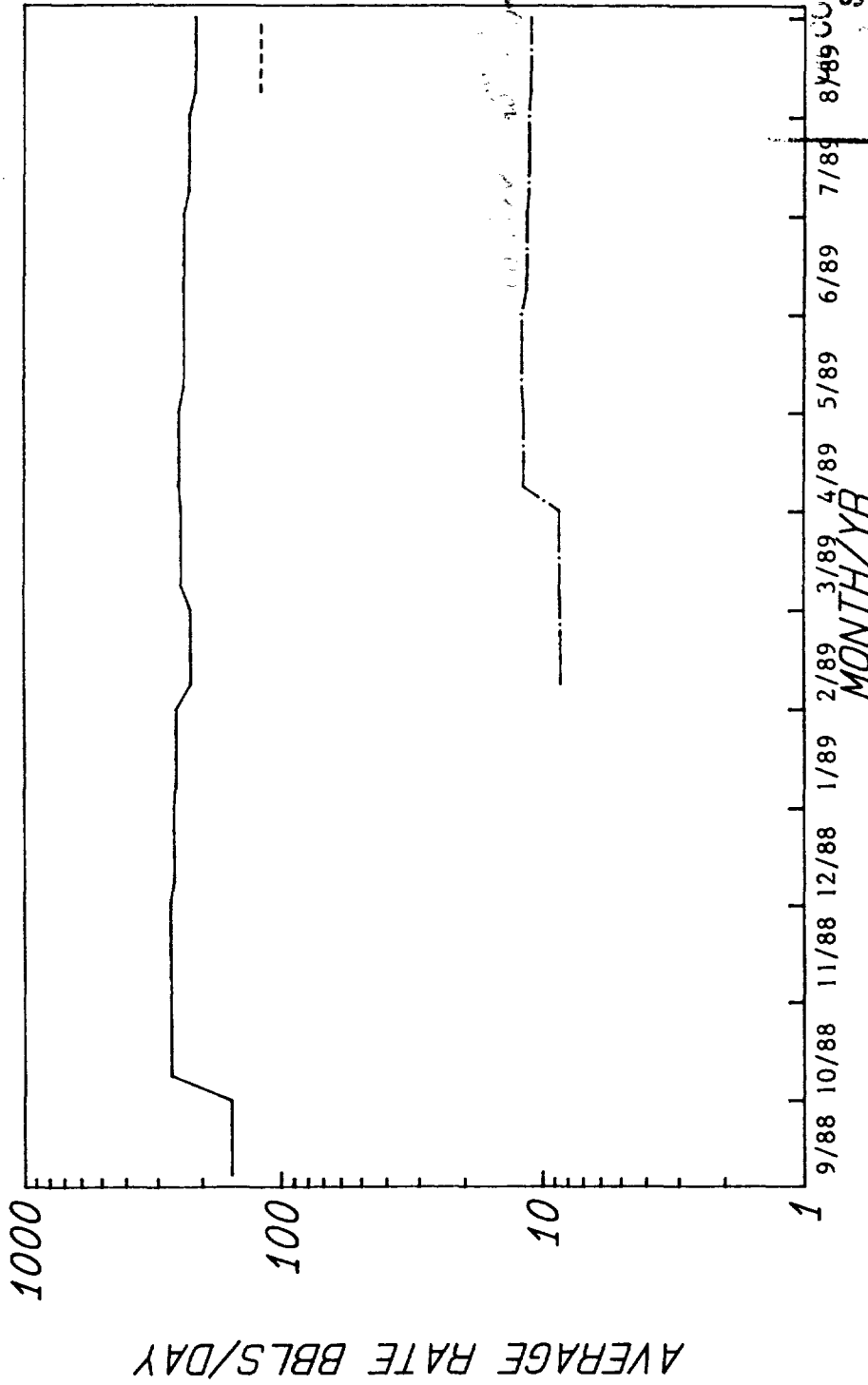
Case No. 1022 Exhibit No. 1

Submitted by ATKINSON

Dating Date 10/1/89

HOLMSTROM FED #1 & DEEMAR FED #1
KING CAMP, N (DEVONIAN)
CHAVES COUNTY, NM

6/2/89
110



HOLMSTROM FED #1
OIL

HOLMSTROM FED #1
WATER

DEEMAR FED #1
OIL

8/89 CONSERVATION COMMISSION
 Santa Fe, New Mexico

Case No. 9207-910 Exhibit No. 9

Submitted by FRANK

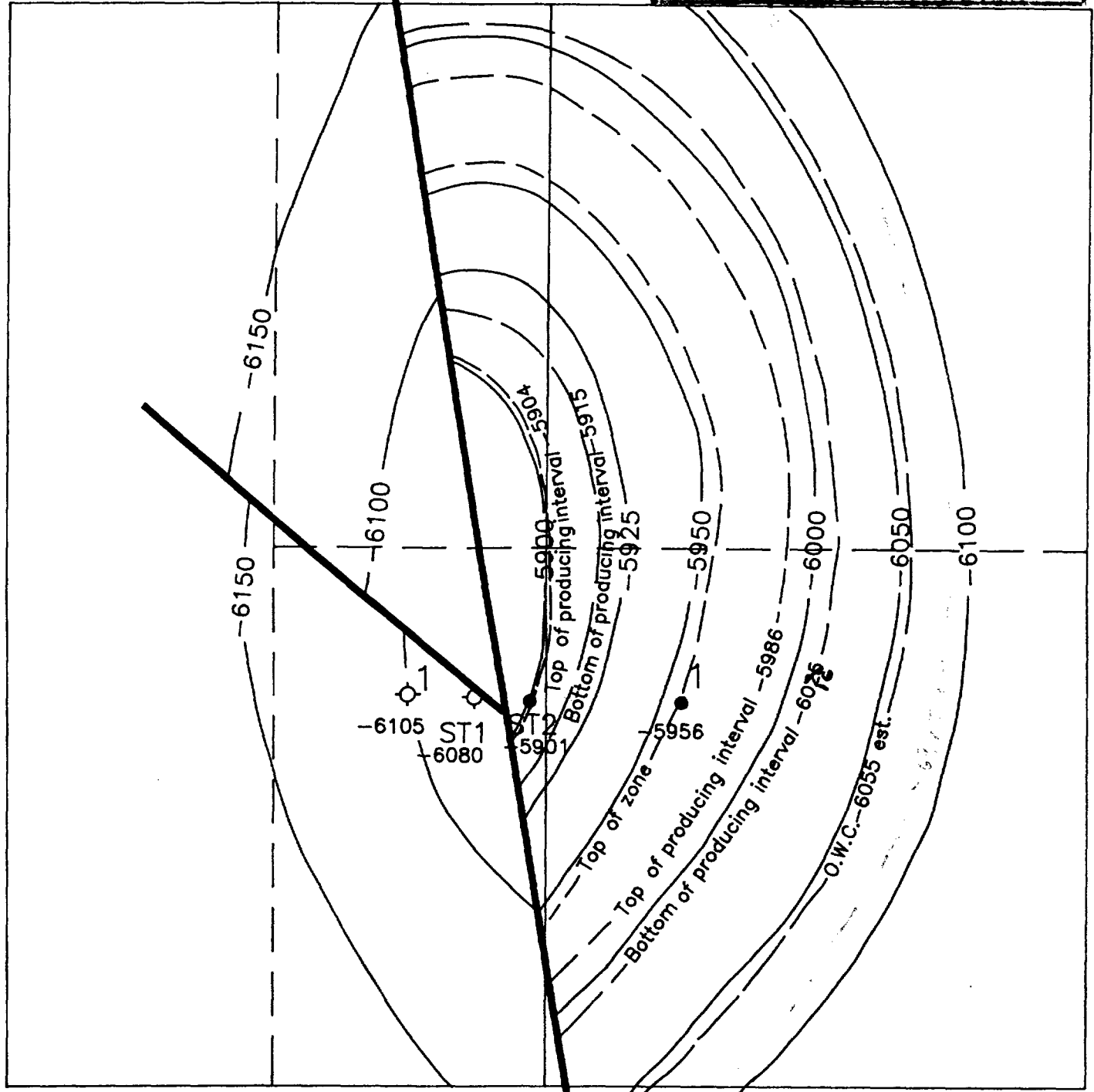
Hearing Date 10/11/89

Case No. 4679 Exhibit No. 10

Submitted by HICKMAN

Hearing Date 10/12/80

R29E



North King Camp
Chaves Co., New Mexico
DEVONIAN
STRUCTURE MAP
Map Scale

0 1000'

Date: 10-10-80

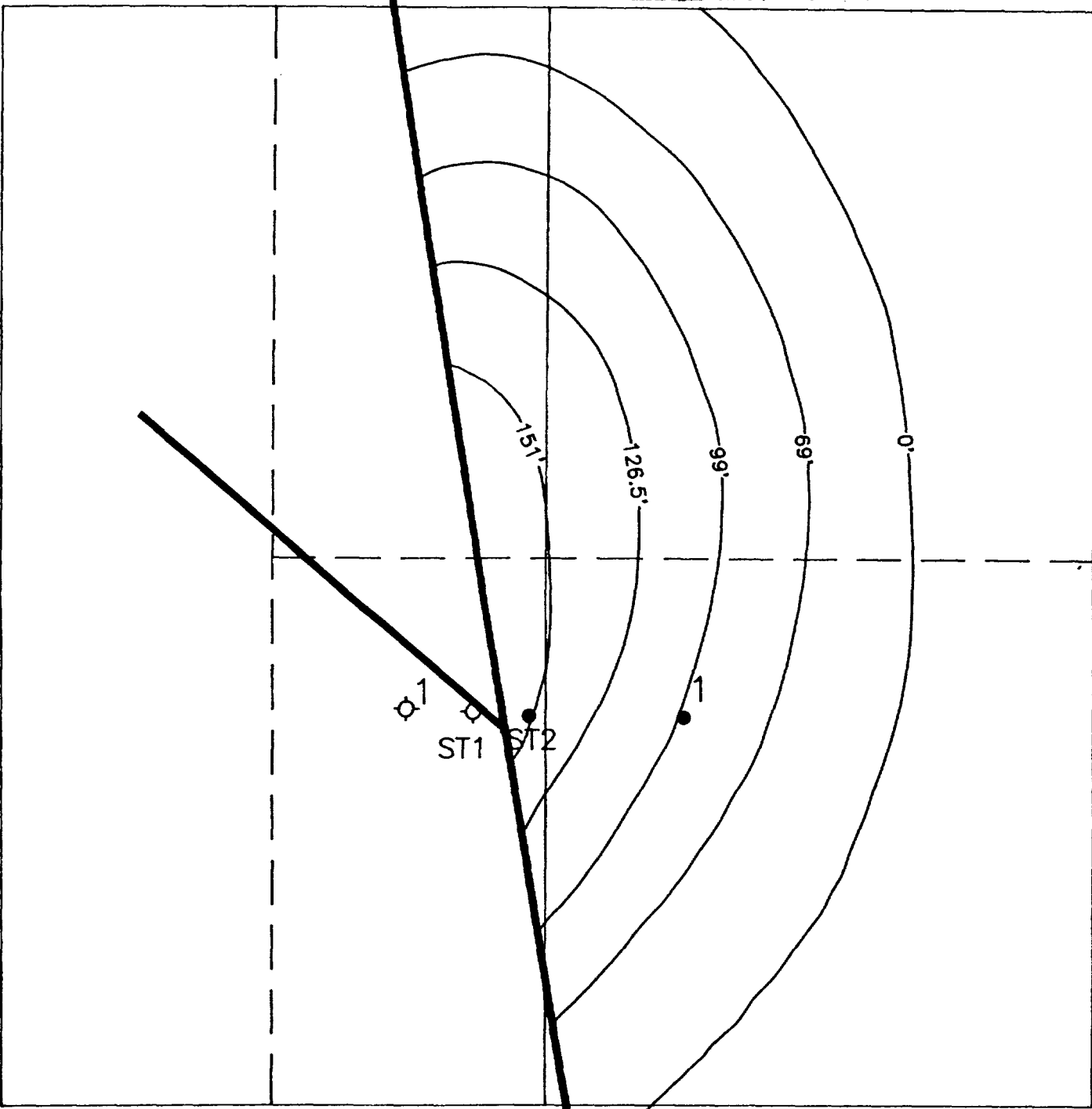
I. SCOTT HICKMAN & ASSOCIATES, INC.
GEOLOGICAL CONSULTANTS

Case No. 9670 Exhibit No. 11

Submitted by HERMAN

Hearing Date 10/29/89

R29E



North King Camp
Chaves Co., New Mexico

GROSS INTERVAL ISOPACH MAP

Map Scale

0 1000'

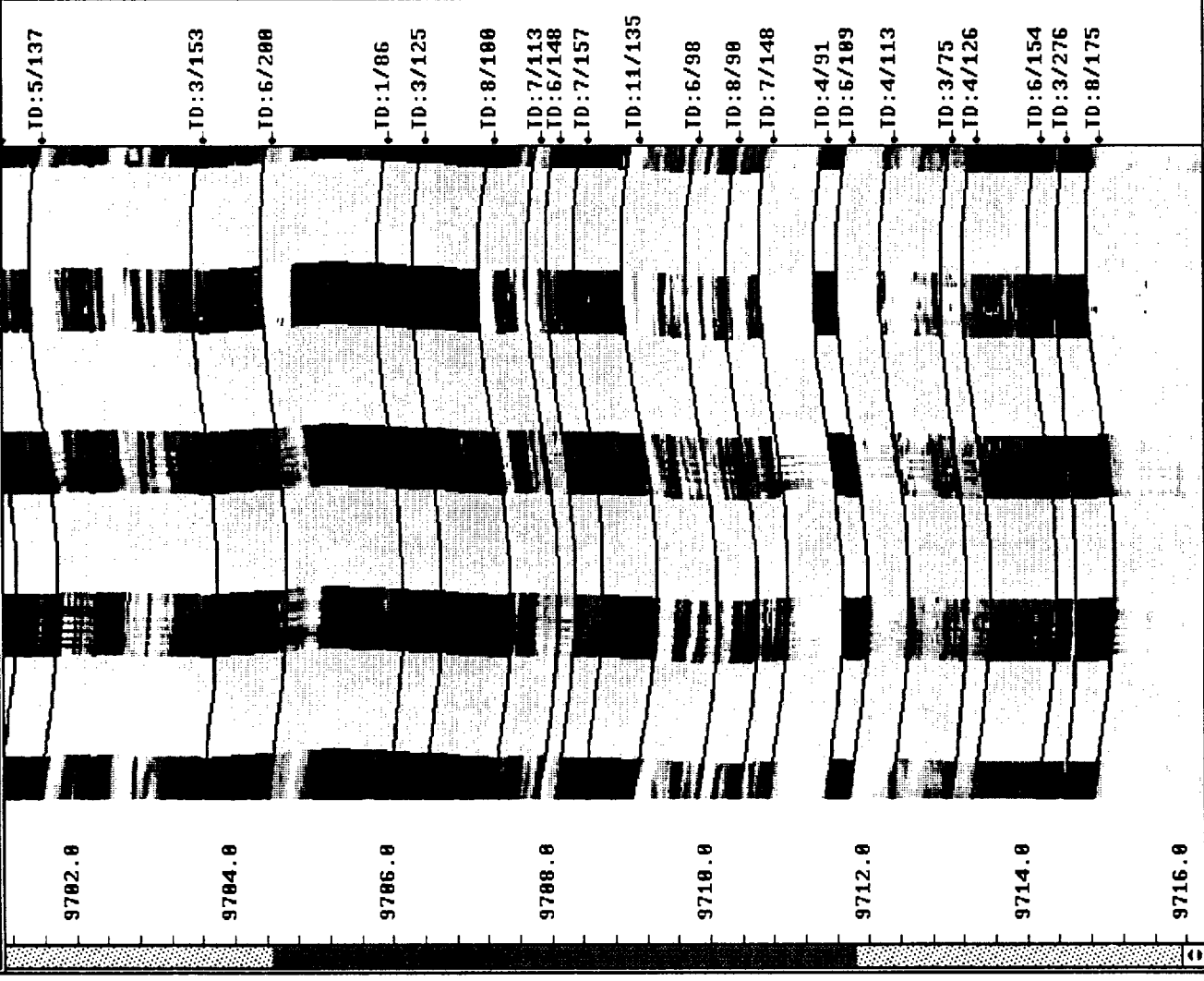
Date: 10-18-89

T. SCOTT HERMAN & ASSOCIATES, INC.
PETROLEUM CONSULTANTS

File browser

Display scale 1/20

0 30 60 90 120 150 180 210 240 270 300 330 360



define depth zone stop zone depth :9654.34 F
 reset depth zone start zone depth :9706.63 F

Zoning has been defined
 plot mode : C Azimuth directions
 38 dips processed for this plot

Dip types
 No type
 Cross_bed
 Fracture
 Fault
 Bed_boundary
 Unconformity
 Other

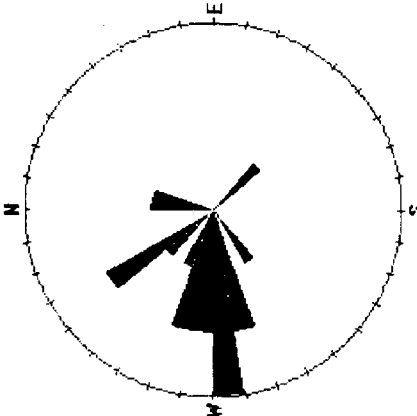
Plot Quit

BEFORE THE
OIL CONSERVATION COMMISSION
 Santa Fe, New Mexico
 9617 4678 Exhibit No. 7
 No. 9697
 filed by Ahler
 Hearing Date 10/19/89

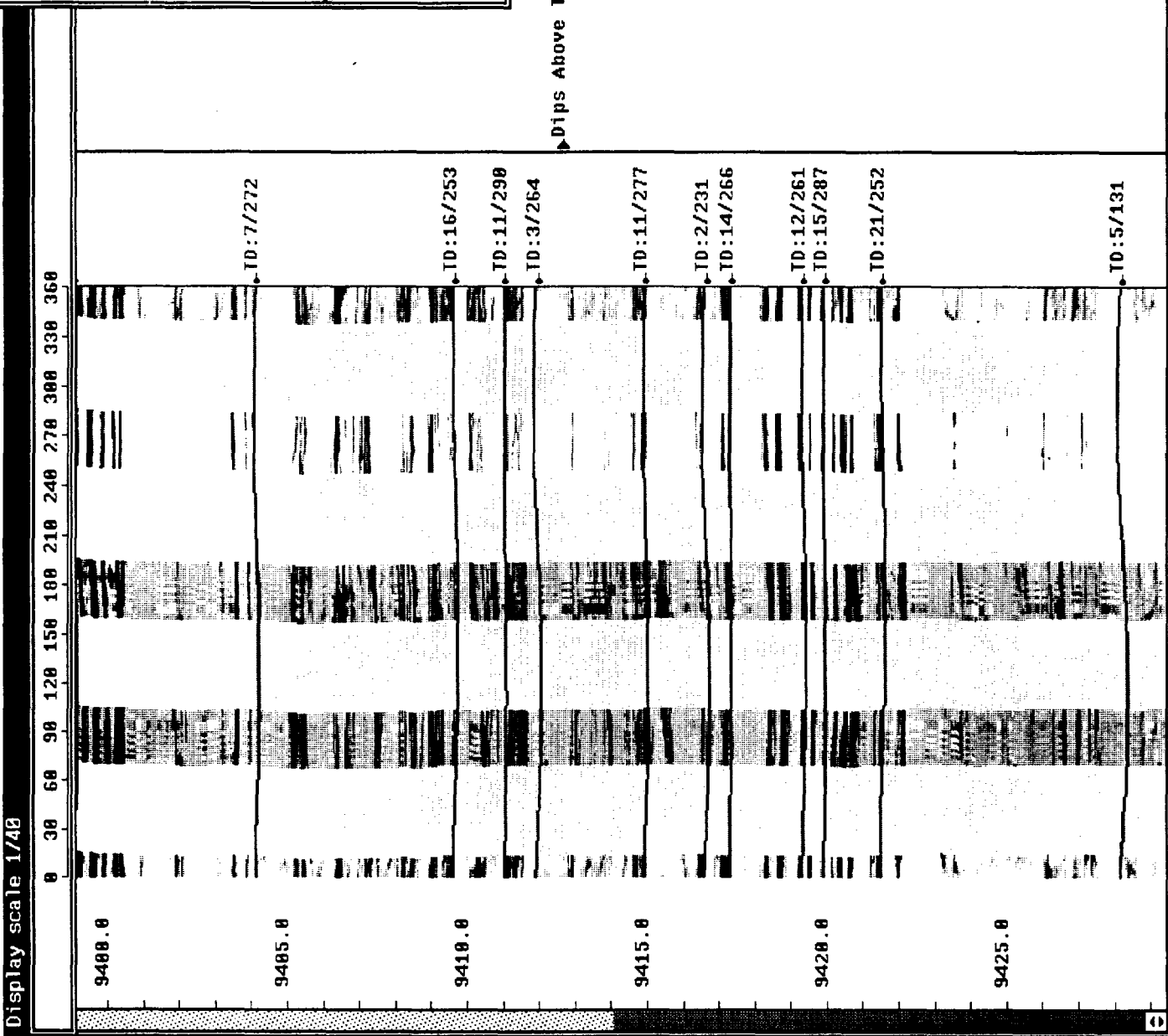
define depth zone :9395.15 F
 stop zone depth :9395.15 F
 reset depth zone :9454.20 F
 start zone depth :9454.20 F

Zoning has been defined
 plot mode : C Azimuth directions
 17 dips processed for this plot

- Dip types
- No type
 - Cross_bed
 - Fracture
 - Fault
 - Bed_boundary
 - Unconformity
 - Other



Plot Quit

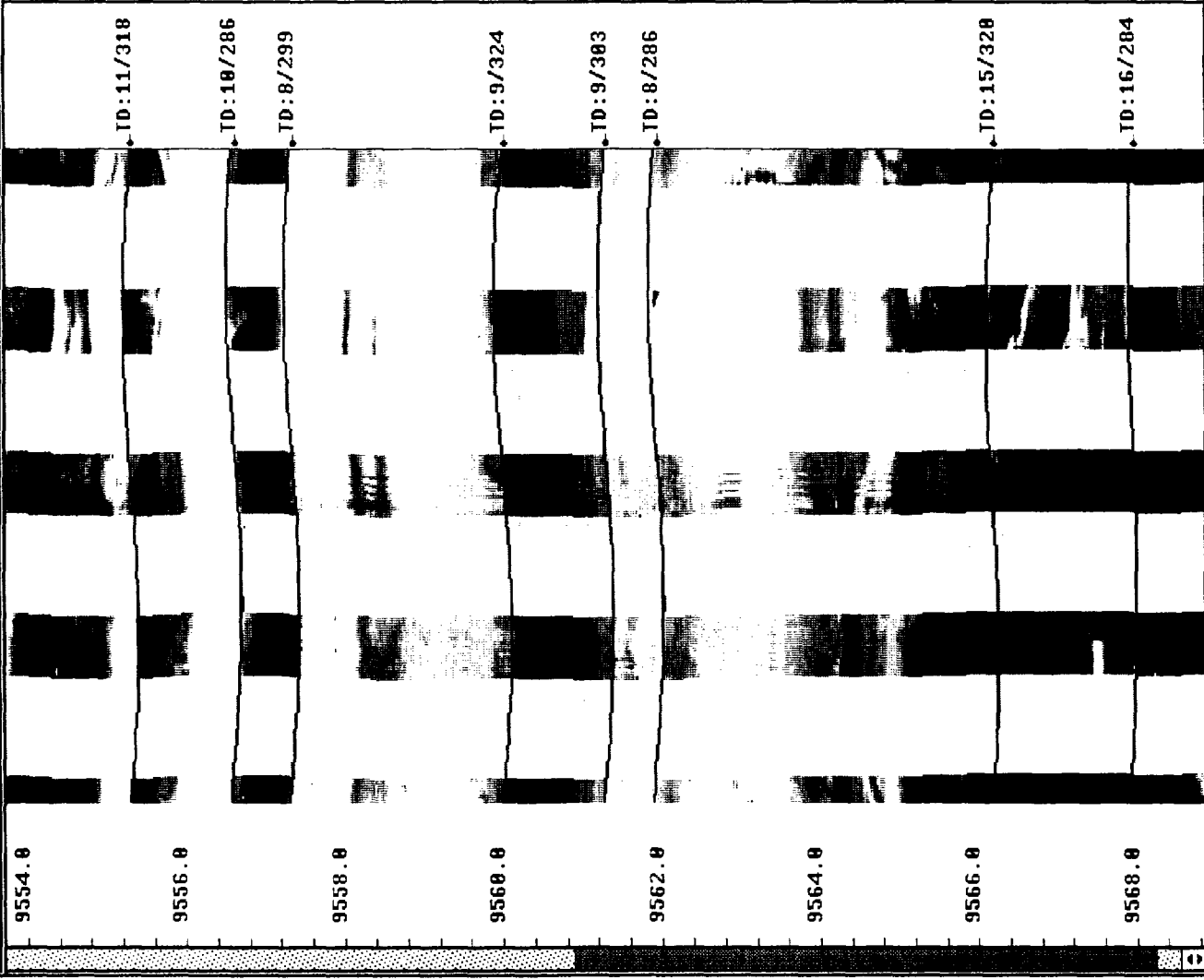


Display scale 1/40

File
by cursor

Display scale 1/20

0 30 60 90 120 150 180 210 240 270 300 330 360

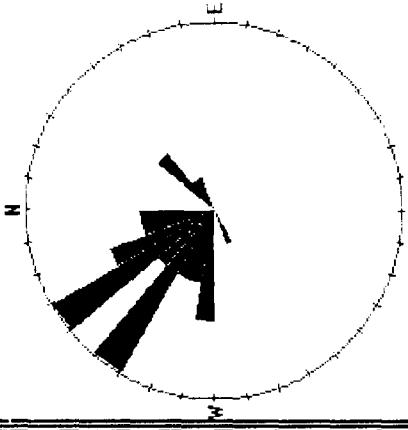


Dip of Beds Between the Faults

define depth zone
reset depth zone

stop zone depth :9466.37 F
start zone depth :9566.44 F

Zoning has been defined
plot mode : Azimuth directions
31 dips processed for this plot



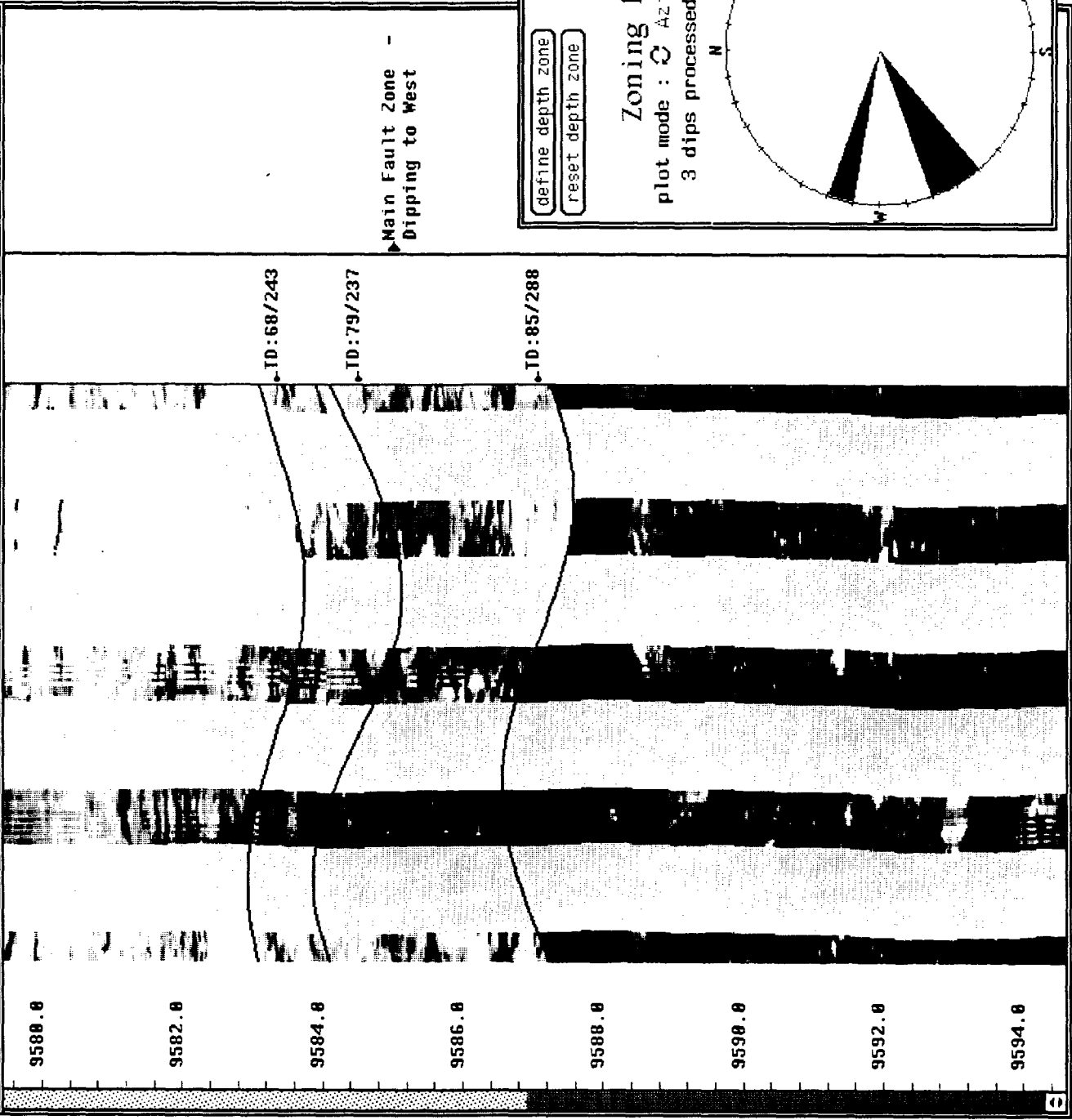
- Dip types
- No type
 - Cross_bed
 - Fracture
 - Fault
 - Bed_boundary
 - Unconformity
 - Other

Plot Quit

File
browser

Display scale 1/20

0 30 60 90 120 150 180 210 240 270 300 330 360



Main Fault Zone -
Dipping to West

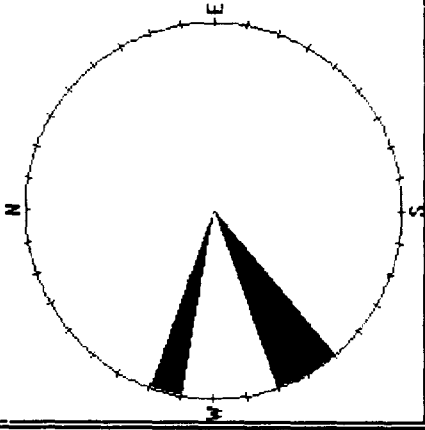
define depth zone
reset depth zone

stop zone depth : 9579.06 F
start zone depth : 9592.14 F

Zoning has been defined

plot mode : C Azimuth directions
3 dips processed for this plot

- Dip types
- No type
 - Cross_bed
 - Fracture
 - Fault
 - Bed_boundary
 - Unconformity
 - Other

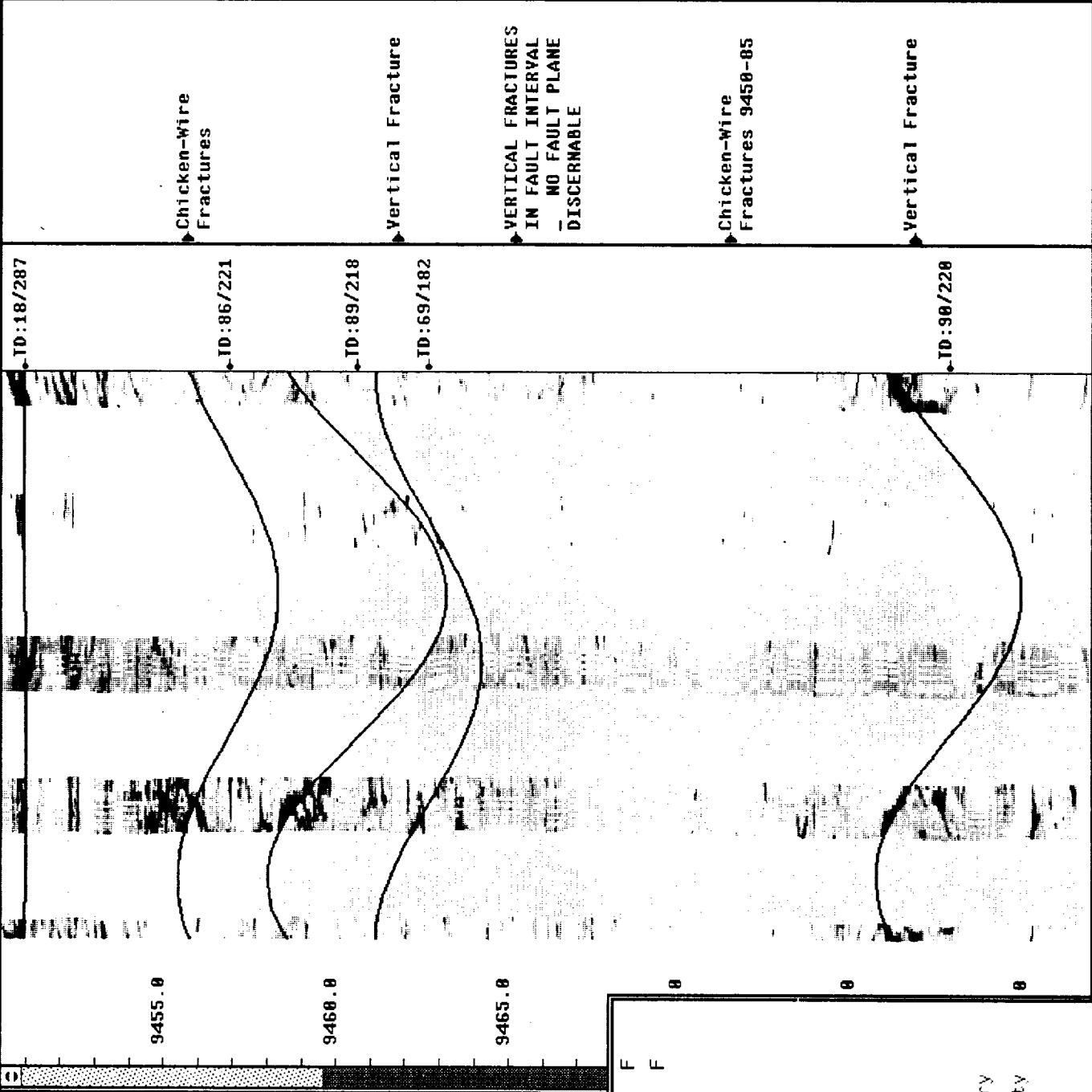


Plot Quit

E

File
browser

Display scale 1/40

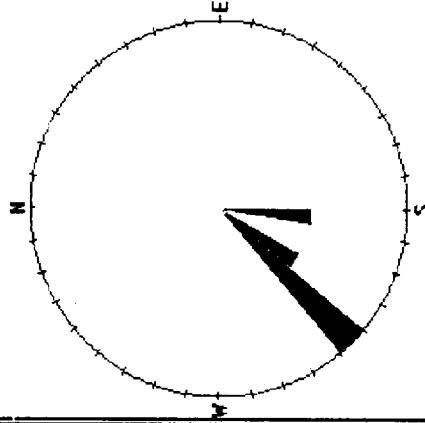


define depth zone stop zone depth :9443.38 F
 reset depth zone start zone depth :9480.80 F

Zoning has been defined

plot mode : C Azimuth directions
 4 dips processed for this plot

- Dip types
- No type
 - Cross_bed
 - Fracture
 - Fault
 - Bed_boundary
 - Unconformity
 - Other



Plot Quit

Using Formation MicroScanner* Images

REPRINTED FROM

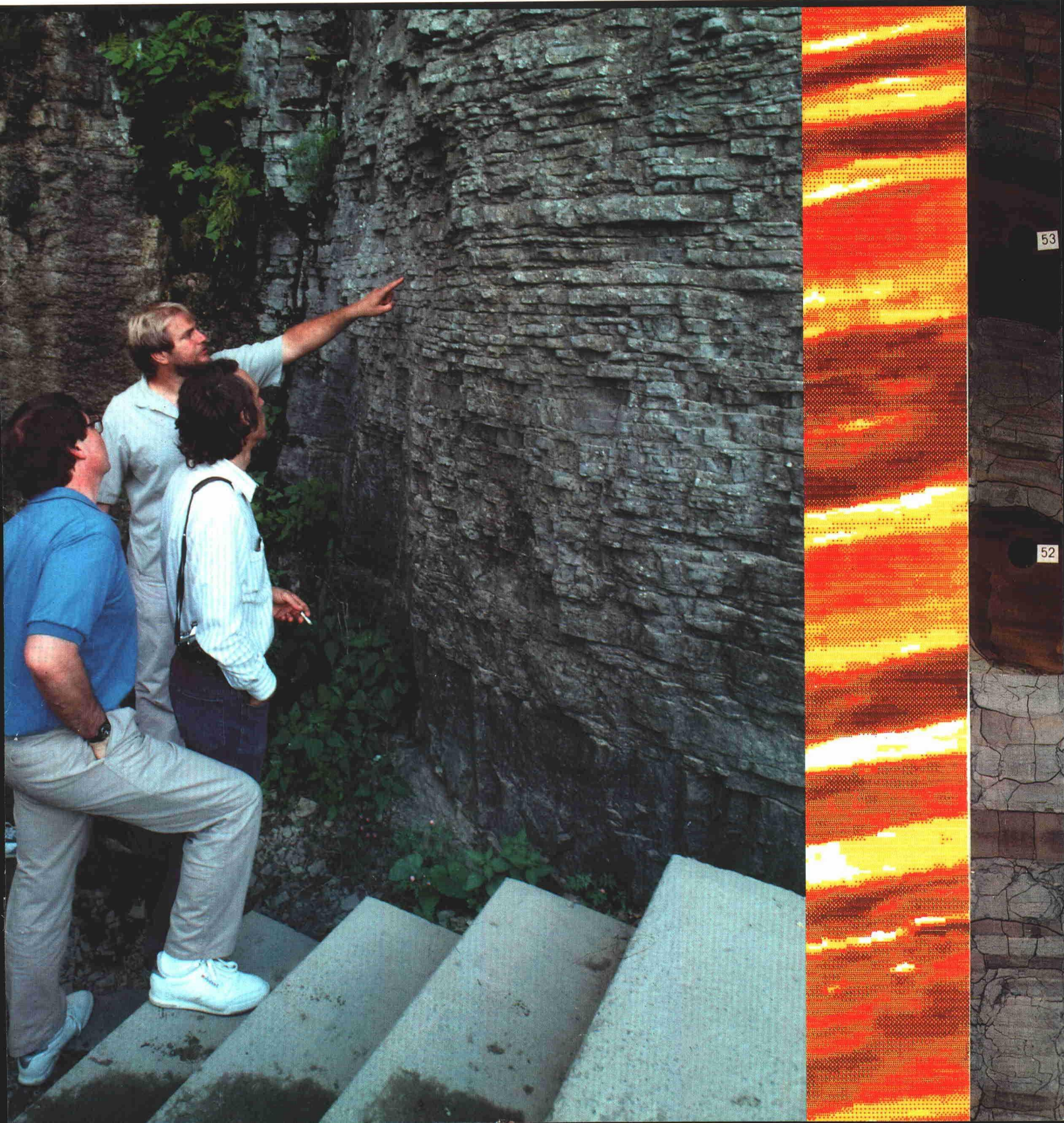
The Technical Review

Volume 37, no. 1 (January 1989): 16-40

BEFORE THE
OIL CONSERVATION COMMISSION
Santa Fe, New Mexico

Case No. 9617, 9670
9697 Exhibit No. 6
Submitted by Ahlen
Hearing Date 10/19/89

Schlumberger



Using Formation MicroScanner

Lawrence Bourke
Aberdeen, Scotland

Pierre Delfiner
Jean-Claude Trouiller
Clamart, France

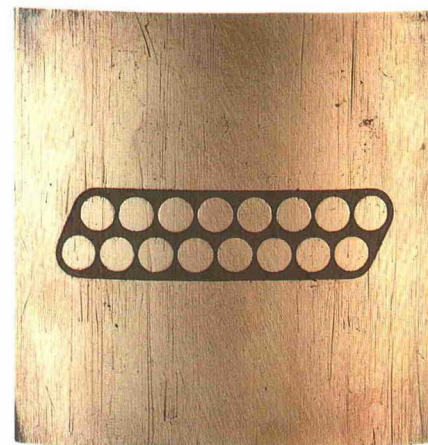
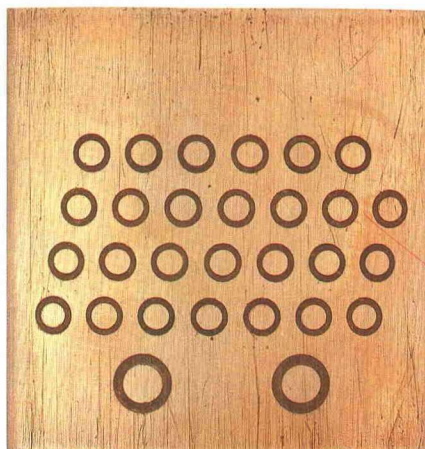
Tom Fett
Corpus Christi, Texas

The dream of the geologist is to shrink to a few inches and, with a strong flashlight, descend the wellbore to settle once and for all what the formation really looks like. To fulfill this dream, various devices were invented for imaging the borehole wall. Television cameras work sometimes, in relatively cool boreholes with clear drilling fluid. Such devices find use in corrosion detection. But to image the borehole wall in a typical oil well, the major advancement was the borehole televiewer [BHTV], developed 20 years ago by Mobil Oil Corp.¹

A second imaging device, the Formation MicroScanner [FMS] tool, caused a minor sensation when it hit the market about three years ago. It gave operators an alternative to the venerable BHTV, which creates an acoustic image of the borehole. Now they could image the borehole wall based on its electrical properties—a technique that complements the televiewer's acoustic image.²

This innovative technology spawned a new field of inquiry. To find a niche for electrical images, studies proliferated comparing Formation MicroScanner logs to cores, BHTV and other open hole logs; physicists refined their understanding of tool response, and engineers fine-tuned hardware and software.³

Today, after three years of commercial trial by fire and miles of logs, interpretation of Formation MicroScanner images is approaching a higher level of sophistication. This article covers some interpretation fundamentals and tips gathered as knowledge



□ Pads of four-pad (right) and two-pad Formation MicroScanner tools. The two-pad tool makes measurements from pads at right angles on a Dual Dipmeter* tool (also called the Stratigraphic High Resolution Dipmeter tool [SHDT]). The two large electrode buttons at the bottom make the dipmeter measurement; the 27 smaller electrodes make the image measurement. The four-pad design uses fewer buttons per pad due to telemetry and data processing constraints. The closer positioning of the buttons reduces saw-tooth effects from imperfect speed correction between button rows (see log, right). The four-pad tool, due to its greater borehole coverage (about 40 percent of an 8 1/2-inch hole, compared with 20 percent for the two-pad tool) takes less time to run because repeat passes are usually unnecessary. The two-pad tool has a slightly higher lateral resolution. Both pads measure about 3 1/4 inches square [≈8 cm²].

of tool response and application improves. To put interpretation in context, we begin by summarizing tool function and reviewing data processing as it bears on interpretation. The article also includes a Formation MicroScanner case study ("Gulf Coast case study: A marine transgressive sequence, wildcat well, South Texas," page 39.)

Tool Function

The Formation MicroScanner tool creates a picture of the borehole wall by mapping its resistivity using an array of small, pad-mounted button electrodes (hence *Micro*). These buttons examine successive small vertical increments of the formation (every 0.1 inch [2.5 millimeters], or 120 samples per electrode per foot) and lateral increments as the tool is pulled uphole (hence *Scanner*) (above). A triaxial accelerometer

permits determination of tool position, and three magnetometers allow determination of tool orientation.

The tool works basically the same way as the dipmeter. During logging, the lower section of the tool emits current into the formation. A portion of this current flows from the buttons on the pads, but the majority is used to focus the button current so that the tool has a moderately shallow depth of investigation and a high resolution (see table, page 31). The button current is recorded as a series of curves that represent relative changes in microresistivity caused by varying electrolytic conduction as a function of pore geometry, or by cation exchange on the surfaces of clays and other conductive minerals. These two effects produce varia-

For reviewing the manuscript for this article or supplying supporting material, thanks to Jean-Noël Antoine, Jean-Pierre Delhomme, Alain Dumont, Herve Ganem and Jean-Marie Lorre, Clamart, France; Ted Bornemann, Anchorage, Alaska; Yves Boutemy, Montrouge, France; Claudia J. Hackbarth, Shell Development Company, Houston; Bill Newberry, Dallas; Roy Nurmi, Dubai; Dick Plumb, Ridgefield, Connecticut; Jon Roestenburg, Jakarta; Gordy Shanor, Kuala Lumpur; and Jacques Tabanou, Houston.

Photos by Tony Bacchiochi

anner Images

Mike Grace
Dallas

Steian Luthi
Ridgefield, Connecticut

Oberto Serra
Montrouge, France

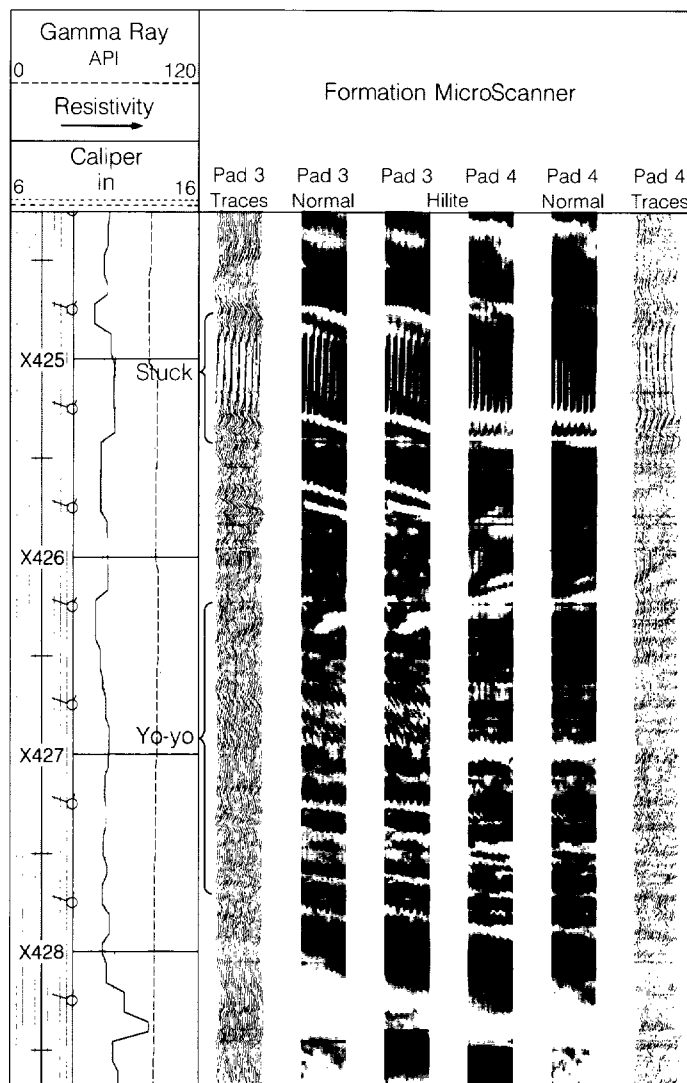
Eric Standen
Calgary, Alberta

tions on the images in response to porosity, grain size, mineralogy, cementation and fluid type. The current intensity measurements, which reflect the microresistivity variations, are converted to variable-intensity gray or color images (right). (The choice of black-and-white or color output is a matter of personal preference. For some, it's easier to discern contrasts in color than in black and white. The color, however, is synthetic and does not indicate lithology or the true color of the formation.) Black, or the darkest color, is lowest microresistivity; white, or the lightest color, is highest microresistivity. For close examination, the image is usually presented at 1:5 scalar reduction (both horizontal and vertical), showing detail that can be scrutinized much like a core photograph.

The tool is designed to work in water-base muds, although it has achieved limited success in oil-base mud. In a study of images made in 16 North Sea wells with oil-base mud, noise reduced image quality, but the tool responded to some textural changes of the rocks, allowing recognition of bed boundaries, carbonate concretions, calcite streaks and other features. Application of the tool in this environment is limited by borehole damage, mudcake buildup and a common lack of resistivity contrast in the invaded zone.

Two versions of the tool are in the field (left). One is a hybrid of the Dual Dipmeter* tool (also known as the Stratigraphic High Resolution Dipmeter [SHDT]) and makes microresistivity measurements from 27 buttons on each of two pads positioned at a right angle. The two-pad design was selected to optimize resolution given the limitations of telemetry and processing (see "Formation Microscanning: Evolution of an Idea," page 18). A newer four-pad version has 16 buttons on each of four pads.

A single pass of the two-pad version covers 20 percent of the borehole wall of an 8 1/2-inch borehole. Two or three repeat



□ Saw-tooth effects on a two-pad Formation MicroScanner log (uncorrected), caused by yo-yoing and intermittent tool sticking at X426.5 to X428 feet. A convention is to have pad 3 data on the left and pad 4 on the right (pads 1 and 2 make only the conventional dipmeter measurement). The output shows, from left, microresistivity traces, the static normalization (sometimes called the "normal" image), and the dynamic normalization (sometimes called the "enhanced" image). HILITE image processing is sometimes run in place of dynamic normalization. See pages 19-20 for discussion of the differences between these processing methods.

1. Zemanek J, Caldwell RL, Glenn EE Jr, Holcomb SV, Norton LJ and Straus AJD: "The Borehole Televiwer—A New Logging Concept for Fracture Location and other Types of Borehole Inspection," *Journal of Petroleum Technology* 2 (June 1969): 762-774.

2. Strictly speaking, the tool measures current intensity, or conductance, and data are presented as microresistivity.

*Mark of Schlumberger

passes are typically run in hopes of rotating the tool, which can increase coverage to about 50 percent. A single pass of the four-pad tool covers 40 percent of an 8½-inch borehole. Although multiple passes with adequate tool rotation may increase coverage, one pass of the four-pad tool is generally sufficient. Data from the four-pad tool therefore require no depth shifting, and are acquired faster than two-pad tool data, which offer slightly better lateral resolution. Details of tool function have been reported elsewhere.⁴

In some heterogeneous formations encountered in oil and gas wells, and in invaded shaly sands in particular, the tool's depth of investigation can be very shallow, perhaps no more than an inch or two. Theoretically, however, its depth of investigation approximates that of the shallow laterolog (1 to 10 inches [2.5 to 25 cm]), depending on the contrast between true and invaded zone resistivity, R_t/R_{xo} . But this maximum depth of investigation is reached only in smooth boreholes with homogeneous beds. According to modeling by Jean-Claude Trouiller of Etudes et Productions Schlumberger, Clamart, France, the tool's depth of investigation can become very shallow: As bed thickness decreases, the effect of inva-

sion becomes more pronounced and the depth of investigation drops from 3 inches [8 cm] in an 8-inch [20-cm] bed to 1 inch [2.5 cm] in a 2-inch [5-cm] bed. Very conductive shoulder beds also decrease the depth of investigation. Rugosity reduces the depth of investigation by diminishing the current flow into the formation. Likewise, the higher the spatial density of vugs, the lower the depth of investigation.

The Formation MicroScanner's theoretical spatial resolution is on the order of 1 inch [2.5 cm], but it can detect hairline features such as fractures, stylolites and shale streaks, provided they have sufficient resistivity contrast with the surrounding material and they are separated by at least 1 inch [2.5 cm]. (See discussion on the resolution threshold of the tool, pages 34-35.)

Data Processing

Data processing converts current intensity measurements of the formation into variable-intensity images. There are six main processing steps:

- 1) Speed correction. A two-step filtering of microresistivity data using accelerometry measurements accounts for curve variations caused by irregular tool movement during logging. The two-pad tool also fine-tunes

this correction with a curve-matching microcorrelation that works much like the speed-button correction of the Dual Dipmeter tool.⁵

Speed correction removes or reduces saw-tooth artifacts, which sometimes occur when the tool sticks at high-resistivity contrast features because each row of sensors does not see the feature simultaneously (see log, page 17).

- 2) Voltage correction of microresistivity traces. This accounts for the effect of the changing current level emitted by the tool. The tool varies this current dynamically during logging to keep the intensity within an optimum operating range even under conditions of great resistivity contrast. It increases the current in front of a resistive formation to allow a significant amount of current to flow into the formation, and reduces current in front of a conductive formation to avoid electrical saturation. (At present, the tool does not give a direct, calibrated quantitative value of formation microresistivity, but this is an area of investigation.) Voltage correction removes image distortion if the tool passes through formations of widely differing resistivities.

- 3) Horizontal equalization of the signal across all buttons. This puts the same dy-

Formation Microscanning: Evolution of an Idea

The Formation MicroScanner tool builds upon a 50-year heritage of resistivity measurements, based on a concept that focused resistivity measurements would yield more detailed information about the formation. What was new was the initial idea of arranging small button electrodes in an array to measure "microresistivity." The first design called for a circular array of buttons on one pad, strictly for fracture detection. (Because open fractures are usually filled with conductive mud—when water-base mud is used—they are far less resistive than the surrounding rock and therefore could be identified as low resistivity anomalies.) The circular array was later changed to linear rows of electrodes when it was realized that rows could cover the same area as a circle but with fewer buttons. The intent of the tool, however, was still fracture detection, a kind of "super dipmeter," in which fractures would be found and analyzed by correlating microresistivity measurements between pairs of buttons.

Progress on the tool stalled when engineers realized that the volume of data from the number of buttons thought necessary would be nearly impossible for computers to handle. With the future of the tool in doubt, the third and most critical evolutionary step changed how the tool would be used: the relative microresistivity measurements could be converted into variable-intensity images. This, tool designers realized, would hold the buttons to a manageable number and permit identification not only of fractures but also of bedding dips and sedimentary features. Now, instead of only traces, log analysts had gray-scale images that could be enhanced, changed in scale, and even correlated with cores. With the technology now on the right track, engineers were free to concentrate on developing the one-pad prototype into the state-of-the-art four-pad version, a task they completed in less than three years.

While refinements in tool hardware and software continue, a major effort has been the development of interactive software and hardware for visualizing and manipulating logs on a workstation. Capabilities of the FMS Image Examiner* program include displaying the image at different horizontal and vertical scales and scrolling up and down the log, automatic dip calculation, viewing the borehole and its azimuth in three dimensions, the ability to annotate the logs within the workstation environment, interactive image processing capability. Other areas of investigation include semiquantitative methods for correlating images from pass to pass and from well to well, and methods for quantifying button microresistivities.

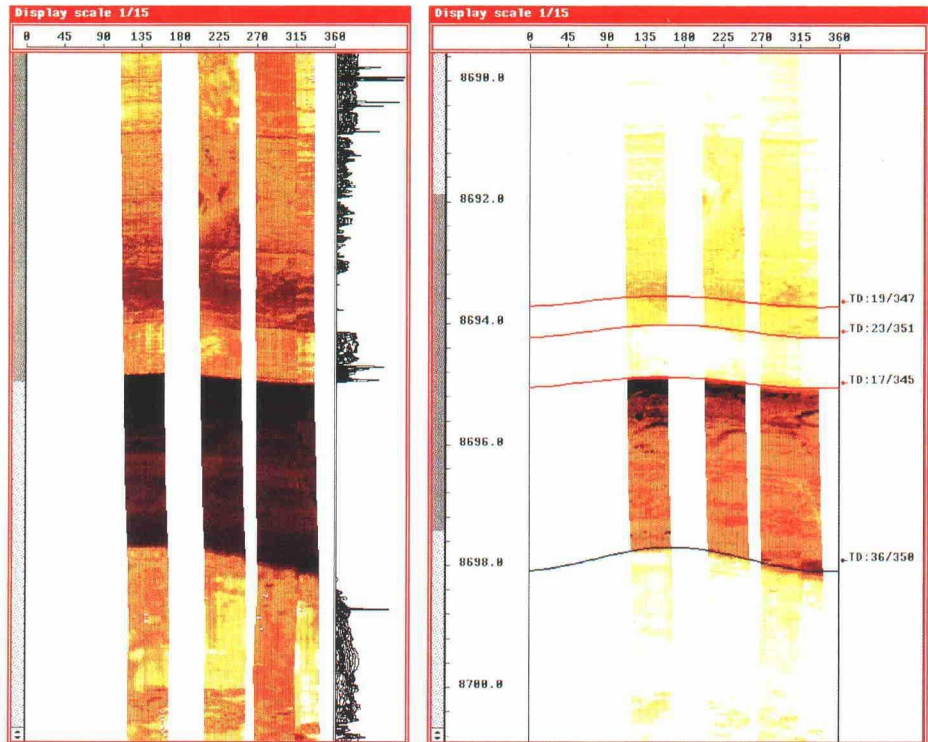
dynamic range on each button and removes stripes in the images, which occur when buttons record different microresistivities. This effect is caused by marginally different gain and offset between buttons and by borehole break-outs or ovalization, which can cause imperfect pad contact.

4) Conversion of current intensity to variable-intensity images. Sixteen gray (or color) scales are represented in printed versions; almost 256 colors and shades can be represented on the FMS Image Examiner* workstation. The conversion of current intensity to images is done by "point-to-point" mapping, in which each pixel in the image has a gray- or color-scale value associated with a particular range of current levels.

There are two schemes for choosing shading levels, depending on what information is needed. For corroborating images with other information about large-scale facies description, gray or color scales may be chosen in the so-called static mode. In this approach, tool response is normalized over a long depth interval, corresponding to a formation or reservoir. This means that a particular shade at one depth indicates the same resistivity as the same shade at another depth. Logs processed this way are typically viewed at scales that result in images 1/2 or 1 inch wide [1 to 2.5 cm] (typically 1:6 or 1:12 vertical scale at 1:3 or 1:6 horizontal scale, respectively).

The advantage of this method is that it permits comparing resistivities over depth by comparing shades of gray or color. This method can be used to obtain a sand count and to infer permeability in water zones. (High-permeability zones with salt muds appear less resistive than low-permeability zones.) A disadvantage of this approach is that small-scale variations in microresistivity may not be visible. To resolve other details, gray and color scales are chosen in the so-called dynamic mode. In this approach, the mapping scheme is changed locally within a small vertical window usually defined as 1 meter [3.3 feet] or 1 foot in the United States. The full range of gray or color levels is used over this window, giving maximum detail. A limitation is that the values of gray or color can only be considered to indicate relative change in microresistivities and do not necessarily indicate like microresistivity values (*right*).

A variation on dynamic normalization is HILITE, which is run instead of dynamic normalization. It uses the entire gray or color scale within a sliding window, which enhances the visibility of small details. (In signal processing terms, dynamic normal-



□ Dynamic (left) and static normalization of merged multiple passes of the two-pad tool, as displayed on the FMS Image Examiner workstation screen and hard copy. The image shows a reverse fault rubble zone (8695 to 8698.5 feet) in Arbuckle limestone, Oklahoma. ("TD: 19/347" means a true dip angle of 19° with a dip azimuth of 347°.) The microresistivity trace appears right of the dynamically normalized image. In this image, nearly all detail of the rubble is lost, but it shows that most of the formation immediately above and below the rubble has a similar resistivity. The dark laminations in the interval from 8690.5 to 8694 feet are probably due to small fractures splaying off the main fault. In the merged right-most tracks, color variation is due to changes in pad pressure. The statically normalized image lacks detail in the rock above and below the rubble zone, but image enhancement in the rubble zone shows that it has some laminations. The fault was identified as reverse based on a repeat section indicated by other open hole logs. (For an explanation of the depth tracks, see log top left, next page.)

3. Dennis B, Standen E, Georgi DT and Calow GO: "Fracture Identification and Productivity Predictions in a Carbonate Reef Complex," paper SPE 16808, presented at the 62nd SPE Annual Technical Conference and Exhibition, Dallas, September 27-30, 1987.

Luthi SM and Banavar JR: "Application of Borehole Images to Three-Dimensional Geometric Modeling of Eolian Sandstone Reservoirs, Permian Rotliegende, North Sea," *AAPG Bulletin* 72 (September 1988): 1074-1089.

Plumb RA and Luthi SM: "Application of Borehole Images to Geologic Modeling of an Eolian Reservoir," paper SPE 15487, presented at the 61st SPE Annual Technical Conference and Exhibition, New Orleans, October 5-8, 1986.

Pezard PA and Luthi SM: "Borehole Electrical Images in the Basement of the Cajon Pass Scientific Drillhole, California; Fracture Identification and Tectonic Implications," *Geophysical Research Letters* 15 (August supplement, 1988): 1017-1020.

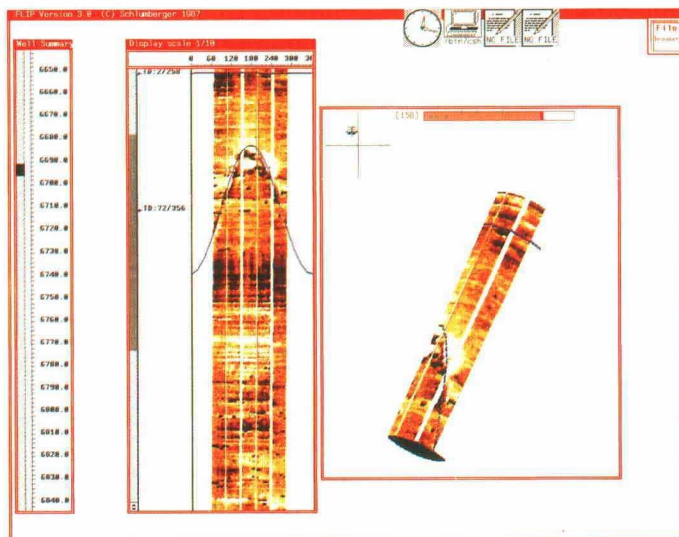
Hackbarth CJ and Tepper BJ: "Examination of BHTV, FMS, and SHDT Images in Very Thinly Bedded Sands and Shales," paper SPE 18118, presented at the 63rd SPE Annual Technical Conference and Exhibition, Houston, October 2-5, 1988.

4. Ekstrom MP, Dahan CA, Chen M-Y, Lloyd PM and Rossi DJ: "Formation Imaging with Microelectrical Scanning Arrays," *Transactions of the SPWLA 27th Annual Logging Symposium*, Houston June 9-13, 1986, paper BB.

Lloyd PM, Dahan C and Hutin R: "Formation Imaging with Micro Electrical Scanning Arrays: A New Generation of Stratigraphic High Resolution Dipmeter Tool," *Transactions of the SPWLA 10th European Symposium*, Aberdeen, Scotland, April 22-25, 1986, paper L.

Formation MicroScanner Applications in Italy. Milano: Schlumberger Italiana S.p.A., March, 1988.

5. For details of speed correction by speed button: *Schlumberger Dipmeter Interpretation*. New York: Schlumberger Limited, 1986.



□ Oriented (left) and three-dimensional images of several passes of a two-pad Formation MicroScanner tool, as presented on the FMS Image Examiner workstation. The sinusoid indicates a steeply dipping fracture. The oriented plot views the borehole as if the viewer were inside the borehole looking out. The eye symbol in the crossplot (right of the oriented plot) indicates the view is north to south. The three-dimensional plot shows that the borehole deviates slightly to the east. This plot can be rotated to choose any view, as if the viewer were walking around the periphery of the borehole from inside the formation. The Well Summary column (far left) indicates where the interval shown—represented as a black rectangle—lies in the well. The shaded rectangle in the column bordering the left of the image represents the unit of computer memory containing the part of the image shown.

ization performs a linear transformation of data, whereas HILITE applies a nonlinear transformation.) HILITE works better in fractured and thin-bed intervals. The transform does not, however, discriminate between low-contrast information and noise. In bad borehole conditions, dynamic normalization may offer the best compromise between enhancement of significant details and suppression of unwanted features.

5) Image display. Two types of displays are available: oriented and three-dimensional plots (left). Oriented plots from the two-pad tool include waveform, or wiggle, traces from each button and variable-intensity images, sometimes presented with an inclinometry grid. Waveform traces can be useful for picking bed boundaries, which are indicated by inflection points on the curves. Features are occasionally easier to see on the waveforms than the image. The waveform traces are not currently presented with four-pad tool data because of limited space on the hard copy. An oriented plot provides a wrap-around view of the borehole with variable-intensity images, oriented with respect to any chosen azimuth, usually north. Multiple oriented plots can be merged to increase borehole coverage. They also show tool rotation. The FMS Image Examiner program can interactively map the

Interpretation of Formation MicroScanner Images		
Features interpretable by themselves		
Structural features ¹	Sedimentary features	Diagenetic features
Fractures Faults Folds	Bedding surfaces Slumps Crossbedding	Stylolites (sometimes)
Features interpretable with the help of other log data		
Clasts Concretions Vugs	Structural shale (clay galls, chips, rip-up clasts; flaser bedding; see photo, right) Grain size changes	Cementation (calcite, dolomite, anhydrite) Sorting (sometimes) "Comparative" porosity
Features interpretable after calibration with core data		
Bioturbation Grain size changes	Sorting Stylolites	Laminations (<1/2 inch [1 cm] thick) "Comparative" permeability



□ Laminated shale clast, Frio sandstone, South Texas. This clast, a little larger than an electrode of the Formation MicroScanner tool, would appear on the image as black against a light background. The overlying clay-rich bed would appear a darker gray than the sand.

1. Structural features are considered those formed mainly by postdepositional deformation. Sedimentary features are considered those formed mainly by processes of deposition and erosion. For more detail on these and other features of Formation MicroScanner interpretation, see: *FMS Image Interpretation Guidebook*. Paris: Schlumberger Limited (in press).

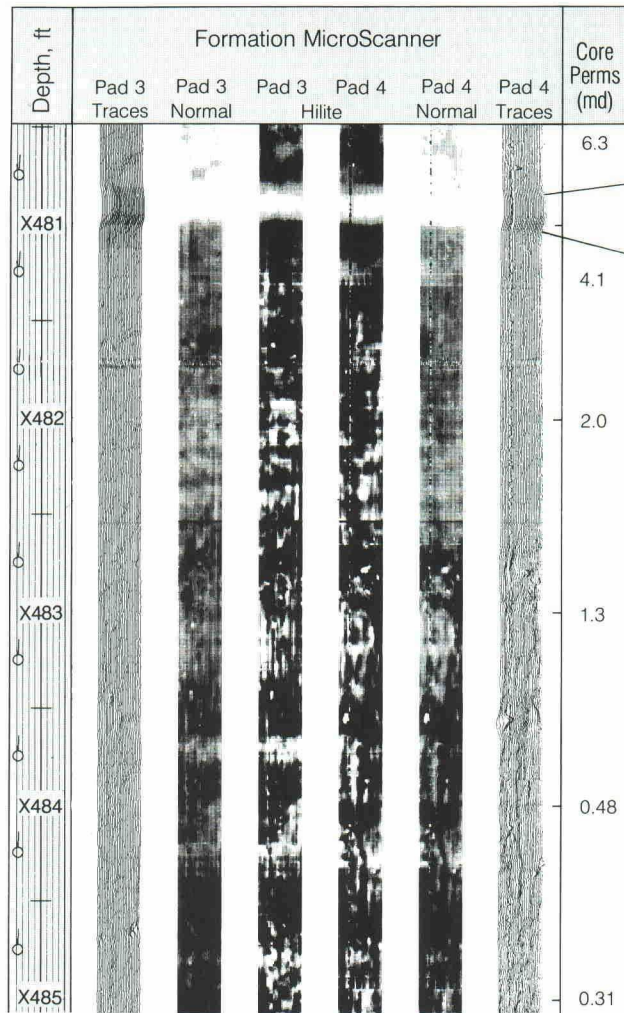
strike and dip of linearly continuous features on the image, and automatically plot borehole deviation. In one study of basement rock, this mapping permitted reorienting the core to within 15 degrees.⁶

6) Image enhancement. This data processing step enables the viewer to emphasize features in a given section that have relatively subtle microresistivity changes compared to other features in the section. For example, dip of a bed of intermediate resistivity might be lost when it is bordered by strongly conductive fractures or highly resistive cemented zones. Image enhancement would reduce the contrast of the end members and enhance that of the middle member. This enhancement is made in a moving window in which the full gray or color scale is applied to a limited area of the electrical current histogram (see page 19, left log).

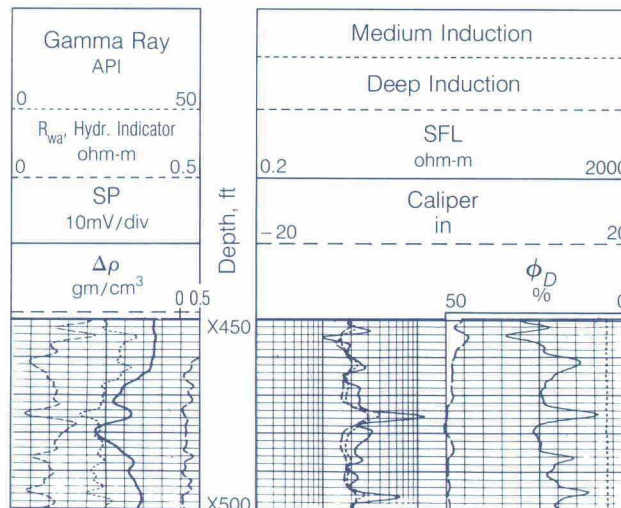
Interpretation

The goal of Formation MicroScanner image interpretation is to characterize formation properties to assist sedimentologic interpretation, determine the presence of permeability paths (open fractures) and permeability barriers (shale beds or compacted massive beds), help calculate net pay, plan perforation and fracturing, and help decide where to drill next. The images support these goals by allowing the user to zone the well on a large scale by dips, and by indicating rock type, features of secondary porosity (vugs and fractures), reservoir fluid contacts, and the direction of rock stresses. Some interpreters also use the images to calculate "comparative permeabilities"—estimating the permeability of beds using core-derived permeabilities from beds of similar resistivity in the same well or in offset wells (right).

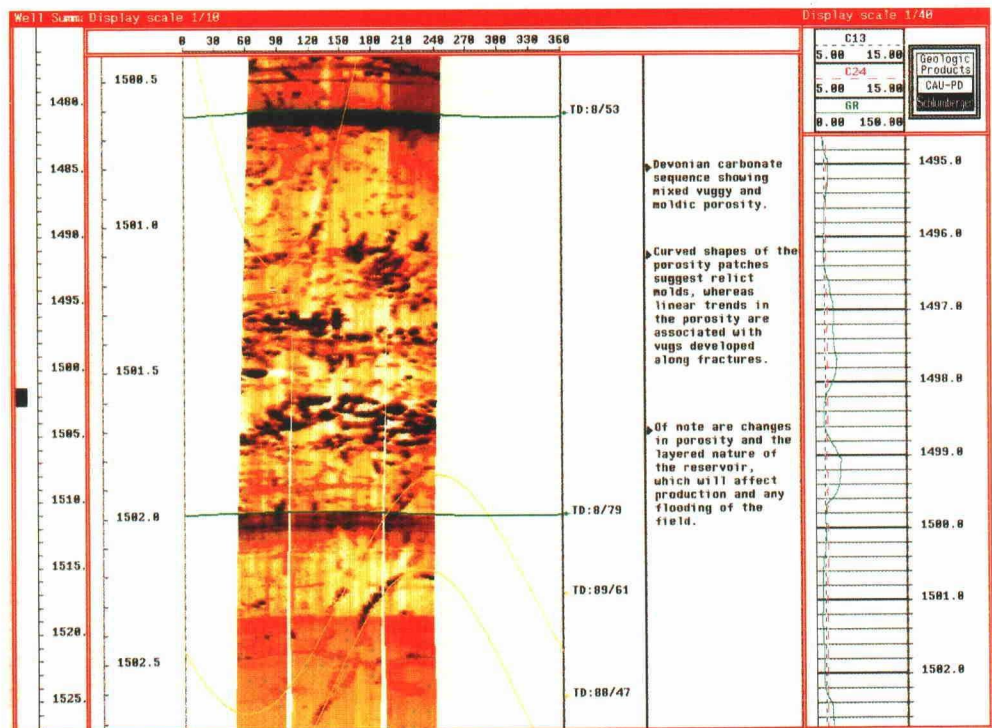
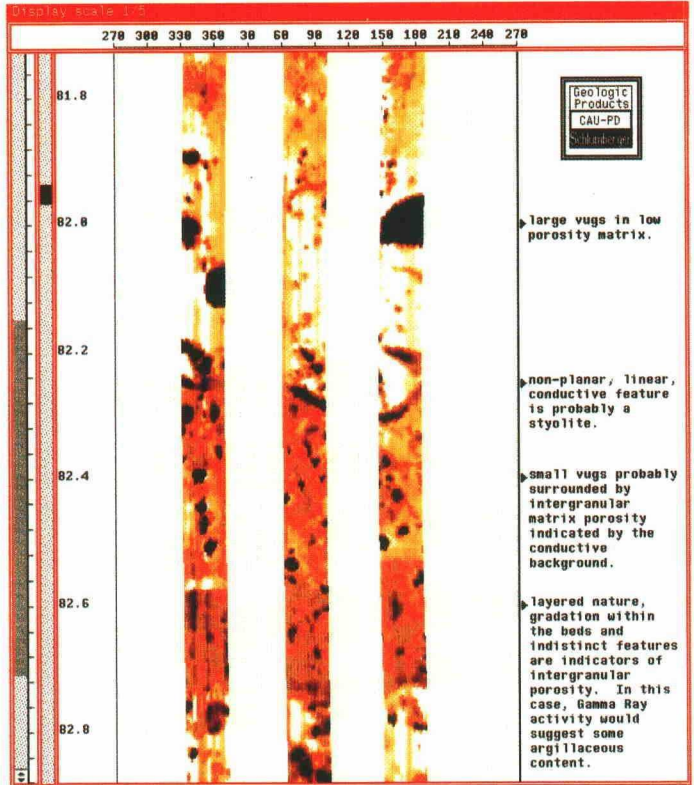
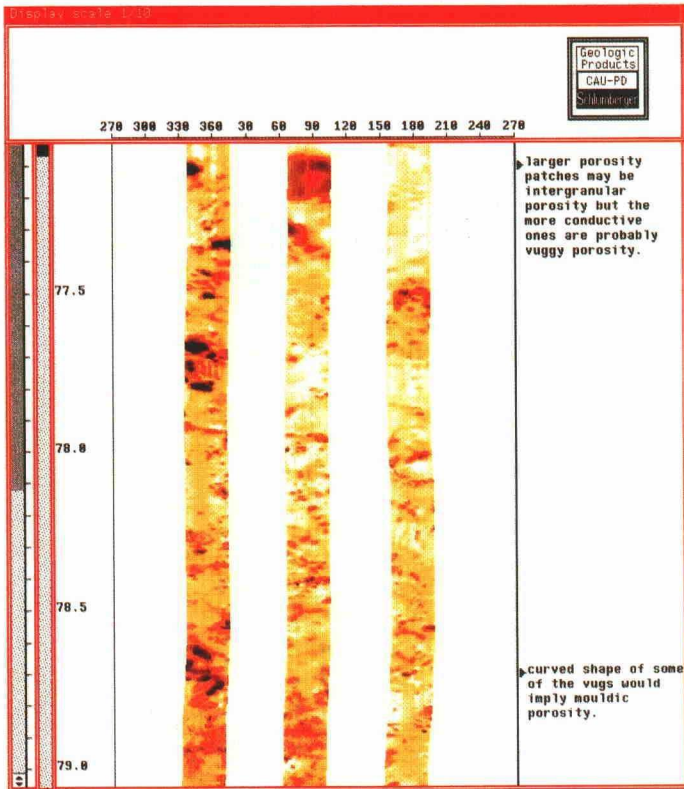
There are three kinds of Formation MicroScanner images: images interpretable by themselves, images interpretable only with the help of other logs and local knowledge, and images interpretable only after calibration with cores (see "Interpretation of Formation MicroScanner Images," left). In practice, Formation MicroScanner images must always be interpreted after lithology has been fairly well defined, so supplemental data are usually necessary to enhance the confidence of image interpretation. For



□ Evidence of a permeability transition zone in the Olmos sandstone, South Texas. Conventional open hole logs show increasing shaliness with depth and a parallel decrease in porosity, suggesting a "tightening up" of the formation. The statically normalized two-pad Formation MicroScanner image (outer two image tracks) shows a high resistivity anomaly just above X481 feet and a gradual downward increase in shaliness. The 2-inch [5-cm] tight streak on the Formation MicroScanner image at X481 feet appears in the core photograph. Core analysis (far right track) shows that this streak separates a high permeability zone above from a lower permeability zone below. Integrating permeability measurements, conventional open hole logs and images could help log analysts find the permeable zone of this 5-foot [1.5-meter] bed in offset wells. (The straight vertical streaks on the images are from a dead button; the horizontal white streaks are from folds on pages of the log.)



6. Reference 3, Pezard and Luthi.



□ Two-pad Formation MicroScanner logs showing a spectrum of vugginess in Canadian carbonates: large vugs, intergranular porosity, mixed vuggy and intergranular porosity, and mixed vuggy and moldic porosity. The examples show marginal notation permitted with the FMS Image Examiner workstation. In the middle figure, right track, C13 and C24 refer to calipers from pads 1-3 and 2-4, respectively; the solid green line is the gamma ray log. Vugs also appear in the image on page 26, top.

Open Fractures

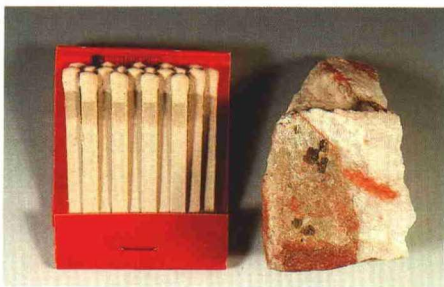
example, local knowledge of a carbonate usually indicates whether dark mottling is due to vugs or shale clasts (*left*).

Interpretation conventions also vary locally. In the North Sea, for example, most wells are cored, so that analysis of nearly all Formation MicroScanner images is combined with core analysis (see "A North Sea Approach to Formation MicroScanner Image Interpretation," page 24). In Monterey, California, core recovery is often so poor that Formation MicroScanner images integrated with other open hole logs, drilling and cuttings data become core substitutes. In most wells, the images reduce, but do not eliminate, the need for cores.

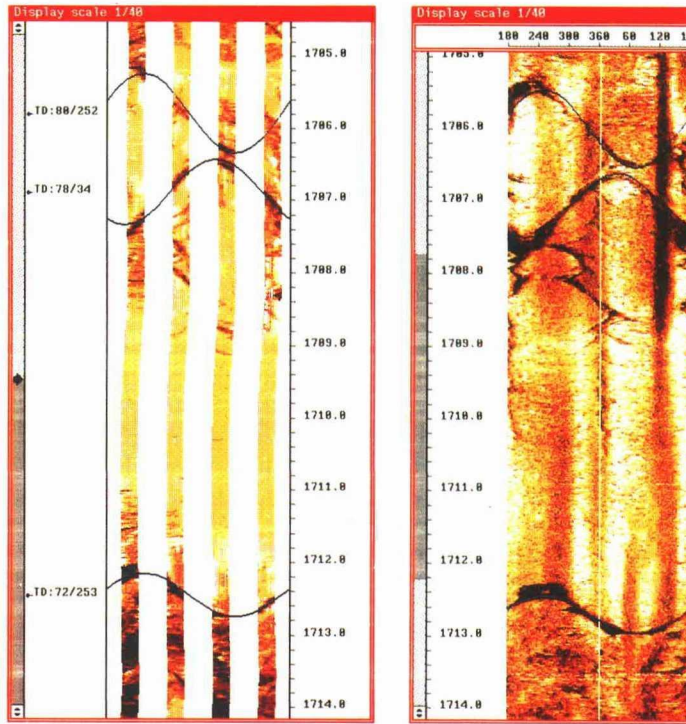
Images interpretable by themselves

Images interpretable by themselves present a fairly unambiguous picture on the log. **Fractures** are one of the most important of such features.⁷ Dark (conductive) lines that typically cut across bedding, and sometimes parallel it, are usually considered open, mud-filled fractures (*right*). But dark lines can also indicate fractures filled with another conductive material. The microresistivity trace offers clues to the type of conductive material. The amplitude of deflection for a mineralized fracture is generally lower than for a fracture of the same aperture filled with conductive mud, and much higher for a fracture filled with very conductive material such as pyrite, graphite or hematite (*below*). Sometimes large clay-filled fractures show an increase in thorium content on the Natural Gamma Ray Spectrometry (NGS*) log. However, this log has a vertical resolution of about 2 feet [60 cm] and should be used guardedly in this application.

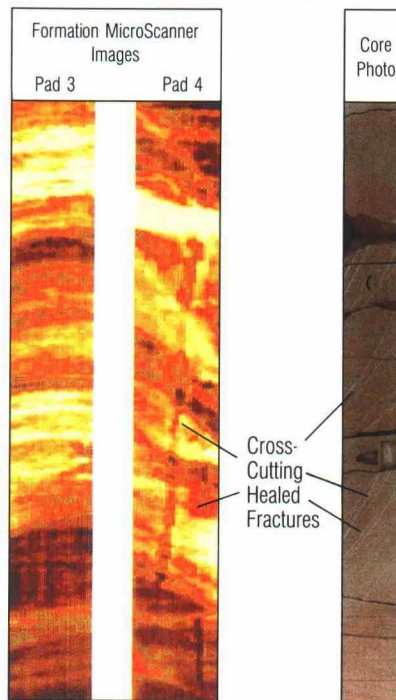
Sometimes fractures appear light instead of dark, with halos near the crest and trough (*next page, left*). Modeling by Trouiller



□ Pyrite crystals embedded in a calcite vein. Although these crystals are about half the size of an electrode on the Formation MicroScanner tool, they are highly conductive and could cause large peaks in the microresistivity curve if an electrode crosses them.

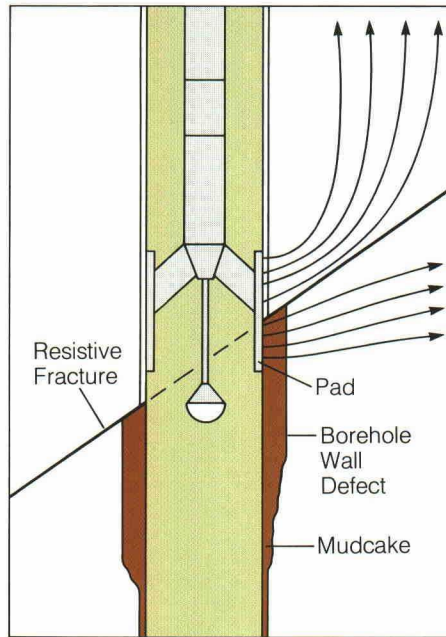
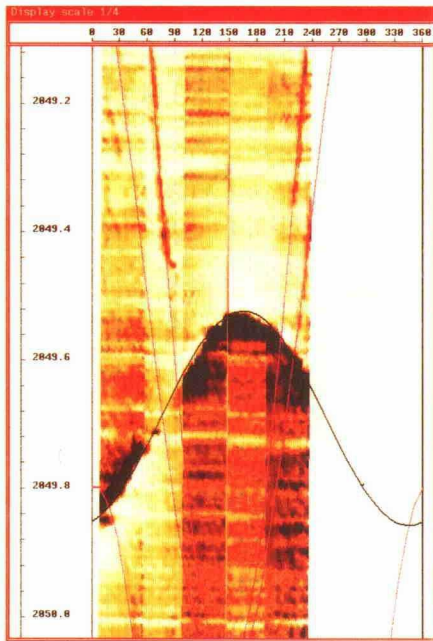


Mineralized Fractures



□ Open fractures shown on four-pad Formation MicroScanner (left) and borehole televiwer logs and mineralized fractures in a different well, on a two-pad Formation MicroScanner log and core. Three open fractures appear on the straight plots of the four-pad Formation MicroScanner tool and on the BHTV log. The scale of the Formation MicroScanner log is slightly more compressed than that of the BHTV. In the other well, mineralized fractures apparent on the core also appear in the Formation MicroScanner image as more conductive (darker) than the surrounding rock. The bottom of the image is about 3 feet [1 meter] above the top of the core.

7. "Fracture Detection with Logs," *The Technical Review* 35, no. 1 (January 1986): 22-34.



□ A statically normalized image from three passes of a two-pad Formation MicroScanner tool, showing a halo effect around a mineralized fracture in a Canadian shale (right) and the mechanism that produced it (tool not to scale). Moving up the well in the updip direction, there is a large overshoot of current (low resistivity) when the pad is opposite the fracture, and large undershoot (high resistivity) when it is above; in the downdip direction the phenomenon is reversed. This is due to compression of tool current as the pad approaches the resistive layer, and expansion as it moves away from the layer. This effect produces a large black section followed by a white section. Unfortunately, since the breakout at the wellbore is a couple of inches, it is below the resolution of the caliper.

shows that such features can be produced by nonuniform pad stand-off over a steeply dipping fracture along which there has been displacement or breakout, or by (calcite) cementation along the fracture plane. The Canadian formation shown at left also had calcite-cemented fractures and steeply dipping fractures that broke out at the wellbore, but neither showed the halo effect. The conclusion was that the halo was produced by the fracture breakout geometry and by calcite cementation. Fractures like this in other wells in the Canadian field did produce and were therefore considered cemented because production increased after acidizing.

There are a few caveats in interpreting images of fractures and fracture-like features. First, not all linear conductive anomalies are fractures. Fracture-like features can also result from grooves in the wellbore produced by stabilizers and drill pipe. These features have a distinctive linearity and uniformity absent in fractures (far right). Second, the image doesn't tell whether a fracture contributes to reservoir production; it tells only that the fracture is present at the wellbore. Determining whether the fracture will produce oil or water, or act as a permeability path or barrier requires integration of more data about the well and the field.⁸

A North Sea Approach to Formation MicroScanner Image Interpretation

An interpretation method for Formation MicroScanner images has grown from FMS image-core integration studies by scientists at Schlumberger and Occidental Petroleum (Caledonia) Limited, in Aberdeen, Scotland.¹ Excluding log quality monitoring, which is done at all stages, the approach has six steps:

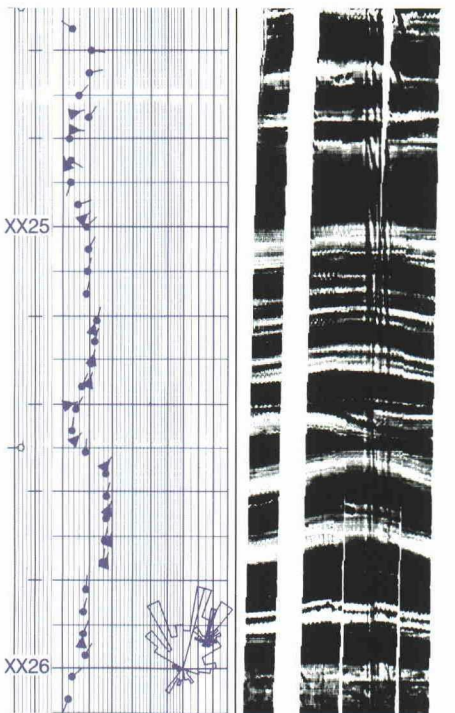
- 1) Zone major depositional units using open hole logs.
- 2) Check dipmeter arrow plots to identify tectonic features and major sedimentary discontinuities. Constrain the range of possibilities based on local knowledge and seismic data.
- 3) Identify hydrocarbon and tightly cemented zones.
- 4) Describe core in detail. Comparing sedimentary features on core and on FMS borehole wall images permits assessment of lateral variation of thin beds and other features at the scale of the borehole. Images also give better visualization of minor faults and slumps that are ambiguous or absent on the dipmeter log and may be too large to interpret from core alone.
- 5) Using local depositional knowledge, place constraints on possible interpretations. Establishing depositional units or individual facies from conventional logs limits the likely sedimentary features.
- 6) Grade FMS image quality based on core correlation in order to assign "confidence limits" to specific features. Confidence limits are assigned a grade, 1, 2 or 3. Grade 1 features can be identified and interpreted from FMS images alone; grade 2 features can be identified from FMS images, but do not have a unique interpretation; grade 3 features have an ambiguous interpretation and require core for interpretation. Confidence grading helps reservoir engineers and geologists weigh the importance of the images when extending interpretation to uncored intervals. Knowledge of expected grading in a given formation also assists future well programming. The higher the image quality, for example, the less emphasis will be needed on coring. Core is not essential for interpreting grade 1 and 2 images. Where grade 3 images are expected, FMS images should be considered a supplement to core interpretation.

1. Harker SD, McGann GJ, Bourke LT and Adams JT: "Methodology of Formation MicroScanner Image Interpretation in Claymore and Scapa Fields (North Sea)," *Journal of the Geological Society of London* (in press).

And finally, fracture detection is best done at a moderately compressed vertical scale, whereas more careful study of individual fractures requires a finer scale, such as 1:5.

Once fractures are identified, what can Formation MicroScanner images reveal about them? On the FMS Image Examiner workstation, fracture strike and dip are determined from simple geometry, knowing the tool orientation and borehole diameter and deviation; fracture density and spacing can be computed from the geometry⁹ (below). Fracture aperture cannot be determined with currently available processing, but fracture porosity can be assessed in a relative sense: an open fracture, because it contains more conducting fluid, will appear darker than a tight one.

The images may distinguish natural fractures from those induced by strain release during drilling or by hydraulic fracturing, even if the fractures have a very small extension. As a rule, zones of induced fractures tend to parallel the borehole axis, usually appear on the image 180 degrees apart, and often contain a succession of small cracks following a complex path. Schlumberger researchers are investigating the effects of loading history, rock strength and rock ductility on where induced fractures originate and how they propagate.

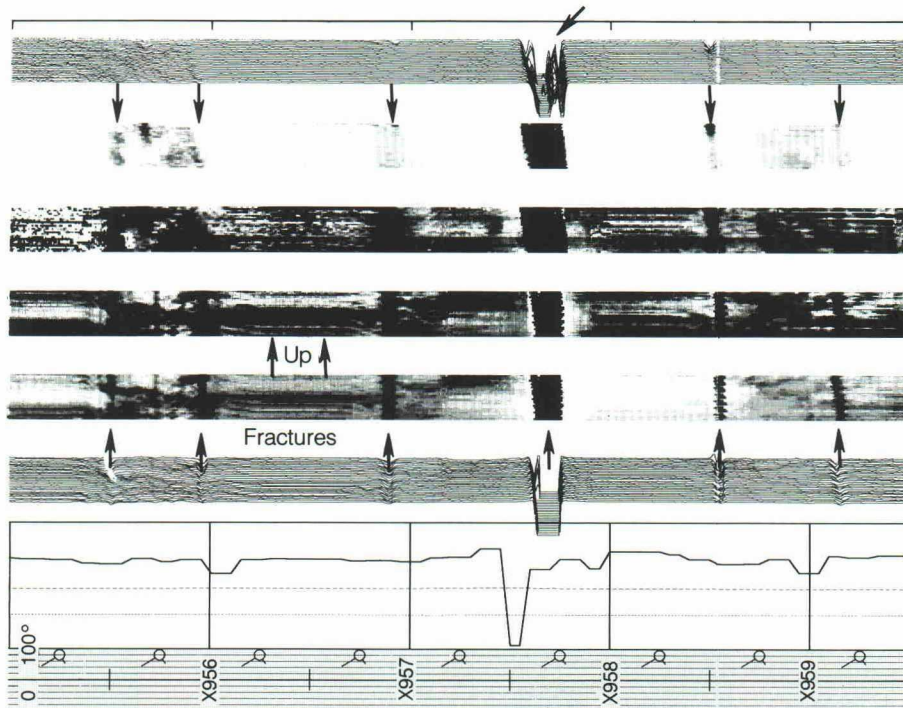
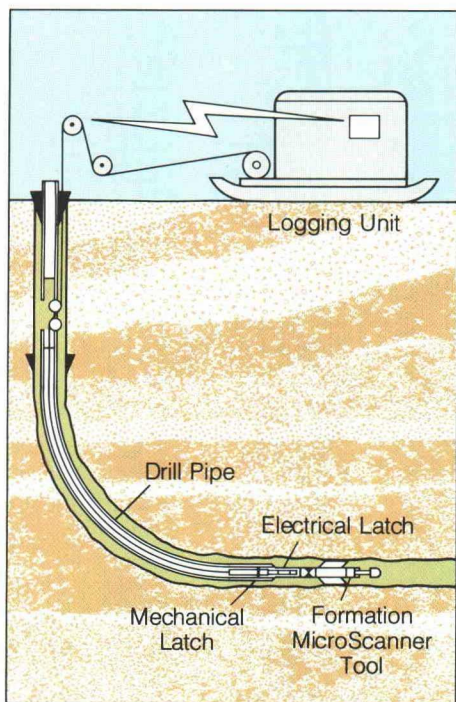


□ Borehole scour marks on a two-pad Formation MicroScanner log in a Canadian crossbedded sand-shale sequence. The uniformity of these marks across both sands and shales suggests they are not of geologic origin. Note the general agreement between the dip magnitude observable on the image and the dip values reported on continuous side-by-side (CSB) and Local Dip processing of dipmeter data.

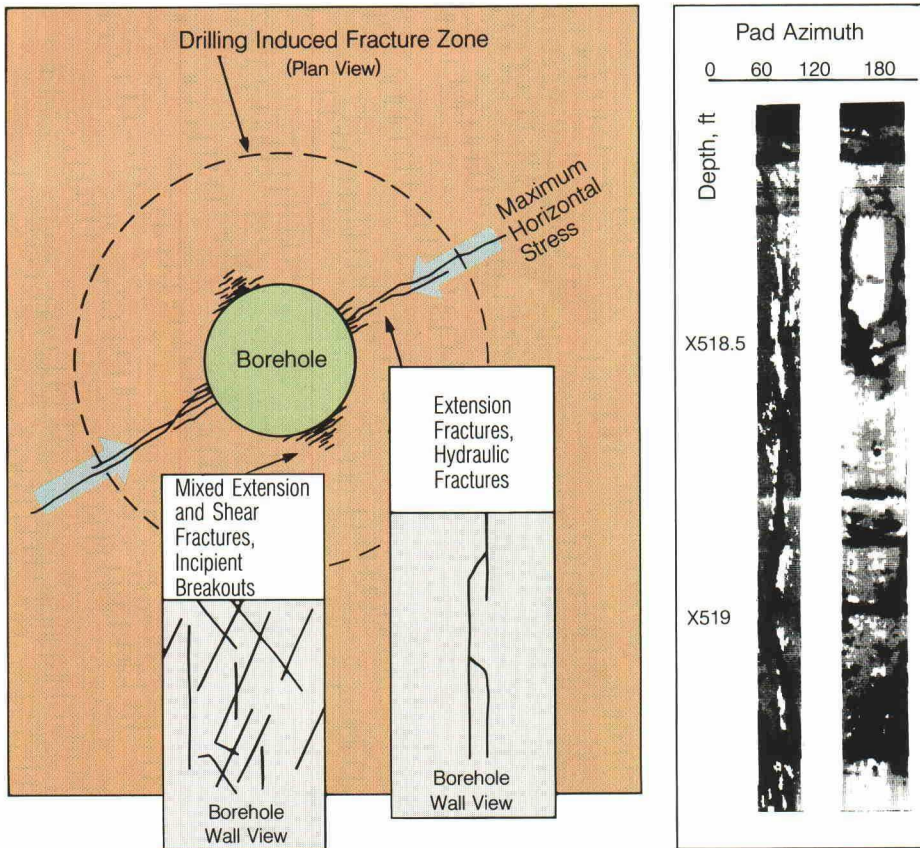
Distinguishing natural from induced and open from mineralized fractures has also been done in basement rock by comparing fracture intensity (how heavily an interval is fractured) from Formation MicroScanner images with fracture porosity obtained from the laterolog.¹⁰ Working in basement rock near the San Andreas fault in California, Philippe Pezard of Columbia University and Schlumberger colleagues found zones with large azimuthal conductivity anomalies that are absent on the laterolog-derived porosity profile. They speculate that these zones may be induced fractures. Natural fractures, both fluid filled and mineralized, were detected by both tools, and, again, a large conductivity anomaly on the Formation MicroScanner log was interpreted as indicating a fluid-filled rather than a mineralized fracture.

Recognizing subtle differences in induced fracture morphology can corroborate information about the stress field, obtained from caliper data in the well or from preexisting

- 8. Reference 3, Dennis et al.
- 9. Reference 3, Plumb and Luthi.
- 10. Pezard PA, Anderson RN, Howard JJ and Luthi SM: "Fracture Distribution and Basement Structure from Measurements of Electrical Resistivity in the Basement of the Cajon Pass Scientific Drillhole, California," *Geophysical Research Letters* 15 (August supplement, 1988): 1021-1024.

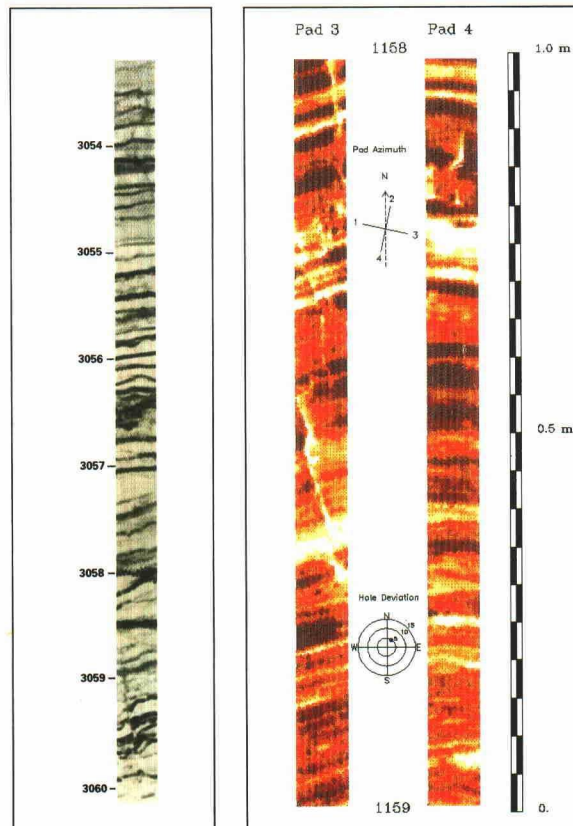


□ Near-vertical fractures in a horizontal borehole appear as dark, steeply inclined lines on a Formation MicroScanner log in the Austin Chalk, South Central Texas. A large fracture appears just left of X958 feet. The log was made with the Tough Logging Condition (TLC*) system (left) in which the tool is attached to the bottom of drill pipe and operated from a wet connect.



□ Models for fracture geometries (left) and drilling-enhanced fractures in a Canadian carbonate shown on two passes of a two-pad Formation MicroScanner image. The log shows the step-like, slanted character common to induced fractures (called en échelon arrangement) at the azimuth of maximum horizontal stress. Dark spots at the bottom of the right track are pin-point vuggy porosity. (Also see log, page 22.)

□ Reverse faults in limestone of a Blanco County, Texas well (left, between 3059 and 3060 feet) and in a Paris basin carbonate, shown on an ALBUM presentation of two-pad Formation MicroScanner images, pad 3 image (see just left and below the pad azimuth diagram). In the ALBUM presentation, the 70° angle between the bedding and fracture suggests that the direction of maximum principal paleostress is near vertical. ALBUM logs are presented in booklets that can be read horizontally, rather than in scrolls that are read vertically. The format is intended to make Formation MicroScanner images easier to compare with core photographs, which are often presented in fold-out albums.

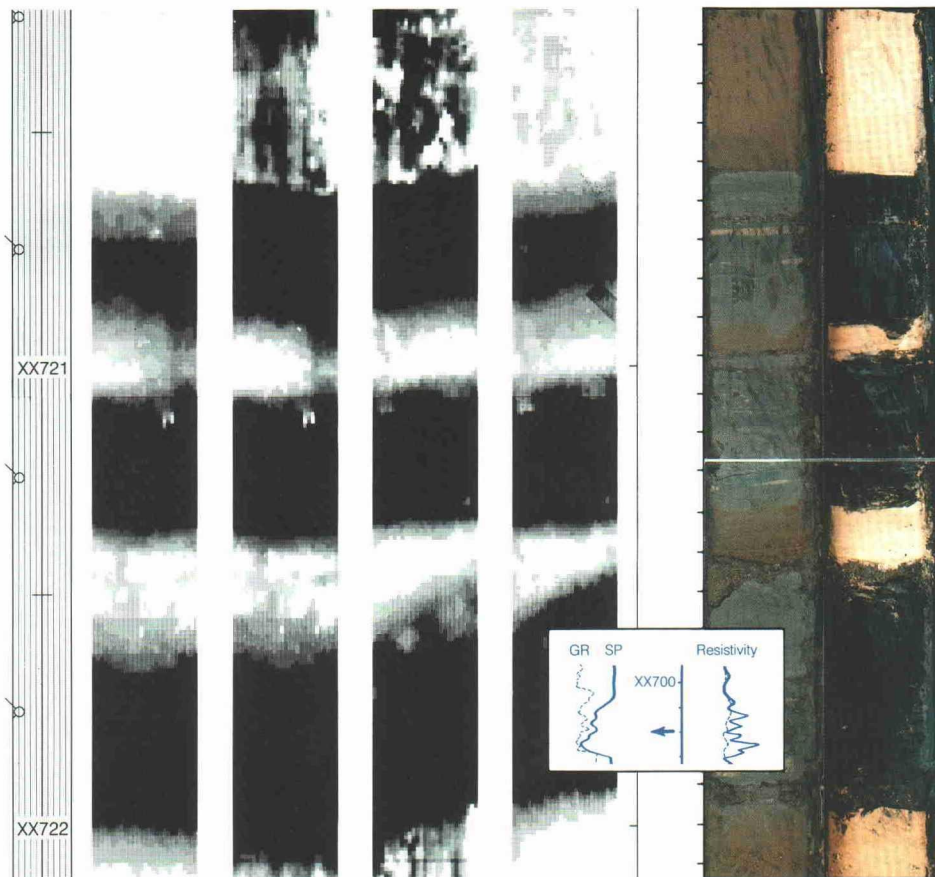


surveys in the area. Fracture morphology can indicate stress orientation and rock strength, according to studies by Richard A. Plumb at Schlumberger-Doll Research, Ridgefield, Connecticut. Plumb has found two kinds of induced fractures on Formation MicroScanner images (left). Fractures that parallel the direction of maximum horizontal stress tend to form en échelon (in a step-like, overlapping fashion), are confined to a relatively narrow azimuth, extend up to hundreds of feet, and form characteristic hooks at their ends. Fractures that form normal to the maximum horizontal stress occupy a wider azimuth, the width of which is controlled by the magnitude of the horizontal stress differences and rock strength. (For a given stress difference, the lower the rock strength, the wider the azimuth; for example, fractures in higher porosity rocks tend to have a greater azimuthal range.) Individual fractures in zones normal to the maximum horizontal stress are often inclined to the wellbore axis by 10 to 30 degrees, and extend up and down the borehole wall no more than 1 foot [30 cm]. In the context of the borehole stress field, this geometry suggests a mixture of shear and extensional components. In general, fractures that are normal to the maximum horizontal stress are thought to represent incipient wellbore breakouts that appear on Formation MicroScanner images as diamond-shaped features or as vaguely diagonal lineaments.

Fractures along which there has been displacement are apparent where beds have been visibly moved (left). Open fractures may be hydrocarbon conduits, whereas cemented fractures can be used to determine paleostress direction when fracture dip and strike can be calculated.

Three other groups of features can be identified from images themselves, given good resistivity contrast and favorable borehole conditions. They are listed here in order of increasing scale—not necessarily the order in which they are considered during interpretation. Interpreters typically move back and forth among scales.

Formation/bedding thickness is the largest scale interpretable on Formation MicroScanner images. The images can reveal the beginning and end of whole depositional sequences, such as those of aeolian, fluvial or deltaic environments. This allows grouping beds within sequences into meaningful units, for example, the channels of a delta and its outwash plains. Narrowing the focus further, the images allow finer subdivision within each group,



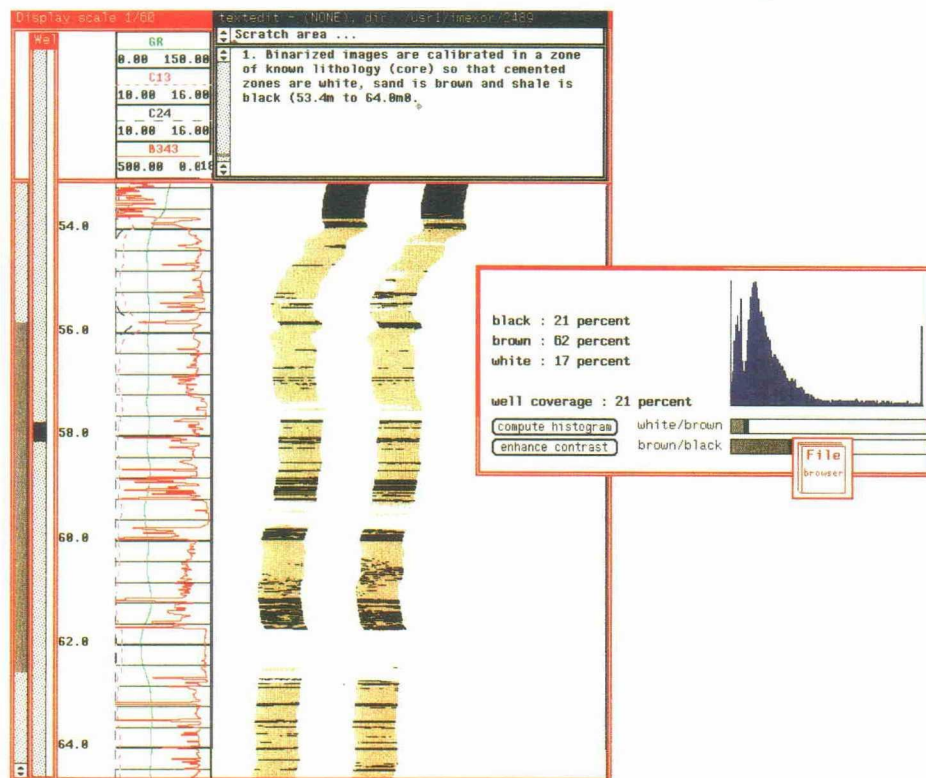
all the way down to beds about 0.5 inch [1 cm] thick, given good borehole conditions, sufficient resistivity contrast, and sufficient spacing between thin beds. In thin beds, the highest resolution can be obtained with dynamic normalization or HILITE processing, whereas static normalization is best suited for doing a sand count in conventional bedding (*below*). A change in bedding composition can be identified from images alone especially where a sharp resistivity contrast exists, such as where sands overlay shales (see *page 19 log and left*).

Sedimentary structures often parallel microresistivity patterns, and may hold the key to understanding the type, shape and size of the reservoir and direction of preferential drainage. On the large scale, discernable sedimentary structures include erosional contacts and unconformities (where one sequence ends and another begins). The images also reveal whether bedding contacts are abrupt or gradual, parallel or lenticular. The local dip of discontinuities can be measured from images, but have to be used carefully since many discontinuities are highly nonplanar at a larger scale.

On the medium scale, within beds, slumps may be determined without ancillary data. When slumps are large enough to be detected, they appear as compressed, folded and swirling features, often interlayered with clay and sand (*left*). On the small scale, images can reveal bedding types,

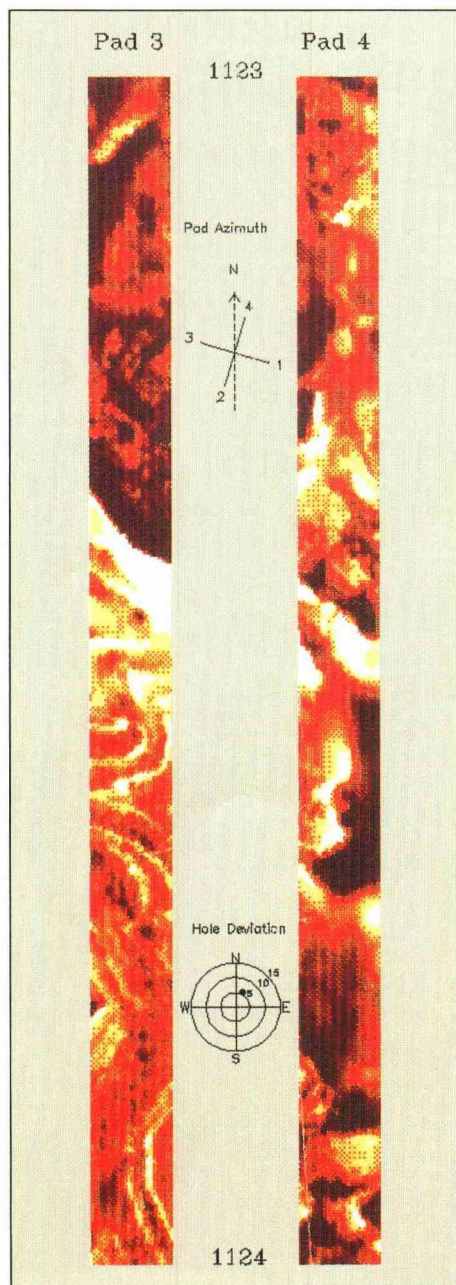
□ Two-pad Formation MicroScanner images, white light and ultraviolet core photographs and open hole logs of a Louisiana sand-shale sequence. The more resistive sands show clearly as white areas with planar and irregular bed boundaries. The white specks may be calcareous concretions within the shale; they are not visible on the core photographs. Divisions by the core photo are 1 inch [2.5 cm].

□ A vertically compressed Formation MicroScanner presentation for estimating sand count, from a two-pad tool measurement of a sand-shale sequence in a Canadian heavy oil zone. This "threshold-derived" 1:60-scale image places thresholds on conductivity based on core calibrations. Cemented zones are white, sand is brown and shale is black. This output includes a histogram showing the relative ratios of cemented to uncemented sand, and uncemented sand to uncemented shale. The vertical scale is frequency, the horizontal scale is conductivity from low to high. The bars below the histogram are scales the operator adjusts to determine the conductivity thresholds.





□ A core photo and ALBUM presentation of a two-pad Formation MicroScanner log of a slump. The core is a shaly sand; the left track of the log shows a sandstone with a high-resistivity cement. The slump appears as folded and overturned beds.



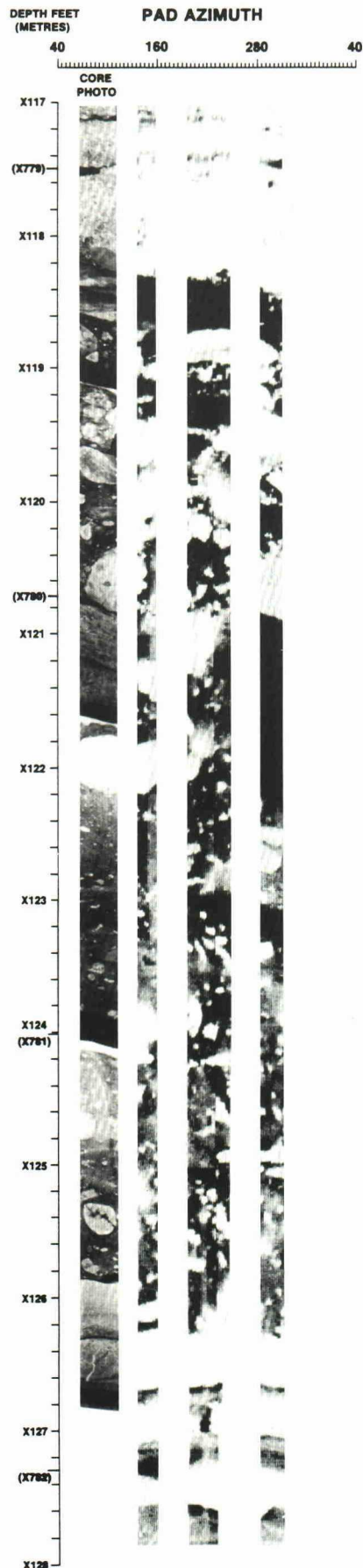
such as crossbedding, massive bedding, bioturbation, and imbrication (tilting of clasts in the same direction; *below left*).

Crossbedding is particularly important because it reveals paleocurrent direction, which can indicate preferential permeability direction and the orientation of the sand body.¹¹ Crossbedding may be more obvious on the images than on the core when the microresistivity contrast is greater than the visual one (*right and opposite page*). Bioturbation often appears as a vague mottling and can be confidently identified only when individual burrows are visible (*page 30, left*). Flaser bedding, when large enough to image, appears as crescent-shaped wisps of clay. Graded bedding is a fining upward or coarsening upward sequence (*page 30, right*).

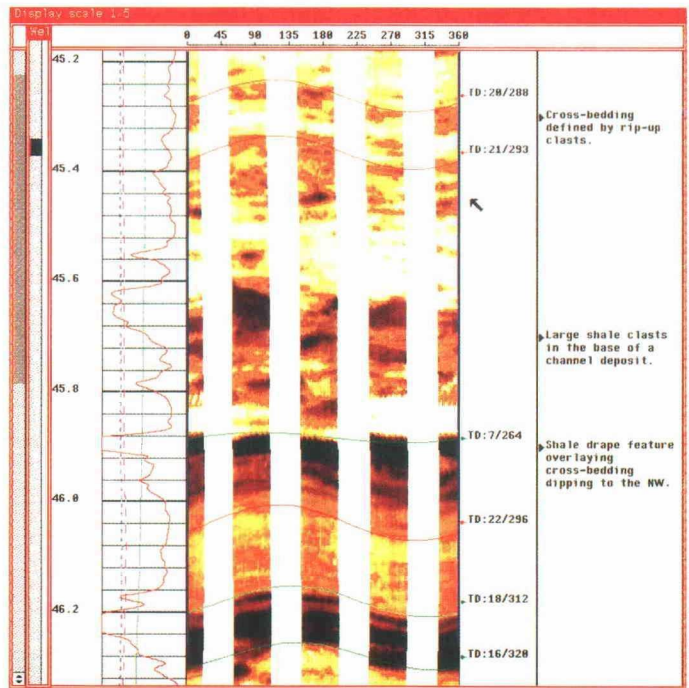
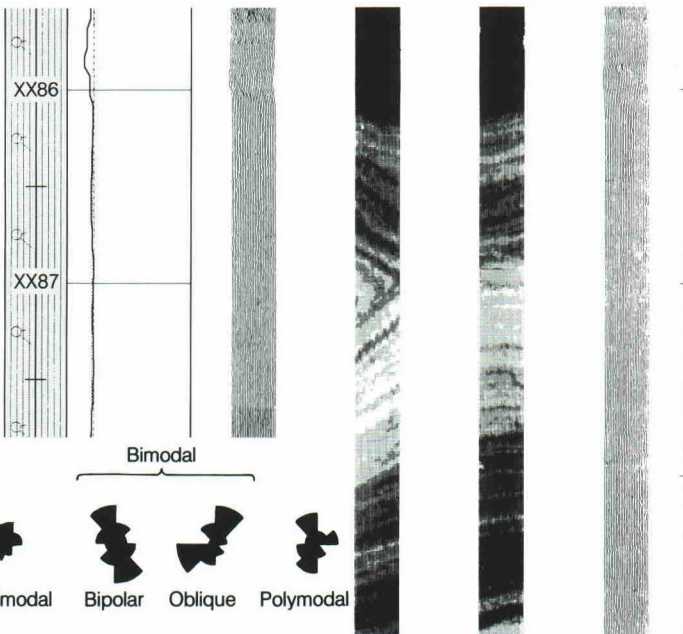
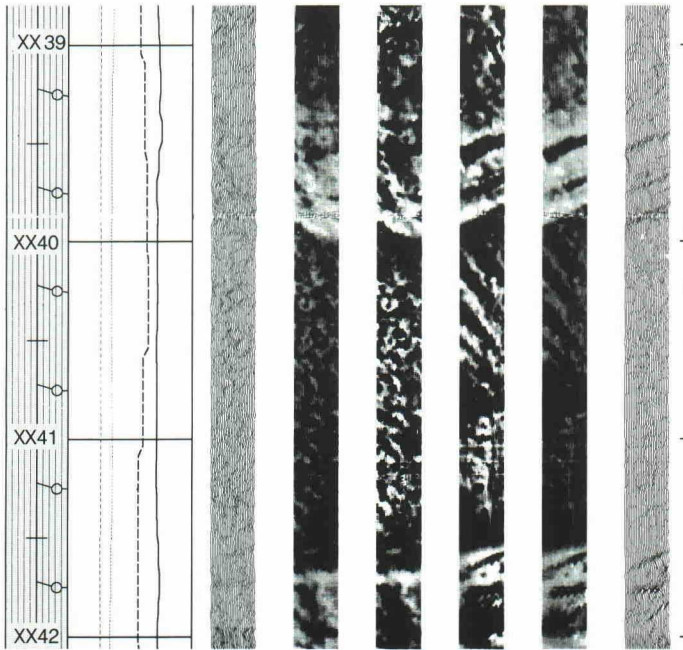
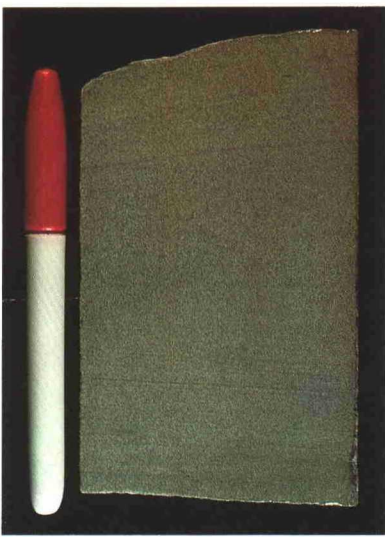
Rock texture is the size, shape and arrangement of the components of a sedimentary rock. Although the Formation MicroScanner tool is sensitive to microfeatures, its resolution is on the macro scale. Therefore, the only texture it can describe is that of a conglomerate or other rock with isolated clasts larger than its electrodes. Based on visible differences in texture, one can distinguish, among other things, angular clasts larger than about 1 inch [2.5 cm] from rounded ones, small clasts from large and whether the clasts are clast- or matrix-supported. Textures visible on images also include those formed by diagenetic nodules and by large shells (see "Images interpretable after calibration with core data," *page 36*).

Artificially produced features can also be identified from images alone. Sidewall core holes and holes from the probe of a formation tester show up clearly, and can be used for depth correlation and determining azimuth of the core or tester sample (*page 30, upper left and right*). Additionally, drilling-induced fractures can be identified (*page 26, upper left*), as well as grooves, bit

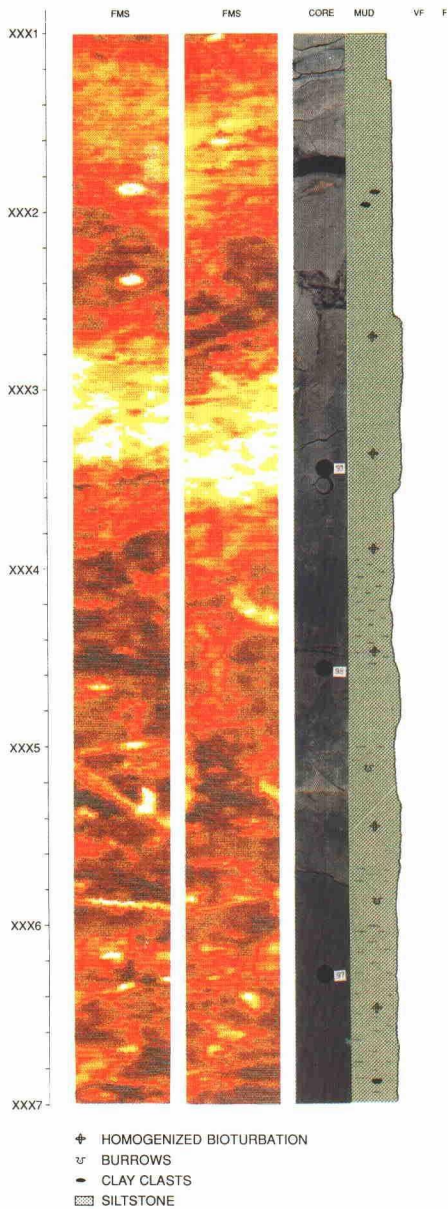
□ Two passes of a two-pad, dynamically normalized Formation MicroScanner log and core photographs of matrix-supported conglomerate, Scapa field, North Sea. Conglomerate is clearly identifiable from images where the resistivity contrast is great between the matrix and clasts. Clast diameter in this sequence is 1/2 inch [≈ 1 cm] to 12 inches [31 cm]. The image shows the clasts to be reverse-graded, although this is not clear from the core. The white areas from X117 to X118 meters are closely interlocked, clast-supported clay pebbles. The poor image definition results from poor resistivity contrast between pebbles and matrix. Between X126 and X128 meters are calcareous nodules, distinguished from the conglomerates by their shape, orientation, sharp bed boundaries and resistivity.



11. For statistical modeling of aeolian sand body geometry, see reference 3, Luthi and Banavar.

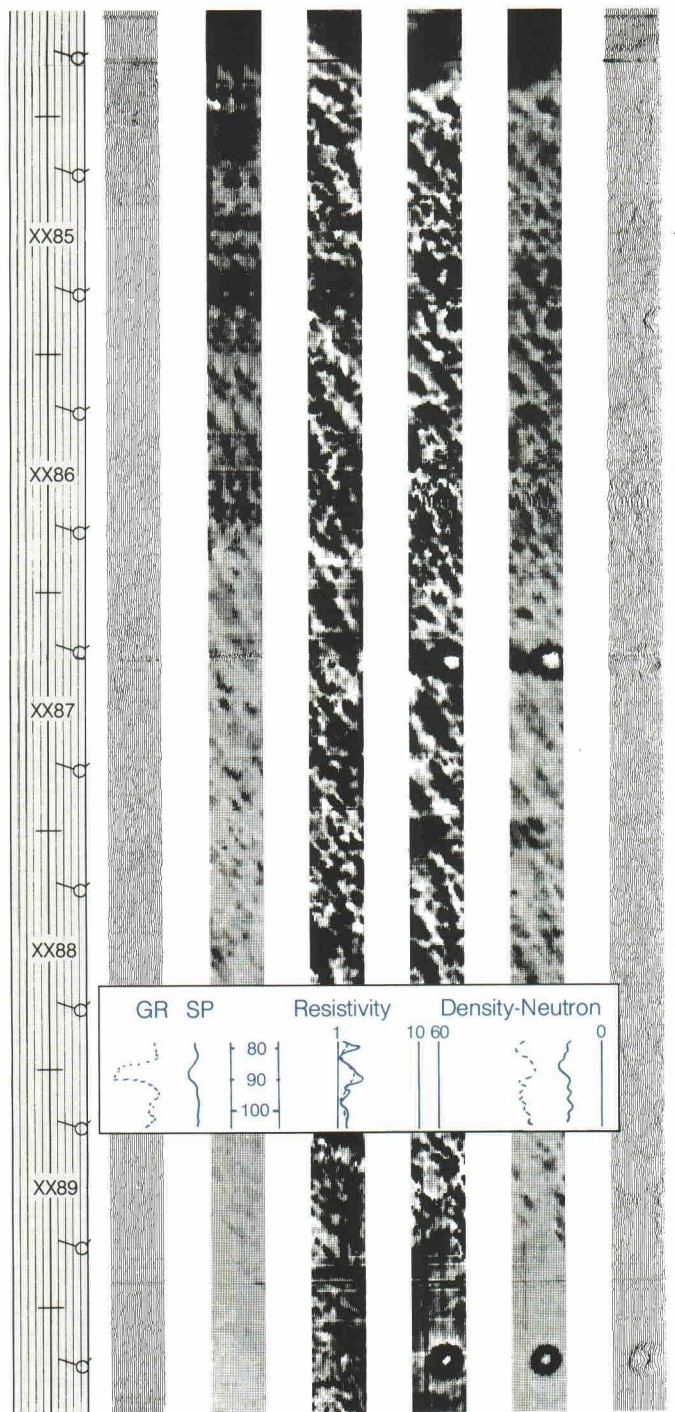


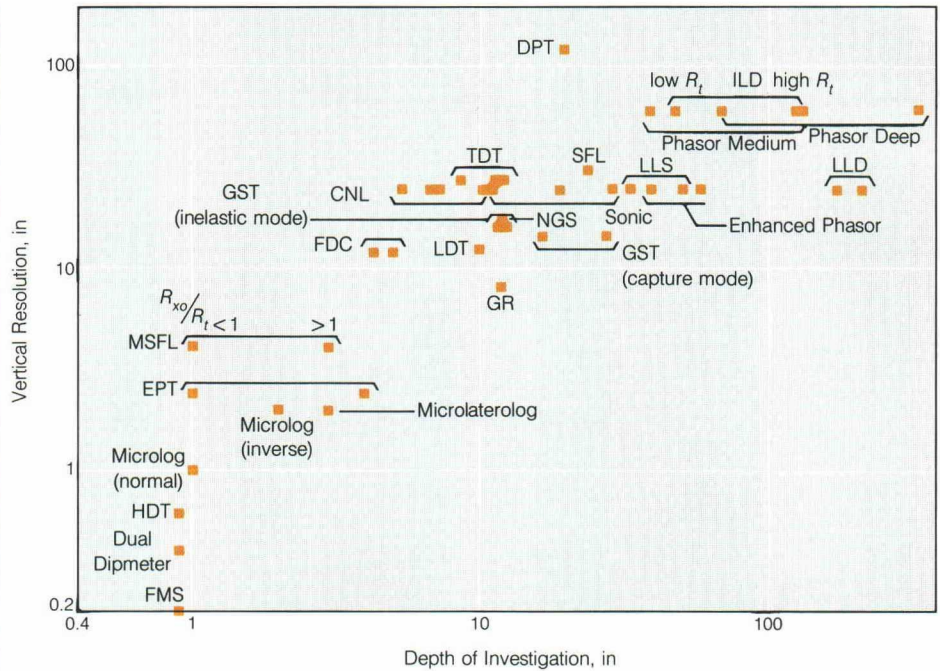
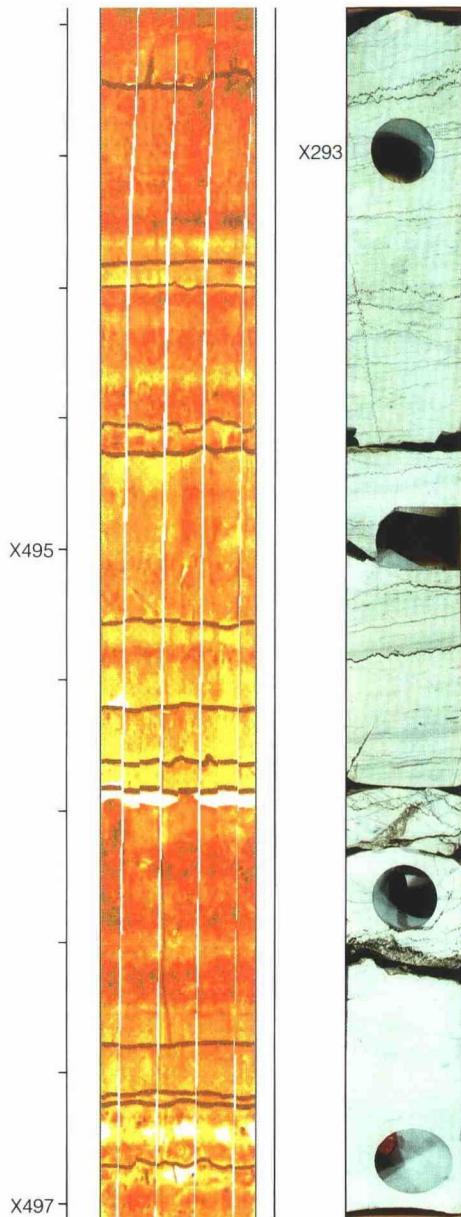
Four expressions of crossbedding. The core photo shows that crossbedding in sandstone can be so faint as to nearly escape detection in a hand specimen. The black-and-white logs show two types of crossbedding in Texas sandstones: bimodal, in which beds dip in any two directions (top log, between XX39 and XX41 feet and at XX42 feet), and a subset of bimodal called bipolar, in which they dip 180° apart (bottom log, around XX87 feet). Bipolar bedding is common in tidal environments; bimodal is common in fluvial environments and is characteristic of trough crossbedding. [Current azimuth models after Selley RC: "A Classification of Paleocurrent Models," Journal of Geology 76, (1968): 99-110.] The FMS Image Examiner presentation (color) illustrates a crossbedded fluvial channel overlain by a shale drape, from the Glauconitic formation, South Alberta, Canada. The presentation shows, from left, two caliper logs, a gamma ray log, an uncalibrated conductivity log obtained from measurement by one of the Formation MicroScanner buttons, and two passes of the two-pad tool. The conductivity trace shows the shales as more conductive than the sands; the image shows shale rip-up clasts and appears to be a better shale indicator than the gamma ray log. Also see log, page 25, top.



□ Two-pad Formation MicroScanner images (1:5 vertical scale) and core photographs of a sand (white, high resistivity) and shale (dark, low resistivity) in a bioturbated oil-bearing interval in a Southeast Asia well. The column headed "Mud VF Fine" refers to grain size based on core analysis. Clay clasts visible in the core appear as lense-shaped spots on the Formation MicroScanner image. A mineralized fracture just below XXX5 meters appears on the left image and core photograph. Several fractures on the core have no counterpart in the electrical image and so probably occurred during or after core retrieval. The images reveal broad variation in porosity and permeability of this otherwise average shaly sand reservoir. Combining Formation MicroScanner images and core enabled sedimentologists to characterize lithofacies changes in other wells in the field.

□ A two-pad Formation MicroScanner log of a fining upward sequence in the Frio sandstone, South Texas, and a hand specimen of South Arkansas sandstone showing flaser bedding formed in a delta. In the statically normalized images (outer tracks), the shale content can be seen gradually increasing upward to the shale bed at the top of the log. The dynamically normalized images show a diagonal trend probably due to borehole damage from vibration of drilling equipment. Holes from a formation tester probe are visible at XX87, XX85.5, and XX89.5 feet.





- CNL*— Compensated Neutron tool
- DPT*— Deep Propagation tool
- Dual Dipmeter* tool— Also known as the Stratigraphic High Resolution Dipmeter [SHDT] tool.
- EPT*— Electromagnetic Propagation tool
- FDC*— Compensated Density tool
- FMS— Formation MicroScanner* tool
- GR— Gamma ray
- GST*— Gamma Ray Spectrometry tool (capture and inelastic modes)
- HDT*— High Resolution Dipmeter tool
- ILD— Dual Induction Laterolog (DIL*) tool, deep

- LDT— Litho-Density* tool
- LLD— Dual Laterolog (DLL*) tool, deep
- LLS— Dual Laterolog (DLL*) tool, shallow
- MSFL— Microspherically focused log (MicroSFL)
- NGS*— Natural Gamma Ray Spectrometry tool
- Phasor*— Induction log (high vertical resolution)
- SFL*— Spherically Focused Resistivity log
- Sonic— Borehole compensated sonic tool
- TDT*— Thermal Decay Time tool

□ The relationship between vertical resolution and depth of investigation for some Schlumberger tools. Seismics would fall about an inch above the upper right corner, and scanning electron microscopy about an inch diagonally below the origin. The borehole televiewer has a depth of investigation of zero and vertical resolution of about 1 inch [2.5 cm] given optimal borehole conditions. The bar next to some measurements represents the range of the depth of investigation. Depth of investigation typically varies with diameter of invasion, drilling fluid resistivity, and resistivities in the invaded and virgin zones. Vertical resolution also varies with these parameters and, for some tools, with the effect of shoulder beds. In homogeneous formations, the High Resolution Dipmeter (HDT*), Dual Dipmeter and Formation MicroScanner measurements can penetrate as deep as the shallow laterolog (LLS), but in the usual setting they are very shallow.

□ Nearly complete borehole coverage from two passes of a four-pad Formation MicroScanner tool in a Paris basin carbonate, showing stylolites—dark, jagged bands that parallel bedding. The vertical gash above the stylolite near the top of the log could be a tension gash. A near-vertical fracture appears at about X496 meters. The core is a mudstone-wackestone from the Maiolica formation, Italy, with numerous stylolites that parallel bedding. Holes in the core are from plug sampling.

scraping, key seating, and helicoidal marks cut by the bit. Stylolites, which are typically found in tight rock, can be identified by their jagged character, although they sometimes must be found on core first (left).

Images interpretable with the help of other open hole logs

Highlights of integrating Formation MicroScanner and other logs appear in "Differentiating Causes of Spots and Mottling on Formation MicroScanner Images," (next page). A few points can be elaborated on here.

A chief consideration when integrating electrical images with other logs is the com-

parability of tool responses (above). Only the Dual Dipmeter and the High Resolution Dipmeter (HDT*) tools have responses that approximate that of the Formation MicroScanner tool. Most other tools view much larger volumes of the formation, both vertically and horizontally. Consequently, they support Formation MicroScanner data only for the largest features. If they respond to a feature at their resolution threshold, they may exhibit a "general trend" indicating that feature. For example, a 1-inch-diameter [2.5-cm] granite clast in conglom-

continued on page 35

Differentiating Causes of Spots and Mottling on Formation MicroScanner* Images

(Decision points in heavy outline)

This flow chart outlines some of the thinking that a geologist undertakes when analyzing images from the Formation MicroScanner tool. It touches on only the highlights of the most common situations, and does not include more complex modes of analysis nor the intuition and local knowledge that is integral to the art of log interpretation.

Log quality control: Can you see similar features on all pads? If not, some features may be artifacts from, for example, pad standoff on the high side of a hole deviated > 15°.

Are the features sharp or diffuse?
Diffuse **Sharp**

Sharp features visible on both pads are most likely formation features, not borehole artifacts.

May be reading mudcake. Check density log for mudcake build up, especially if diffuse image only on high side of a deviated hole. Also check that tool rotation is < 1 per 20 feet (excessive rotation wedges mud between the pad and borehole wall). Borehole breakouts may also produce diffuse images and tool sticking.

You want to determine what causes light (high resistivity) and dark (low resistivity) spots on a Formation MicroScanner Image
Clastics **Carbonate**

Examine gamma ray, resistivity and SP logs to grossly distinguish sands from shales.

Examine the shape and fabric of the spots.
shape **fabric**

Are the spots light (high resistivity)?

Examine the dark spotted (lower resistivity) interval on other open-hole logs.

Are very conductive peaks visible on Dual Dipmeter* log or resistivity traces of the Formation MicroScanner log?

Are they rounded?

Suspect a conglomerate or anhydrite nodules; compacted shale clasts often are rounded. Examine the spotted interval on other open-hole logs.

Angular light spots suggest:
 ● Shells (not commonly seen)
 ● Breccia
 ● Debris flow
 ● Anhydrite in-filling
 ● Borehole rugosity

● A few white spots suggests a **debris flow**, where matrix-supported pebbles or boulders tend to be spread out; upward coarsening common.
 ● A high density of white spots that touch each other suggests a grain-supported **conglomerate**; clasts that are well-rounded, well-sorted, imbricated and clast-supported suggest a high-energy depositional environment, such as a **beach**. Conglomerate at the bottom on a sand unit suggests **lag**.
 ● Clasts larger than the borehole diameter may look like beds; they suggest a high flow regime, commonly seen in **submarine canyon sill**; rare in fluvial settings. (Examine the boundary shape to distinguish clasts from beds. Clasts often have a concave top and convex bottom, whereas beds do not.)
 ● Mottling may be due to a **conglomerate of compacted clay clasts**.

Suspect pyrite nodules or crystals.

Does the gamma ray increase? and
 Do thorium and potassium increase? and
 Is there separation of neutron-porosity [ϕ_N] and density-porosity [ϕ_D] curves?

Suspect "vugs" in sandstone, which can occur if pebbles fall out of the borehole wall.

Suspect shale. Examine shapes of conductive spots and mottling on the Formation MicroScanner image.

● Is $P_e < 3$? and
 ● Is the gamma ray 50 to 80 API? and
 ● Are there slight increases in thorium and potassium?

$P_e > 3$, decrease in neutron-density porosity [ϕ_{ND}], gamma ray < 50 API, and slight increase in ρ_{ma} suggests anhydrite or calcite nodules in sandstone.

Probably a clastic conglomerate.

To differentiate anhydrite and calcite nodules, examine the Matrix Identification Plot (CP-21, Schlumberger Chart-book); alternatively, is there a large increase in ρ_{ma} ?

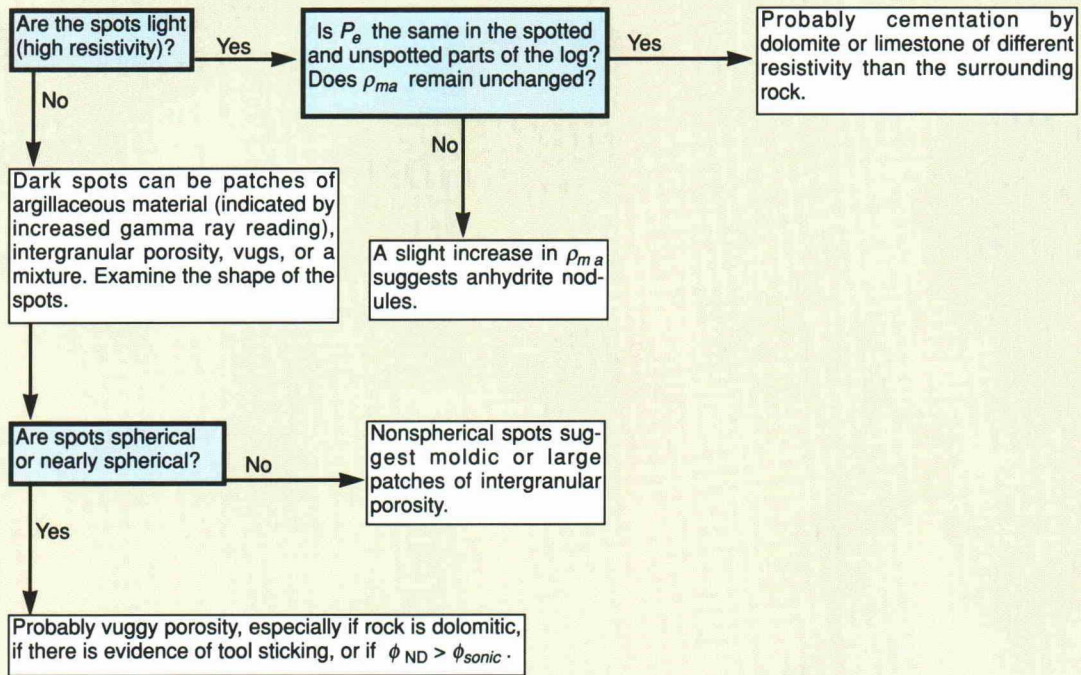
A small increase in ρ_{ma} usually indicates calcite.

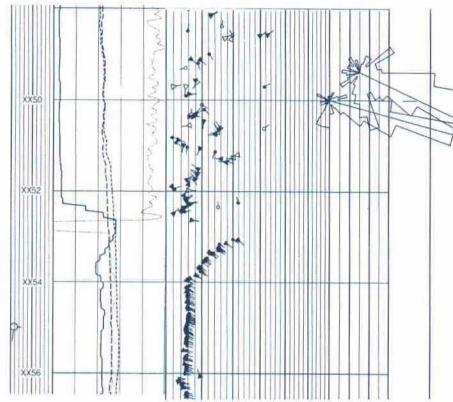
Probably anhydrite nodules, but because anhydrite and calcite have a similar P_e , a medium amount of anhydrite will look the same as a large amount of calcite nodules.

Flat **Rounded**

Wavy mottling suggests **Flaser bedding** (derives from fines deposited in a trough; laminations sometimes visible; common in deltas); **angular spots or mottling** suggests structural shale (shale in the form of chips, grains, or both) or rip-up clasts; may be a low volume of pyrite.

Rounded to oval spots suggest burrows (common in barrier systems).



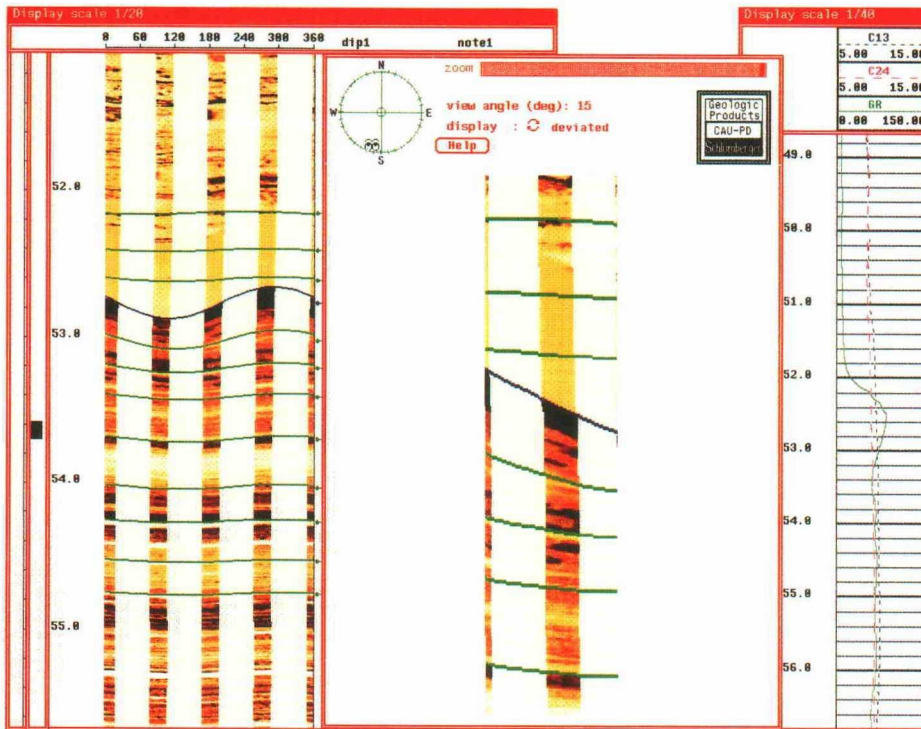


between these extremes—with some exceptions. In a study of a Canadian carbonate reef, adding flowmeter data to a full logging suite and Formation MicroScanner images enabled engineers to identify zones of well-developed intergranular porosity, where flow into the wellbore was greatest.¹²

The four-pad Formation MicroScanner tool will eventually replace the conventional dipmeter because it allows dip determination in all types of borehole drift, even in the presence of fractures and when lateral continuity is partially lost. Until then, however, the Dual Dipmeter tool is one of the most useful ancillary logs, since it is made from the same pads as the two-pad Formation MicroScanner measurement and requires minimal depth shifting. The dipmeter is used to estimate the shape, depth and azimuth of the sand body to help position offset wells. In a US Gulf Coast study of braided stream environments, integrating dipmeter and Formation MicroScanner data resulted in hitting the target sand in 73 percent of offset wells, whereas the typical success rate without the two logs was 26 percent (left).¹³

With the industry trend toward deep-water and younger reservoirs, often of turbiditic origin, more attention is being paid to analysis of "thin beds"—for logging purposes beds below the resolution of conventional open hole logs. This is a key area where Formation MicroScanner and other open hole logs can work together (right, far right). Formation MicroScanner images have received mixed reviews in thin beds: some report that FMS images are not much better than BHTV images;¹⁴ others find that FMS images can compensate for deficits in BHTV logs.^{12,15}

In some thinly bedded reservoirs of the Middle East, North America and the North Sea, conventional logs will report an accurate porosity across a given interval, but won't reveal its distribution. When beds are more than 1 inch [2.5 cm] thick, Formation MicroScanner images can help determine the distribution of porosity anisotropy and assist in estimating the location of vertical permeability barriers (next page, top). Experience in thin turbidites of the Scapa field in the North Sea shows that Formation MicroScanner images can assist calculation of net pay of porous zones determined by high-resolution sampling (1.2-inch, rather than 6-inch) of porosity logs.¹⁶ The key to

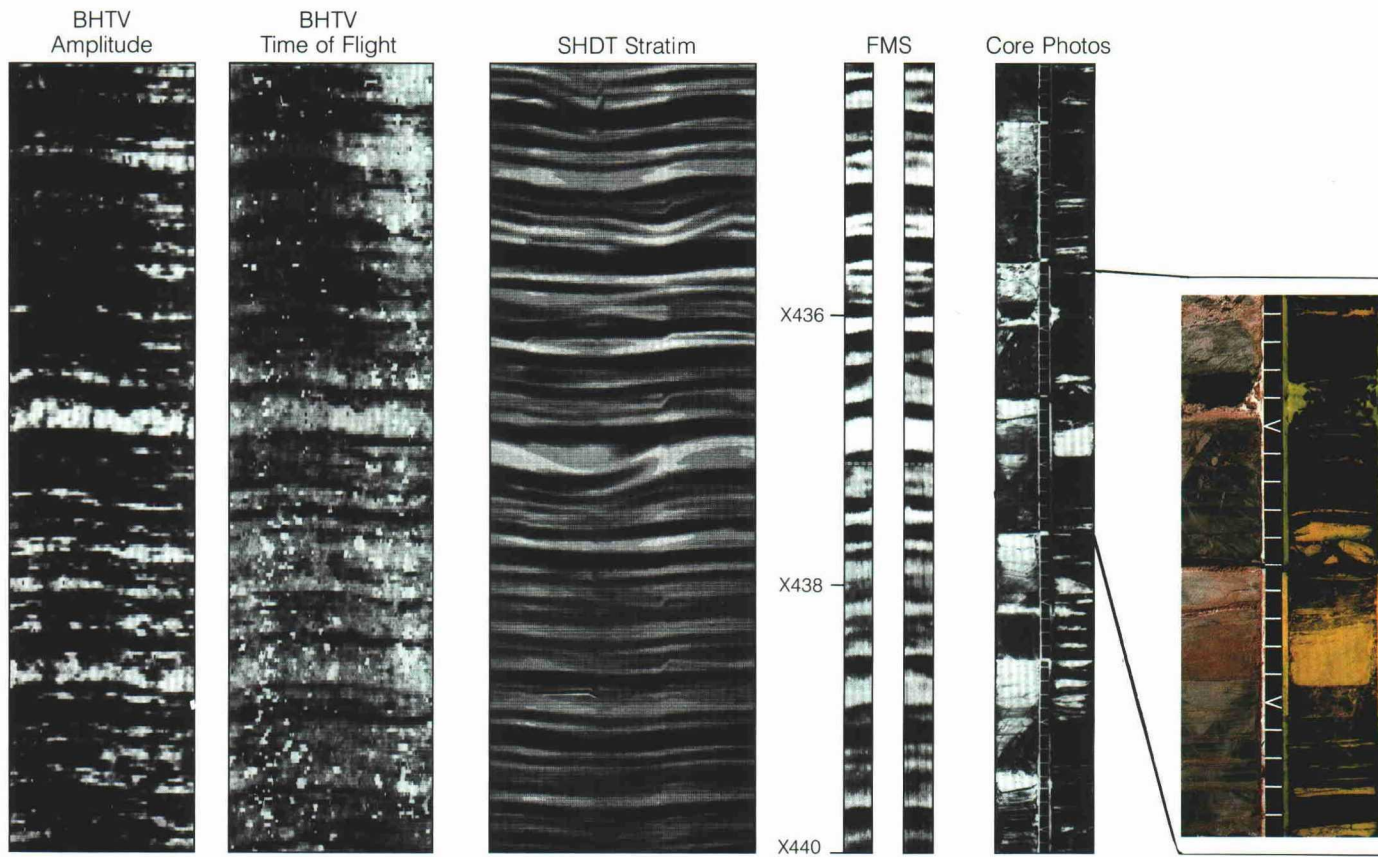


□ Identification of a normal fault in Canadian Mississippian carbonates and shales using the Dual Dipmeter tool (above, right) and one pass of the four-pad Formation MicroScanner tool, static normalization over 1 meter. The tracks in the dipmeter log are, from left, gamma ray, two calipers and conductivity. The dipmeter log shows random dips above the fault zone, a jump in conductivity at the fault zone, then dips decreasing with depth below the fault. The decrease in dips is clearly visible on the straight (left) and three-dimensional Formation MicroScanner outputs. The gamma ray track clearly marks the change in lithology above and below the fault at XX52.5 feet.

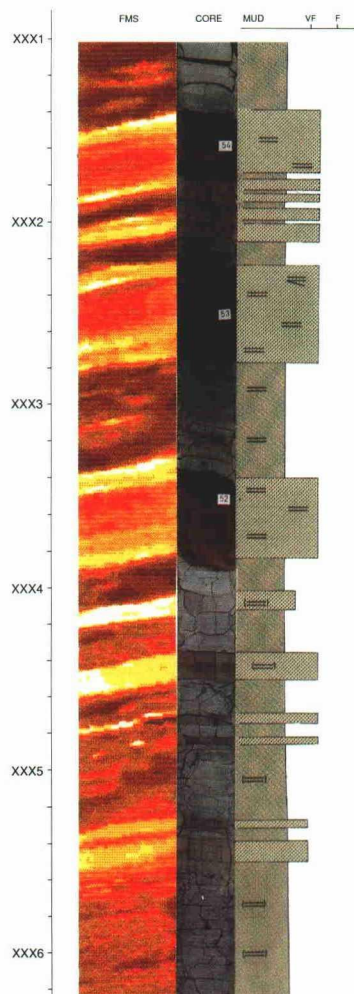
erate is far below the resolution of the NGS tool, but if the granite is rich enough in thorium and potassium, and there are enough similar clasts over a large enough interval, an increase in the thorium and potassium curves may register across the conglomerate. Likewise, the Litho-Density* tool can help distinguish coal and nodules of anhy-

drite, calcite and pyrite if they represent 5 to 10 percent of the rock volume, depending on the mean atomic number of the nodules.

Which open hole logs are integrated with images varies tremendously. In some development areas, for example, the log analyst is lucky to have more than a gamma ray, a spontaneous potential (SP) log, and a resistivity log. In more complex formations, a complete suite of nuclear, electrical and sonic logs may accompany the Formation MicroScanner images—as well as core photographs and comprehensive drilling and mud logs. The typical well lies somewhere



□ Two-pad Formation MicroScanner images at their resolution threshold in a thinly bedded sand and silty shale interval in a US Gulf Coast well. Comparison of borehole televiwer images, computed stratigraphic Stratim* imaging from the Dual Dipmeter tool, Formation MicroScanner images, and white-light and ultraviolet core photos (with 1/10-foot divisions) shows that the thinnest beds consistently reported by all tools is 1 1/2 inches [=4 cm]. No tool measurement represents each bed, but the resistivity logs more accurately reflect the true number of beds seen on the core photographs. In general, one would expect the televiwer to show more sand beds than the resistivity tools, which tend to show conductive features more clearly than resistive ones. The Formation MicroScanner image was processed in the dynamic normalization mode, which maximizes locally the number of gray shades for the microresistivity contrasts. This processing blurred the distinction between sands and shales, since similar gray shades do not indicate similar resistivities. Reprocessing with static normalization solved this problem but did not change the bed resolution of the images.



□ Well-defined alternation of thinly-bedded sandstone and siltstones in an oil-bearing zone of a Southeast Asia well. Shallow marine shales appear dark red on the Formation MicroScanner image; fine- to very fine-grained siltstones appear as white or yellow streaks. Wide spacing of these beds, some as thin as 1 inch (2.5 cm), permits good correlation between the images and the core. Clay clasts appear in the image as white ellipses and thin lenses.

12. Reference 3, Dennis et al.
13. Grace LM and Stephens WC Jr: "Exploration in Braided Stream Environments Using Dipmeter Analysis," *AAPG Bulletin*, 71 (1987): 238-239 (abstract).
- Grace LM, Luthi SM and Pirie RG: "Stratigraphic Interpretation Using Formation Imaging and Dipmeter Analysis," paper SPE 15611, presented at the 61st SPE Annual Technical Conference and Exhibition, New Orleans, October 5-8, 1986.
14. Reference 3, Hackbarth and Tepper.
15. Laubach SE, Baumgardner RW Jr, Monson ER, Hunt E and Meador KJ: "Fracture Detection in Low-Permeability Reservoir Sandstone: A Comparison of BHTV and FMS Logs to Core," paper SPE 18119, presented at the 63rd SPE Annual Technical Conference and Exhibition, Houston, October 2-5, 1988.

- ≡ FAINT BEDDING
- ≡ HORIZONTAL LAMINATION
- ≡ LOW ANGLE NON-LAMINATION AND HORIZONTAL LAMINATION
- ▨ SILTSTONE
- ▨ SHALE

this application of Formation MicroScanner logs is using images with static normalization, in which like porosities are indicated by like gray or color scales, rather than dynamic normalization (see page 19).

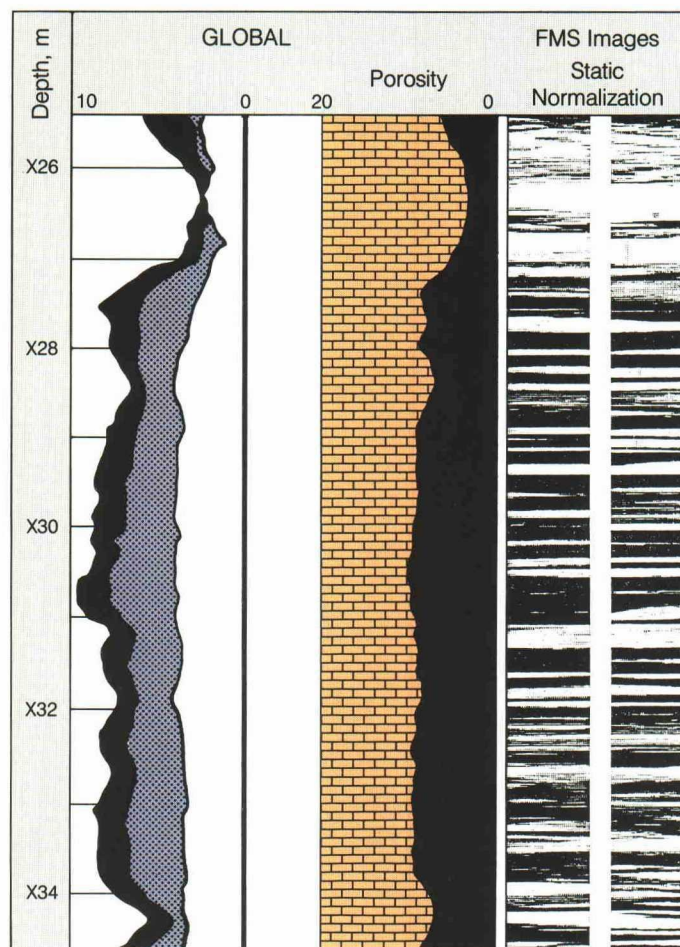
The degree of sorting is sometimes apparent on images alone. When it is equivocal, however, porosity logs can provide a rough indicator. In general, if total porosity is less than 25 percent, suspect poor sorting; if it exceeds 25 percent, suspect good sorting. In carbonates, images do not reveal the nature of the cement (calcitic, dolomitic or anhydritic), which is needed to understand diagenetic events that may indicate the location of the oil leg. In general, a high photoelectric cross-section index, P_e , and low matrix density, ρ_{ma} , indicate calcite, a high P_e and high ρ_{ma} indicate anhydrite, and a low P_e and high ρ_{ma} dolomite. As a further test (on cuttings, for example) hydrochloric acid [HCl] will dissolve calcite, slightly attack dolomite, but not anhydrite.

Images interpretable after calibration with core data

Core calibration of Formation MicroScanner images is needed in many heterogeneous formations in which mottling has no self-evident pattern and no conclusive signature on open hole logs. For example, bioturbation that is conductive may show up as an increase in the gamma ray log if the creatures concentrated clays. But the burrows may be filled with calcite (low neutron porosity, bulk density of 2.71 gm/cc) or coal (high neutron porosity, bulk density less than 2 gm/cc.) Once bioturbation is identified, the orientation of the burrows tells something of the depositional environment. Vertical burrows suggest a high-energy, shallow-water environment, in which the animals "dig in" vertically to escape scouring currents. Horizontal burrows suggest a low-energy, deep-water environment.

Fossils are often key indicators of depositional environment, not only by species, but by sorting, distribution, and orientation. Once they are identified on core, they may be recognizable on Formation MicroScanner images, which can help extend interpretation to offset wells (*right*).

Stylolites are jagged, teeth-like sutures that occur in carbonates and occasionally in sandstones. They contain insoluble compo-



□ Porosity indicated by GLOBAL* output computed from conventional open hole logs and layering by a statically normalized two-pad Formation MicroScanner image, Shuaiba chalk, Middle East. Porosity is black in both presentations. Although the GLOBAL output correctly predicts the average porosity value, the Formation MicroScanner images show porosity distribution and strong anisotropy caused by thinly bedded layers. Porosity in conductive and resistive beds varies by up to three orders of magnitude, from 2 porosity units (p.u.) to almost 9 p.u. Evaluating thin beds like these is also crucial in the US Gulf Coast where half the oil in some wells is in sands thinner than 2 inches [5 cm].

nents of the rock—clay, carbon and iron oxides—and are usually parallel to bedding in tight zones, acting as vertical permeability barriers. They are also known to be paths for diagenetic processes and as such become sites for development of secondary porosity.¹⁷ Once identified on core, they may be correlated on images and may become powerful predictors of vertical permeability barriers.

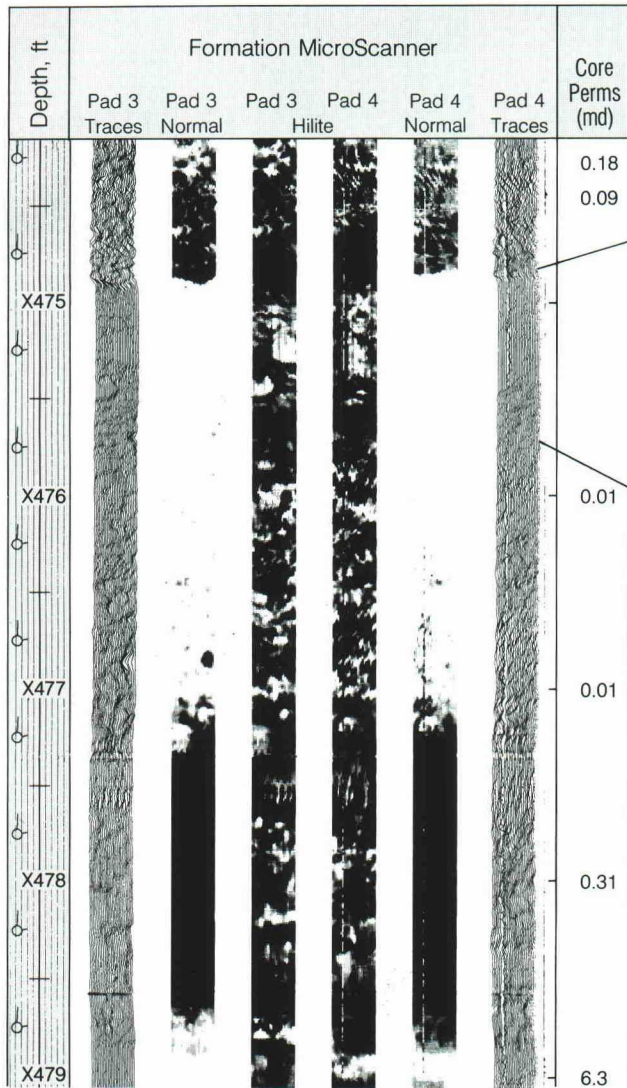
Emerging interpretation methods

The cutting edge of Formation MicroScanner interpretation is concerned with the integration of images with data from several techniques. A particularly active area of investigation is how to use information about rock texture provided by the images.

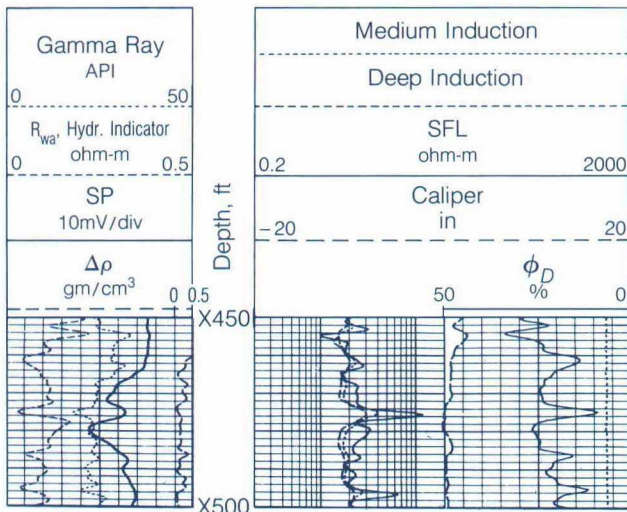
In carbonates, identifying heterogeneities in porosity can be crucial for reservoir development. These heterogeneities often have a textural component that is evident on Formation MicroScanner images. Scientists with Schlumberger Middle East have integrated these images with core data and porosity logs run at high sample rate, and

proposed a geometrical classification of "porosity heterogeneities." This classification focuses on the distribution and density of features on the decimeter scale (about 4 inches)—such as vugs, molds, fractures and micropores.¹⁸ The purpose of this classification is to assist mapping and correlation of facies, identify permeability anisotropy, and aid modeling of depositional environment and diagenesis.

In this scheme, carbonate porosity is grouped into three geometric types: layered, isolated and interwoven. Layered porosity beds have maximum flow parallel to bedding; isolated porosity beds have poor permeability in any direction even with medium to high porosity; and beds of interwoven porosity have a mixture of porous and non-porous intervals. This scheme is useful for reservoir engineers who average porosity data with mathematical models. They model layered porosity as a parallel permeability system, isolated porosity as a series permeability system, and interwoven porosi-



□ An oil-water transition zone between glauconitic sands with and without fossil shells, Olmos formation, South Texas. From conventional open hole logs and the two-pad Formation MicroScanner images, it is impossible to tell that shells are abundant below X475 feet. Shaliness increases and porosity drops from X476 to X480 feet; the large kick in the induction indicates a limy interval; the cross-over between shallow and other measurements signals the shaly interval, and the curve separation below flags a clean sand. No definite features are visible on the images. The core, however, shows the top of the shell debris section, which marks the top of the oil-water zone. The sand below the shell debris was a marginal producer, yielding no more than 20 barrels of oil per day and some water.



ty as either parallel or series, depending on how the porous components are oriented with respect to flow. Formation MicroScanner images supply useful information about each of these porosity types (see "Identifying Carbonate Porosity Types with Formation MicroScanner Images," next page).

Another development is a texture-recognition computer program that permits interpreters working on the FMS Image Examiner workstation to quickly and interactively pick key lithofacies.¹⁸ Now users must do this manually, scrolling sometimes through hundred of feet of images. The program was devised mainly to save time, but it can also provide, for example, an automatic sand count based on the texture differences between sands and shales.

The program assumes that textures discernable on Formation MicroScanner images correlate with lithofacies characteristics. In this system, the user selects an image texture of interest (for example, a conglomerate or a mudstone) and the computer finds similar Formation MicroScanner images using a histogram-similarity transform.

In tests, S.A. Wong of Texas A&M University and Schlumberger coworkers, found that the algorithm located 30 to 50 percent of the lithofacies it was expected to find. The success rate increased to 65 percent if two targets of the same lithofacies were selected, giving the system better knowl-

16. McGann GJ, Riches HA and Renoult DC: "Formation Evaluation in a Thinly Bedded Reservoir A Case History: Scapa Field, North Sea," *Transactions of the SPWLA 29th Annual Logging Symposium*, San Antonio, Texas, June 5-8, 1988, paper V.
17. Carozzi AV and Von Bergen D: "Stylolitic Porosity in Carbonates: A Critical Factor for Deep Hydrocarbon Production," *Journal of Petroleum Geology* 10, (1987): 267-282.
18. Nurmi R, Charara M and Waterhouse M: "Heterogeneities in Carbonate Reservoirs: Detection and Analysis Using Borehole Electrical Imagery," presented at the London Geological Society, London, June 1988.

Identifying Carbonate Porosity Types with Formation MicroScanner Images¹⁸

Porosity Type	Characteristic Features Visible on Images
"Layered"	Resistive vs conductive cementation ("selective cementation") Crossbedded grainstone Stylolites (after core calibration) Thin beds
"Isolated"	Anhydrite nodules (after conventional open hole log calibration) Patchy distribution of cements Vuggy porosity (with open hole and caliper data) Leached fossils (after core calibration)
"Interwoven"	Dual (or multiple) porosity system indicated by various shades on statically normalized images. Although usually free of clay, the higher porosity component appears darker (more conductive) than the lower porosity component. (Images can help determine the vertical extent of high and low porosity components. For example, fractures often predominate in the lower porosity component.)

edge of the texture. Due to natural variations within lithofacies, the limited resolution of the scanner and other data processing constraints, Wong and colleagues suspect that an 80 percent success rate may be the limit.

A method for calculating fracture aperture at the borehole has also been developed using information from conventional logs and the Formation MicroScanner tool.¹⁹ The core of the method is an algorithm developed by Stefan Luthi of Schlumberger-Doll Research, Ridgefield, Connecticut, which extended work begun by Philip Souhaité, formerly of Etudes et Productions Schlumberger, Clamart, France. The algorithm relates aperture to the additional current flow from the tool caused by a fracture,

mud resistivity (R_m), and R_t . Based on studies of a well in granite-gneiss in Connecticut, fracture apertures calculated by this method are close to those calculated from an investigational sonic method using Stoneley wave reflection data.²⁰ This method takes a step toward calculating fracture hydraulic permeability, but much remains to be done before a commercial service is available.

The Formation MicroScanner tool has ushered in an era in which improving the resolution of other log measurements has become a priority. But solving an oil company's problems involves more than seeing the well in finer vertical detail. Scientists are hoping that the better they can see features that intersect the well, the better they will be able to find ways to quantify their lateral extent. The ultimate goal is not only to characterize the borehole wall—that infinitesimally small but critical part of the reservoir—but also the unprobed territory beyond.

—JMK

19. Luthi SM: "Width Determination of Fractures Intersecting a Borehole," U.S. Patent Application Serial Number 252,958, filed October 3, 1988.

20. Johnson DL, Hornby BE, Winkler KW and Plumb RA: "Fracture Evaluation from the Borehole Stoneley Wave," 1987 AGU Fall Meeting Program, *Eos* 68 (1987): 1503 (abstract T51C-07); *Geophysics* (in press).

Plumb RA and Hornby BE: "In-situ Stress Directions and Permeable Fractures in the Moodus #1 Well: Measurements from Experimental Ultrasonic Image and Stoneley Wave Logs," *SDR Research Note*, May 11, 1988.

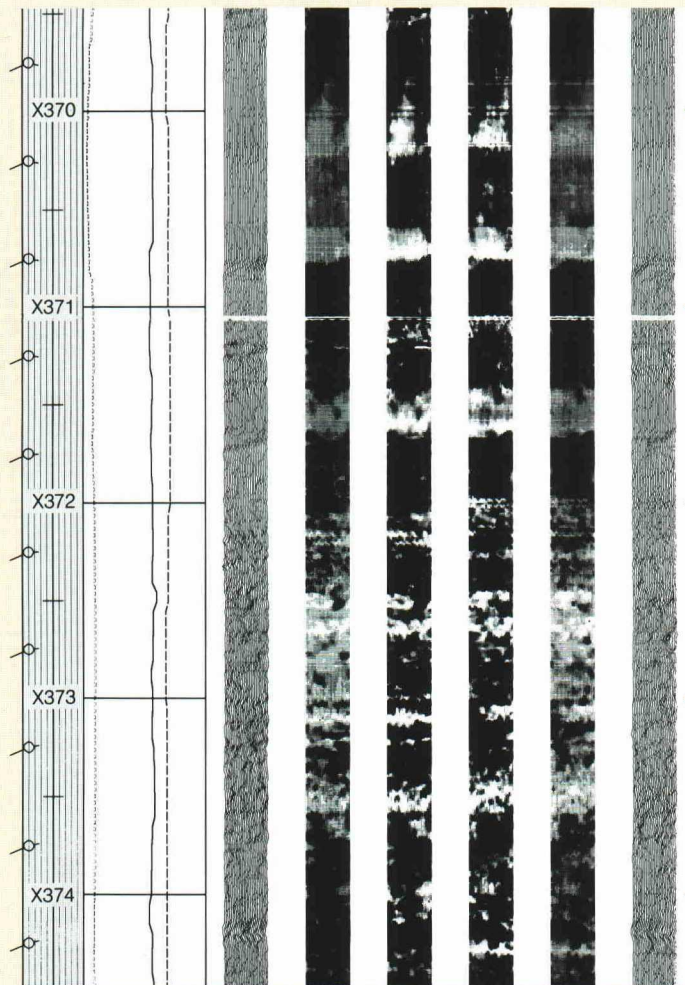
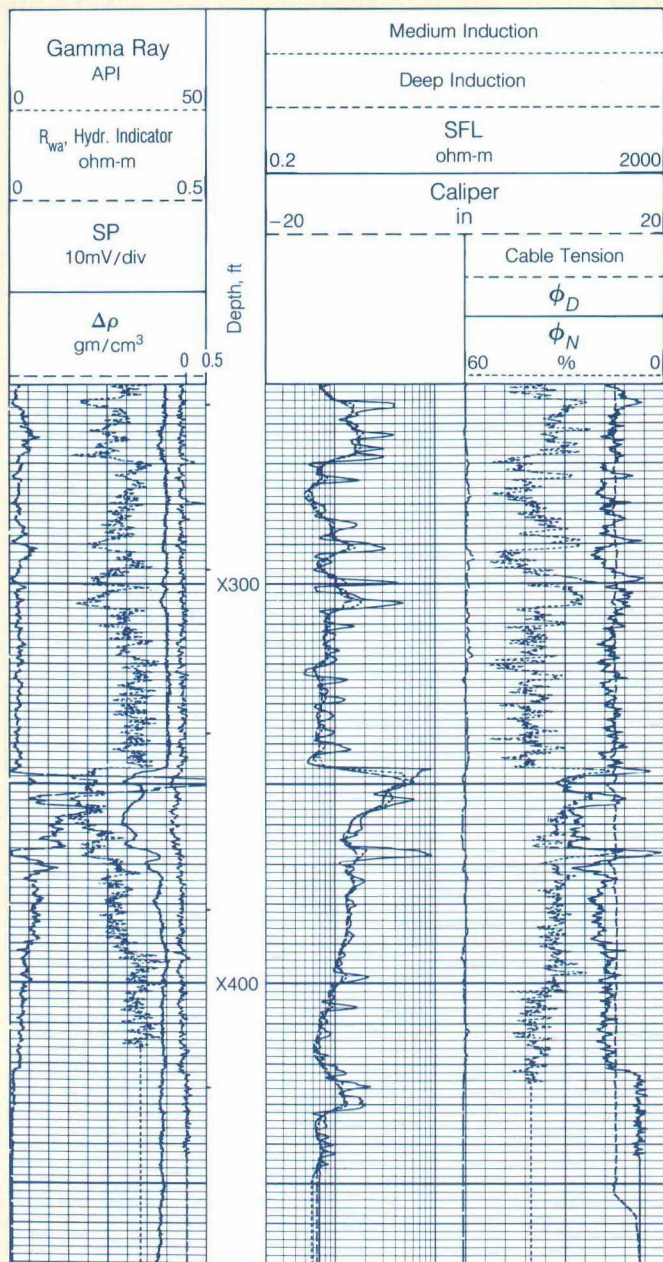
The basic question in interpreting logs of wildcat wells is what depositional environments the well intersects. Local knowledge suggested this well was probably in a regressive or transgressive sequence or a delta, so the interpreter, Tom Fett, of Schlumberger, Corpus Christi, Texas, at least had a place to hang his hat. Here is how he approached the logs and core.

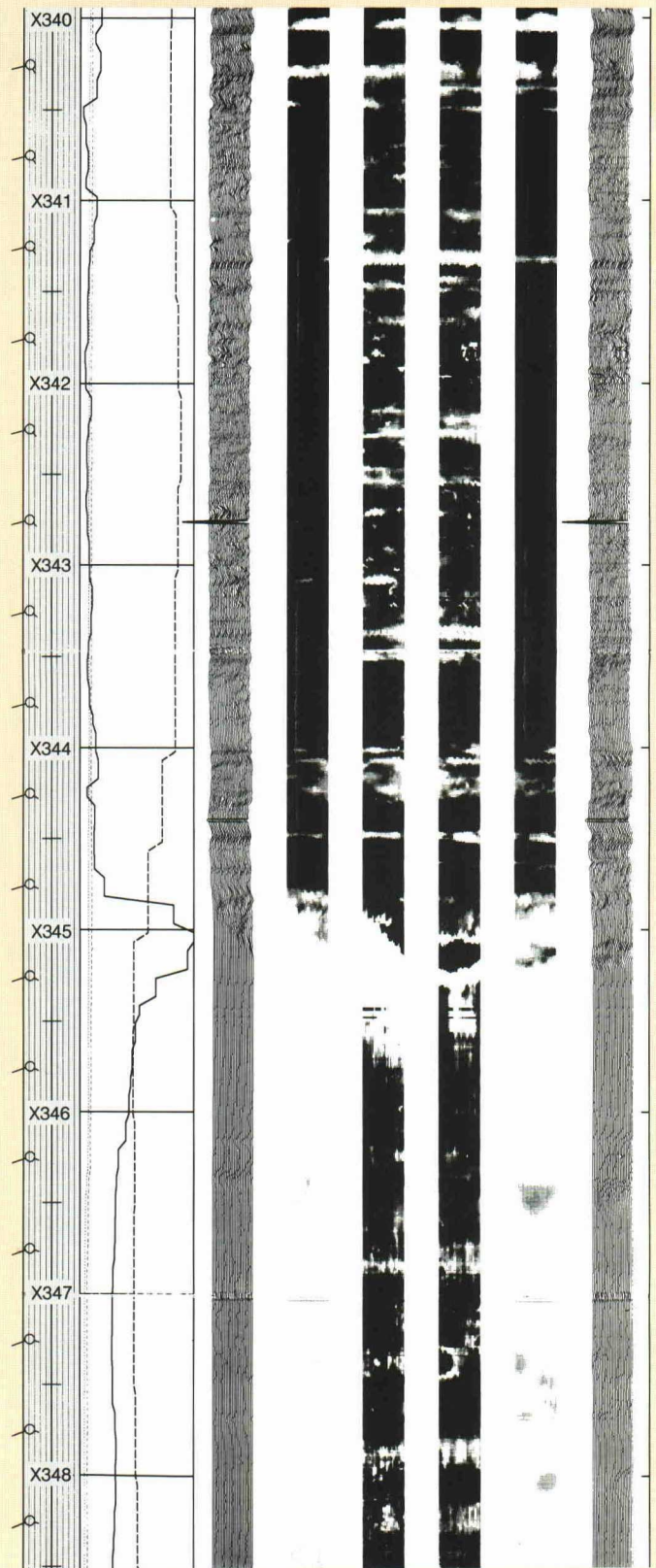
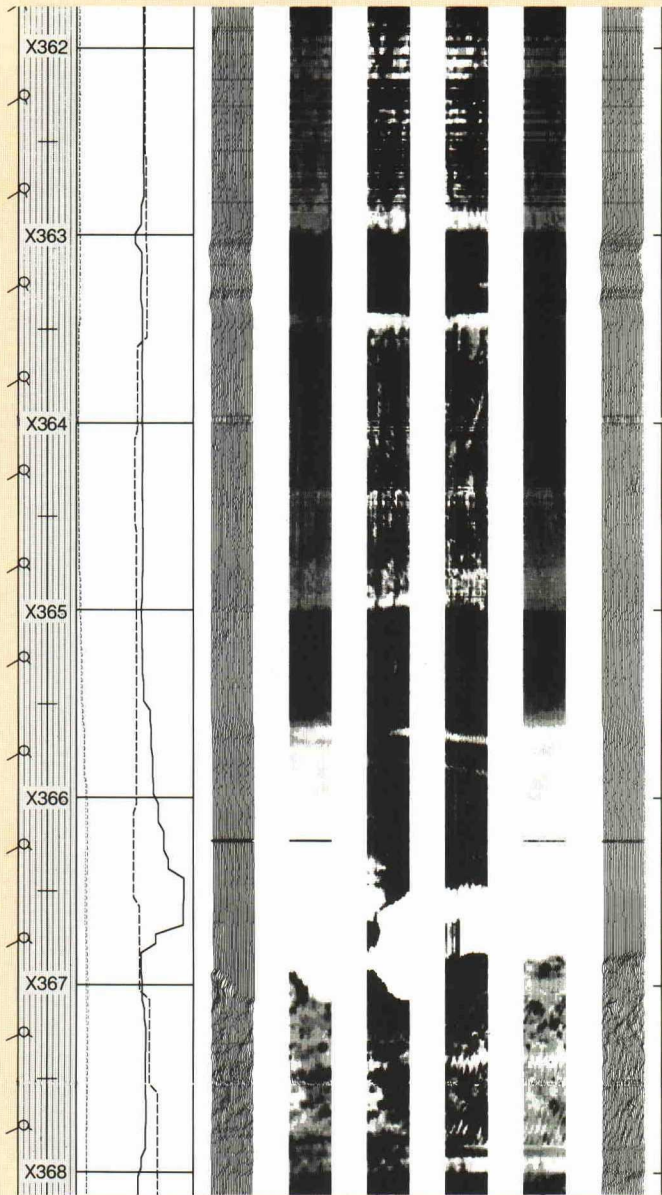
Beginning at the bottom of the interval, from 7396 to about 7372 feet, the logs show a mottled, heterogeneous shale with rounded conductive features that suggest burrowing. At 7371 feet, the gamma ray and spontaneous potential logs kick to the left, indicating a drop in shaliness. The image shows a corresponding sand pulse at 7371.5 feet, and another at 7370 feet. With each sand comes a decline in mottling in the image. At 7367 feet, a resistive (bright white) feature appears on the image and as a low point on the density logs. This is possibly a cobble indicating a lag deposit, and an increase in depositional energy. The image above 7366 feet shows a nonburrowed sand, possible crossbedded, also suggesting an increase in depositional energy. At 7363 feet, a pulse of shale intrudes into the sand, but the next 12 to 15 feet are largely shaly, silty sands. This is supported by the high permeabilities of sidewall cores from 7347 and 7348 feet (core holes are visible on the statically normalized image).

The story changes again at 7345 feet, where the dark, homogeneous images indicate a marine shale. (Continental and near-shore shales tend to be gray and mottled; deep-water shales are usually dark black and nearly featureless.) Analysis of a sidewall core at 7341.5 feet bears this out—a massive, low permeability silty shale. (The hole from this core is visible on the image.)

This is the most basic interpretation—primarily a description of what is seen on the logs and images. This interpretation can be expanded to include depositional environment. A probable scenario is a lagoonal deposit, rich in bioturbation, followed by an influx of silty, muddy sand, which choked off the organisms living in the mud, followed by intermittent pulses of silty, muddy sand. Finally, the sea encroached over the land, burying the sand in deep marine sediments which became shales.

Gulf Coast Case Study: A Marine Transgressive Sequence, Wildcat Well, South Texas





Cover

Bob Demicco (pointing), associate professor of geologic sciences at the State University of New York at Binghamton, discusses a thinly bedded Devonian limestone of the Catskill (New York) delta with Russ Hertzog (left), a nuclear physicist with Schlumberger Houston, and Ulf Bayer, a visiting mathematical geologist at Schlumberger-Doll Research, Ridgefield, Connecticut. The subtidal limestone, with beds 1 to 10 centimeters thick [2.5 to 25 inches] is known locally as ribbon limestone. The outcrop is part of the Indian Ladder escarpment, Manlius formation, Helderberg group, in John Boyd Thatcher State Park, about 20 miles southwest of Albany, New York. At right is a core photograph and Formation MicroScanner log of a thinly bedded sand-shale sequence from Southeast Asia.

Pictures Worth a Thousand Words!

Put *Technical Review* to work with color view-graphs and 35-mm color slides of the illustrations from your favorite articles. Hurry your order by calling 713-928-4920.



Technical Review color view-graphs and slides are perfect for

- Lectures
- Courses
- Sales presentations
- Technical publications
- Continuing education

View-graph sets are delivered in protective plastic sleeves for easy storage in a three-ring binder. Slide sets are prepared by a custom lab to meet the highest standards of clarity and color rendition. They are mounted in sturdy, jam-resistant plastic mounts.

Select the view-graphs and slide sets you want and fill in the appropriate information from the table on the business reply card. Please allow 3 weeks for delivery. Rush service—1-week delivery within the US and 2-week delivery outside the US—doubles the cost of each set.

For more information, contact Schlumberger Educational Services, P.O. Box 2175, 5000 Gulf Freeway, Houston, Texas 77252, (713)-928-4920.

The Technical Review

The Quarterly Magazine for the Oil-Field Professional

Set No.	Article Title	No. of Slides	Set Price
1	The LOGNET® Communications Network: Bringing the Well Site to the Client (April 1986)	11	\$110
2	Logging Through Glass: Telemetry for the 1990s (April 1986)	10	\$100
3	Offset Seismic Profiling in the Jatibarang Volcanics, Java (April 1986)	8	\$ 80
4	Oil-Water Dynamics in Porous Media (April 1986)	14	\$140
5	The Perforation: Crucial Link in the Production Chain (July 1986)	13	\$130
6	Tubing-Conveyed Perforating (July 1986)	15	\$150
7	Perforated Completions: Design and Test (July 1986)	9	\$ 90
8	A Millisecond of Shaped-Charge Physics (July 1986)	11	\$110
9	Making Shaped Charges (July 1986)	9	\$ 90
10	Horizontal Fractures: Debunking a Myth (October 1986)	4	\$ 40
11	Basics of Failure Mechanics (October 1986)	21	\$210
12	Fracturing: Theory Behind the Practice (October 1986)	18	\$180
13	Formation Collapse in a Producing Well (October 1986)	10	\$100
14	Raymond Sauvage: Recollections of Schlumberger Wireline's First Four Years (January 1987)	16	\$160
15	Acoustic Waveforms Explained (January 1987)	12	\$120
16	Fracture Detection with Logs (January 1987)	12	\$120
17	Induction Logging: Evolution of a Technique (January 1987)	16	\$160
18	Elements of Borehole Seismics (April 1987)	20	\$200
19	Jim Carroll: The Gulf Coast WID Kid (April 1987)	13	\$130
20	The Emergence of Geochemical Well Logging (April 1987)	11	\$110
21	The Quest for True Formation Resistivity (April 1987)	15	\$150
22	Basics of Nuclear Logging (July 1987)	16	\$160
23	Evaluating Porosity and Permeability in Oomoldic Carbonates (July 1987)	9	\$ 90
24	The Generalized Radon Transform: A Breakthrough in Seismic Migration (July 1987)	15	\$150
25	Strategies for Dipmeter Interpretation: Part I (July 1987)	30	\$300
26	Layered Reservoir Testing (October 1987)	15	\$150
27	Sonic Logging in Cased Wells: Opportunities for Enhancing Old Fields (October 1987)	8	\$ 80
28	Strategies for Dipmeter Interpretation: Part II (October 1987)	11	\$110
29	Logging Techniques for Casing Corrosion (October 1987)	17	\$170
30	Probing Permeability: An Introduction to Measurements (January 1988)	24	\$240
31	Looking Sideways for Oil (January 1988)	18	\$180
32	Fractals and Rocks (January 1988)	9	\$ 90
33	Mineral Logging Parameters: Nuclear and Acoustic (January 1988)	14	\$140
34	Advances in High-Resolution Logging (April 1988)	15	\$150
35	Measuring Flow Downhole (April 1988)	15	\$150
36	New Environmental Corrections for the Compensated Neutron Porosity Log (April 1988)	12	\$120
37	Rock Wettability (April 1988)	8	\$ 80
38	Archie's Law: Electrical Conduction in Clean, Water-Bearing Rock (July 1988)	22	\$220
39	High Resistivity in Oklahoma (July 1988)	4	\$ 40
40	Detecting Seismic Waves in the Borehole (July 1988)	21	\$210
41	Log Interpretation in Igneous and Metamorphic Rock (July 1988)	24	\$240
42	Logging for Science (October 1988)	8	\$ 80
43	Archie II: Electrical Conduction in Hydrocarbon-Bearing Rock (October 1988)	18	\$180
44	Measuring Porosity, Saturation and Permeability from Cores: An Appreciation of the Difficulties (October 1988)	16	\$160
45	IMPULSE® Testing (October 1988)	18	\$180
46	PVT Analysis for Oil Reservoirs (January 1989)	21	\$210
47	Using Formation MicroScanner® Images (January 1989)	36	\$360
48	The Annulus Effect (January 1989)	13	\$130
49	Bacteria in the Oil Field: Bad News, Good News (January 1989)	9	\$ 90



2103 Market, Midland, Texas 79703, Phone: (915) 694-9517

SURVEY CERTIFICATION SHEET

STATE OF TEXAS
COUNTY OF MIDLAND

I, TIM STEPHENS, in the employ of Eastman Christensen, Inc. did on the days of JUNE 23, 19 89 thru JUNE 23, 19 89 conduct or supervise the taking of a GYROSCOPIC MULTI-SHOT survey by the method of magnetic orientation from a depth of 0 feet to 3900 feet, with recordings of inclination and direction being obtained at approximate intervals of 100 feet.

This survey was conducted at the request of STEVENS OPERATING CORPORATION for their DEEMAR FEDERAL WELL #1, CHAVES County, State of NEW MEXICO, in the field.

This data for this survey and the calculation were obtained and performed by me according to standards and procedures as set forth by Eastman Christensen, Inc. and is true and correct to the best of my knowledge.

Signature of Tim Stephens, Directional Supervisor/Surveyor

The data for this survey has been examined by me and conforms to principles and procedures set forth by Eastman Christensen, Inc. Signature of E. J. ...

Before me, the undersigned authority, on this day personally appeared, known to me to be the person whose name is subscribed to this instrument, who after being by me duly sworn on oath, states that he has knowledge of all the facts stated above and that this instrument is a true statement of facts therein recited.

Subscribed and sworn to before me on this day of 19

BEFORE THE OIL CONSERVATION COMMISSION Santa Fe, New Mexico No. 9677 9670 Exhibit No. 5 Attest by Ahlen Date 10/19/89

Notary Public in and for the County of Midland, Texas My commission expires

STEVENS OPERATING CORPORATION
 DEEMAR FEDERAL WELL NO 1
 CHAVES COUNTY, NEW MEXICO

DATE PRINTED : 02--AUG--89
 OUR REF. NO. : S01364.05Z
 DECLINATION : 10.00 JOB NUMBER :

PAGE NO.

MEASURED DEPTH	DRIFT ANGLE D M	DRIFT DIRECTION D M	COURSE LENGTH	TRUE VERTICAL DEPTH	R E C T A N G U L A R C O O R D I N A T E S	DOGLE SEVERI
7900.00	2 15	N 81 0 E	0.00	7898.37	63.34 N 77.79 E	0.0
8004.00	4 45	S 78 0 E	104.00	8002.17	63.17 N 84.10 E	2.6
8064.00	6 0	S 76 0 E	60.00	8061.90	61.91 N 89.58 E	2.1
8126.00	6 45	S 77 0 E	62.00	8123.52	60.30 N 96.27 E	1.2
8220.00	7 45	S 81 0 E	94.00	8216.77	58.04 N 107.91 E	1.1
8315.00	9 0	S 81 0 E	95.00	8310.75	55.88 N 121.58 E	1.3
8407.00	10 30	S 85 0 E	92.00	8401.42	53.98 N 137.04 E	1.7
8510.00	12 0	S 84 0 E	103.00	8502.44	52.05 N 157.04 E	1.4
8595.00	13 15	N 89 0 E	85.00	8585.38	51.24 N 175.59 E	2.3
8689.00	15 0	N 87 0 E	94.00	8676.54	52.04 N 198.51 E	1.9
8745.00	15 30	N 88 0 E	56.00	8730.56	52.68 N 213.23 E	1.0
8814.00	13 30	N 87 0 E	69.00	8797.36	53.44 N 230.49 E	2.9
8877.00	12 0	N 89 0 E	63.00	8858.81	53.92 N 244.38 E	2.4
8968.00	10 0	S 89 0 E	91.00	8948.13	53.92 N 261.74 E	2.2
9062.00	8 0	S 90 0 E	94.00	9040.97	53.79 N 276.45 E	2.1
9155.00	6 30	S 81 0 E	93.00	9133.22	52.88 N 288.13 E	2.0
9248.00	5 15	S 77 0 E	93.00	9225.73	51.06 N 297.48 E	1.4
9377.00	5 45	S 72 0 E	129.00	9354.14	47.76 N 309.39 E	0.5
9502.00	5 0	S 76 0 E	125.00	9478.59	44.53 N 320.64 E	0.6
9623.00	5 0	S 75 0 E	121.00	9599.13	41.89 N 330.85 E	0.0
9748.00	4 45	S 71 0 E	125.00	9723.67	38.78 N 341.01 E	0.3
9872.00	4 45	S 71 0 E	124.00	9847.25	35.44 N 350.72 E	0.0
9899.00	4 45	S 71 0 E	27.00	9874.16	34.71 N 352.83 E	0.0

CLOSURE - DISTANCE : 354.53
 DIRECTION : N 84 23 E
 REPORT UNITS : Feet
 SURVEY CALCULATION METHOD : Radius of curvature

SURVEY RUN INFORMATION

Sioc Track 1



5/6 of 2

11/11/89

STEVENS OPERATING CORPORATION
DEEMAR FEDERAL WELL NO 1
CHAVES COUNTY, NEW MEXICO

DATE PRINTED : 01-AUG-89
OUR REF. NO. : S01365.4SZ

PAGE NO.

DECLINATION : 10.00 JOB NUMBER :

MEASURED DEPTH	DRIFT ANGLE D M	DRIFT DIRECTION D M	COURSE LENGTH	TRUE VERTICAL DEPTH	R E C T A N G U L A R C O O R D I N A T E S	DOGLEG SEVERITY
0.00	0 0	N 0 0 E	0.00	0.00	0.00 N 0.00 E	0.00
100.00	0 15	S 83 0 E	100.00	100.00	0.03 S 0.22 E	0.25
200.00	0 30	N 79 0 E	100.00	200.00	0.00 S 0.87 E	0.27
300.00	0 15	N 85 0 E	100.00	300.00	0.09 N 1.52 E	0.25
400.00	0 30	S 71 0 E	100.00	399.99	0.01 N 2.16 E	0.29
500.00	0 15	S 74 0 E	100.00	499.99	0.19 S 2.79 E	0.25
600.00	0 30	S 90 0 E	100.00	599.99	0.28 S 3.44 E	0.27
700.00	0 30	N 20 0 W	100.00	699.98	0.33 N 3.86 E	0.82
800.00	0 30	S 43 0 E	100.00	799.98	0.66 N 4.40 E	0.98
900.00	0 30	N 52 0 E	100.00	899.98	0.59 N 5.19 E	0.68
1000.00	0 30	S 35 0 E	100.00	999.97	0.48 N 5.96 E	0.73
1100.00	0 30	S 43 0 W	100.00	1099.97	0.33 S 5.90 E	0.63
1200.00	0 15	N 50 0 E	100.00	1199.97	0.64 S 6.20 E	0.75
1300.00	0 15	S 62 0 E	100.00	1299.97	0.60 S 6.61 E	0.28
1400.00	0 30	N 67 0 W	100.00	1399.96	0.98 S 6.43 E	0.75
1500.00	0 15	S 35 0 E	100.00	1499.96	1.36 S 6.12 E	0.72
1600.00	0 30	N 21 0 W	100.00	1599.96	1.15 S 6.51 E	0.75
1700.00	0 30	N 26 0 W	100.00	1699.96	0.35 S 6.17 E	0.04
1800.00	1 0	N 16 0 W	100.00	1799.95	0.87 N 5.70 E	0.51
1900.00	1 0	N 42 0 W	100.00	1899.93	2.38 N 4.86 E	0.45
2000.00	0 45	N 15 0 W	100.00	1999.92	3.71 N 4.14 E	0.48
2100.00	1 0	N 4 0 W	100.00	2099.91	5.21 N 3.89 E	0.30
2200.00	1 15	N 16 0 W	100.00	2199.89	7.14 N 3.55 E	0.34
2300.00	1 30	N 19 0 W	100.00	2299.86	9.43 N 2.82 E	0.26
2400.00	1 0	N 26 0 W	100.00	2399.84	11.44 N 1.99 E	0.52
2500.00	1 0	N 49 0 W	100.00	2499.82	12.82 N 0.94 E	0.40
2600.00	1 0	N 28 0 W	100.00	2599.81	14.18 N 0.15 W	0.36
2700.00	0 45	N 34 0 W	100.00	2699.79	15.49 N 0.93 W	0.27
2800.00	1 30	N 46 0 W	100.00	2799.77	16.99 N 2.19 W	0.78
2900.00	1 30	N 35 0 W	100.00	2899.74	18.97 N 3.89 W	0.29



CONTINUED ON NEXT PAGE ...

MEASURED DEPTH	DRIFT ANGLE D M	DRIFT DIRECTION D M	COURSE LENGTH	TRUE VERTICAL DEPTH	R E C T A N G U L A R C O O R D I N A T E S	DOGLEG SEVERITY
3000.00	1 15	N 39 0 W	100.00	2999.71	20.89 N 5.33 W	0.27
3100.00	1 30	N 17 0 W	100.00	3099.68	22.99 N 6.45 W	0.58
3200.00	1 30	N 22 0 W	100.00	3199.65	25.46 N 7.32 W	0.13
3300.00	1 0	N 7 0 W	100.00	3299.62	27.57 N 7.87 W	0.59
3400.00	1 30	N 13 0 W	100.00	3399.60	29.71 N 8.25 W	0.52
3500.00	1 0	N 4 0 W	100.00	3499.58	31.87 N 8.57 W	0.54
3600.00	0 45	N 2 0 E	100.00	3599.56	33.40 N 8.60 W	0.27
3700.00	1 0	N 23 0 E	100.00	3699.55	34.88 N 8.27 W	0.40
3800.00	0 30	N 35 0 E	100.00	3799.54	36.02 N 7.63 W	0.52
3900.00	0 30	N 56 0 E	100.00	3899.54	36.63 N 7.01 W	0.18
4000.00	1 0	N 66 0 E	100.00	3999.53	37.26 N 5.87 W	0.51
4100.00	0 30	N 29 0 E	100.00	4099.52	38.13 N 4.92 W	0.67
4200.00	0 45	N 35 0 E	100.00	4199.52	39.06 N 4.34 W	0.26
4300.00	1 0	N 67 0 E	100.00	4299.50	40.01 N 3.17 W	0.54
4400.00	0 45	N 86 0 E	100.00	4399.49	40.36 N 1.70 W	0.38
4500.00	0 30	N 77 0 E	100.00	4499.49	40.52 N 0.62 W	0.27
4600.00	0 30	N 40 0 E	100.00	4599.48	40.97 N 0.11 E	0.32
4700.00	0 15	N 82 0 E	100.00	4699.48	41.28 N 0.68 E	0.36
4800.00	1 0	N 74 0 E	100.00	4799.47	41.51 N 1.74 E	0.75
4900.00	1 0	N 80 0 E	100.00	4899.46	41.90 N 3.44 E	0.10
5000.00	1 0	N 46 0 E	100.00	4999.44	42.68 N 4.97 E	0.58
5100.00	1 15	N 63 0 E	100.00	5099.42	43.82 N 6.57 E	0.41
5200.00	1 15	N 74 0 E	100.00	5199.40	44.61 N 8.59 E	0.24
5300.00	0 45	N 42 0 E	100.00	5299.38	45.53 N 10.05 E	0.73
5400.00	1 0	N 64 0 E	100.00	5399.37	46.44 N 11.27 E	0.41
5500.00	1 0	N 81 0 E	100.00	5499.36	46.96 N 12.92 E	0.30
5600.00	1 0	N 68 0 E	100.00	5599.34	47.43 N 14.60 E	0.23
5700.00	1 15	N 68 0 E	100.00	5699.32	48.16 N 16.42 E	0.25
5800.00	1 15	N 79 0 E	100.00	5799.30	48.78 N 18.51 E	0.24
5900.00	1 30	N 79 0 E	100.00	5899.27	49.24 N 20.87 E	0.25



EVENS OPERATING CORPORATION
 EMAR FEDERAL WELL NO 1
 AVES COUNTY, NEW MEXICO

DATE PRINTED : 01-AUG-89
 OUR REF. NO. : S01365.4SZ
 DECLINATION : 10.00JOB NUMBER :

MEASURED DEPTH	DRIFT ANGLE D M	DRIFT DIRECTION D M	COURSE LENGTH	TRUE VERTICAL DEPTH	R E C T A N G U L A R C O O R D I N A T E S	DOGLEG SEVERITY
6000.00	0 30	N 87 0 E	100.00	5999.25	49.45 N 22.60 E	1.01
6100.00	2 15	N 84 0 E	100.00	6099.22	49.64 N 24.99 E	1.75
6200.00	1 30	N 89 0 E	100.00	6199.17	49.84 N 28.25 E	0.77
6300.00	1 15	N 70 0 E	100.00	6299.14	50.28 N 30.60 E	0.52
6400.00	1 30	N 74 0 E	100.00	6399.11	51.02 N 32.88 E	0.27
6500.00	1 45	N 67 0 E	100.00	6499.07	51.96 N 35.55 E	0.32
6600.00	2 0	N 73 0 E	100.00	6599.01	53.08 N 38.63 E	0.32
6700.00	2 0	N 79 0 E	100.00	6698.95	53.93 N 42.01 E	0.21
6800.00	2 0	N 79 0 E	100.00	6798.89	54.59 N 45.44 E	0.00
6900.00	2 0	N 83 0 E	100.00	6898.83	55.14 N 48.88 E	0.14
7000.00	1 15	S 85 0 E	100.00	6998.79	55.19 N 51.71 E	0.82
7100.00	1 30	N 74 0 E	100.00	7098.76	55.42 N 54.09 E	0.56
7200.00	2 0	N 76 0 E	100.00	7198.71	56.21 N 57.04 E	0.50
7300.00	1 45	N 61 0 E	100.00	7298.66	57.40 N 60.07 E	0.55
7400.00	2 0	N 74 0 E	100.00	7398.61	58.65 N 63.09 E	0.49
7500.00	1 45	N 68 0 E	100.00	7498.55	59.72 N 66.18 E	0.32
7600.00	1 45	N 79 0 E	100.00	7598.51	60.58 N 69.11 E	0.34
7700.00	1 45	N 77 0 E	100.00	7698.46	61.22 N 72.09 E	0.06
7800.00	1 30	N 60 0 E	100.00	7798.42	62.25 N 74.72 E	0.54
7847.00	1 15	N 53 0 E	47.00	7845.41	62.87 N 75.66 E	0.64
7940.00	2 45	S 74 0 E	93.00	7938.35	63.44 N 78.74 E	2.40
8033.00	6 15	S 72 0 E	93.00	8031.05	61.31 N 85.72 E	3.77
8126.00	6 30	S 76 0 E	93.00	8123.47	58.47 N 95.64 E	0.55
8219.00	8 0	S 82 0 E	93.00	8215.72	56.23 N 107.16 E	1.80
8312.00	9 15	S 88 0 E	93.00	8307.67	55.01 N 121.04 E	1.65
8406.00	10 30	N 89 0 E	94.00	8400.28	54.87 N 137.16 E	1.44
8499.00	12 15	S 88 0 E	93.00	8491.45	54.71 N 155.50 E	1.99
8592.00	13 0	N 89 0 E	93.00	8582.20	54.53 N 175.82 E	1.07
8685.00	15 0	N 89 0 E	93.00	8672.43	54.93 N 198.32 E	2.15
8778.00	16 15	N 89 0 E	93.00	8761.99	55.36 N 223.36 E	1.34



EVENS OPERATING CORPORATION
 EMAR FEDERAL WELL NO 1
 AVES COUNTY, NEW MEXICO

DATE PRINTED : 01-AUG-89
 OUR REF. NO. : S01365.4SZ
 DECLINATION : 10.00JOB NUMBER :

MEASURED DEPTH	DRIFT ANGLE D M	DRIFT DIRECTION D M	COURSE LENGTH	TRUE VERTICAL DEPTH	R E C T A N G U L A R C O O R D I N A T E S	DOGLEG SEVERITY
8871.00	17 15	S 84 0 E	93.00	8851.04	54.20 N 250.12 E	2.42
8965.00	18 45	S 76 0 E	94.00	8940.44	49.16 N 278.70 E	3.07
9058.00	20 15	S 77 0 E	93.00	9028.10	41.91 N 308.89 E	1.65
9151.00	21 0	S 74 0 E	93.00	9115.14	33.71 N 340.60 E	1.39
9244.00	22 15	S 74 0 E	93.00	9201.60	24.26 N 373.55 E	1.34
9337.00	23 0	S 76 0 E	93.00	9287.44	15.00 N 408.10 E	1.16
9430.00	25 0	S 74 0 E	93.00	9372.39	5.21 N 444.64 E	2.32
9524.00	26 45	S 76 0 E	94.00	9456.97	5.40 S 484.26 E	2.08
9617.00	27 0	S 78 0 E	93.00	9539.92	14.86 S 525.22 E	1.01
9710.00	25 30	S 77 0 E	93.00	9623.33	23.76 S 565.37 E	1.68
9739.00	25 45	S 76 0 E	29.00	9649.47	26.69 S 577.57 E	1.72

CLOSURE - DISTANCE : 578.19
 DIRECTION : S 87 21 E

REPORT UNITS : Feet
 SURVEY CALCULATION METHOD : Radius of curvature

SURVEY RUN INFORMATION

=====

